Faculté **e**nvironnement **n**aturel, **a**rchitectural et **c**onstruit - ENAC

MCS MAINTENANCE CONSTRUCTION SÉCURITÉ
INSTITUT D'INGÉNIERIE CIVILE

ÉCOLE POLYTECHNIQUE FÉDÉRALE DE LAUSANNE

Test Report MCS 23.09.01-part 1

# Tensile fatigue test of Ultra-High Performance Fibre Reinforced Composites (UHPFRC)

Doctoral assistant Tohru Makita
Director Professor Eugen Brühwiler

Lausanne, February 2014

**Table of Contents**

**List of Figures**

**List of Tables**

## 1 Objectives

The experimental campaign was intended to study the tensile fatigue behaviour of UHPFRC. UHPFRC carries tensile stress thanks to its relatively high tensile strength and tensile strain-hardening behaviour. Especially, when applied to bridge deck slabs, UHPFRC is subjected to tensile fatigue stress at the cantilever part (circled part in Fig. 1). It is necessary to understand the tensile fatigue behaviour of UHPFRC for the practical application.

The test results were expected to be utilised for determination of fatigue endurance limit of UHPFRC, comprehension of characteristic tensile fatigue behaviour and fatigue fracture process of UHPFRC and deduction of empirical laws for UHPFRC under tensile fatigue.

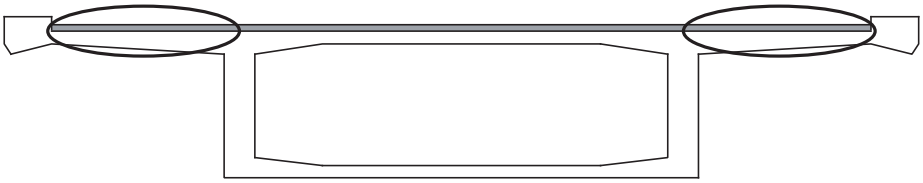

**Figure 1** Bridge deck slab improved with UHPFRC layer

## 2 Specimens, test set-up and instrumentation

### 2.1 Material

The mix of UHPFRC used in experimental tests is HIFCOM 13 developed by MCS, EPFL. This mix is characterised by 3.0 vol.- % content of 13 mm long steel fibres with a diameter of 0.16 mm and by the use of CEM III/B type cement which contains a high percentage of blast furnace slag (66%~80%) (Table 1). Specimens of preliminary tests, S1 and S2 series were cast at the same day, so were specimens of S2.5 series and so were specimens of S3 and S4 series. Three prisms with section of 40 mm × 40 mm and length of 160 mm were produced for each casting with the same UHPFRC as used for the fabrication of monolithic UHPFRC specimens. Three prisms made for preliminary tests, S1 and S2 series were tested 28 days after casting and the average compressive strength and modulus of elasticity were 206.2 MPa and 49.5 GPa respectively (Table 2). Three prisms made for S2.5 series were tested 8 days after casting and the average compressive strength and modulus of elasticity were 182.5 MPa and 46.0 GPa respectively (Table 3). Three prisms made for S3 and S4 series tests were tested 61 days after casting and the average compressive strength and modulus of elasticity were 215.5 MPa and 50.8 GPa respectively (Table 4).

**Table 1** Composition of UHPFRC mix "HIFCOM 13"

| Component | Type | Mass [kg/m$^3$] | Remarks |
|---|---|---|---|
| Cement | CEM III/B | 1277.4 | |
| Silica fume | Elkem Microsilica 971 U | 95.8 | 7.5 % of cement mass |
| Sand | Quartz sand MN 30 | 664.6 | $d_{max}$ < 0.5mm |
| Steel fibres | Bekaert OL 13/0.16 mm | 235.5 | 3.0 vol.-%, brass coating |
| Superplasticiser | Sikament P5 | 42.3 | 3.3 % of cement mass |
| Water | | 198.0 | W/C=0.155 |

**Table 2** Test results of UHPFRC prisms 40mm × 40mm × 160mm fabricated for preliminary test, S1 and S2 series on 04.11.2009

| Report No. | ID No. | Age [days] | Compressive Strength [MPa] | Modulus of Elasticity [GPa] | Modulus of Rupture [MPa] |
|---|---|---|---|---|---|
| 398/09/LMC<br>399/09/LMC | 1967 | 28 | 205.9 | 49.5 | 50.2 |
| | 1968 | | 204.7 | 50.0 | 37.1 |
| | 1969 | | 208.1 | 49.0 | 38.4 |
| | Average | | 206.2 | 49.5 | 41.9 |

**Table 3** Test results of UHPFRC prisms 40mm × 40mm × 160mm fabricated for S2.5 series on 25.08.2009

| Report No. | ID No. | Age [days] | Compressive Strength [MPa] | Modulus of Elasticity [GPa] | Modulus of Rupture [MPa] |
|---|---|---|---|---|---|
| 254/09/LMC<br>255/09/LMC | 1332 | 8 | 177.8 | 47.0 | 24.6 |
| | 1333 | | 162.8 | 44.5 | 25.1 |
| | 1334 | | 206.9 | 46.5 | 37.6 |
| | Average | | 182.5 | 46.0 | 29.1 |

**Table 4** Test results of UHPFRC prisms 40mm × 40mm × 160mm fabricated for S3 and S4 series on 25.11.2009

| Report No. | ID No. | Age [days] | Compressive Strength [MPa] | Modulus of Elasticity [GPa] | Modulus of Rupture [MPa] |
|---|---|---|---|---|---|
| 019/10/LMC<br>020/10/LMC | 2124 | 61 | 212.8 | 51 | 46.1 |
| | 2125 | | 216.6 | 50.5 | 42.1 |
| | 2126 | | 217.2 | 51 | 37.6 |
| | Average | | 215.5 | 50.8 | 41.9 |

**2.2 Specimen**

The dimension of specimen is 750 mm long with a cross section of 150 mm × 40 mm (Fig. 2). Specimens were cast in wooden forms and demouled seven days after casting, and then kept in the testing hall of IIC, EPFL at constant climate condition for more than 72 days for S1 and S2 series, more than 830 days for S2.5 series and more than 329 days for S3 and S4 series. In order to cause fracture within the 250 mm-long central zone of the specimen, aluminium plates (250 mm long, 150 mm wide and 2 mm thick) were glued using epoxy resin to both surfaces of the specimen end parts as strengthening elements.

**2.3 Measuring Devices**

Two 250 mm-long Linear Variable Differential Transducers (LVDT) and five displacement transducers with a 50mm measurement length were used to measure the specimen deformation (Fig.2). LVDTs were set up on both of specimen sides such as to capture global specimen deformation. In this report the average of deformation as measured by the two LVDTs are always referred to as global deformation. The five displacement transducers were set up on the specimen surface to measure local specimen deformation in five consecutive zones. LVDT 1 was installed on the eastern side of the specimen and LVDT 2 was on the western side. The five transducers were installed on the north surface of the specimen. Force was measured by the load cell installed in the actuator of the 1,000 kN servo-hydraulic testing machine (SCHENCK universal machine).

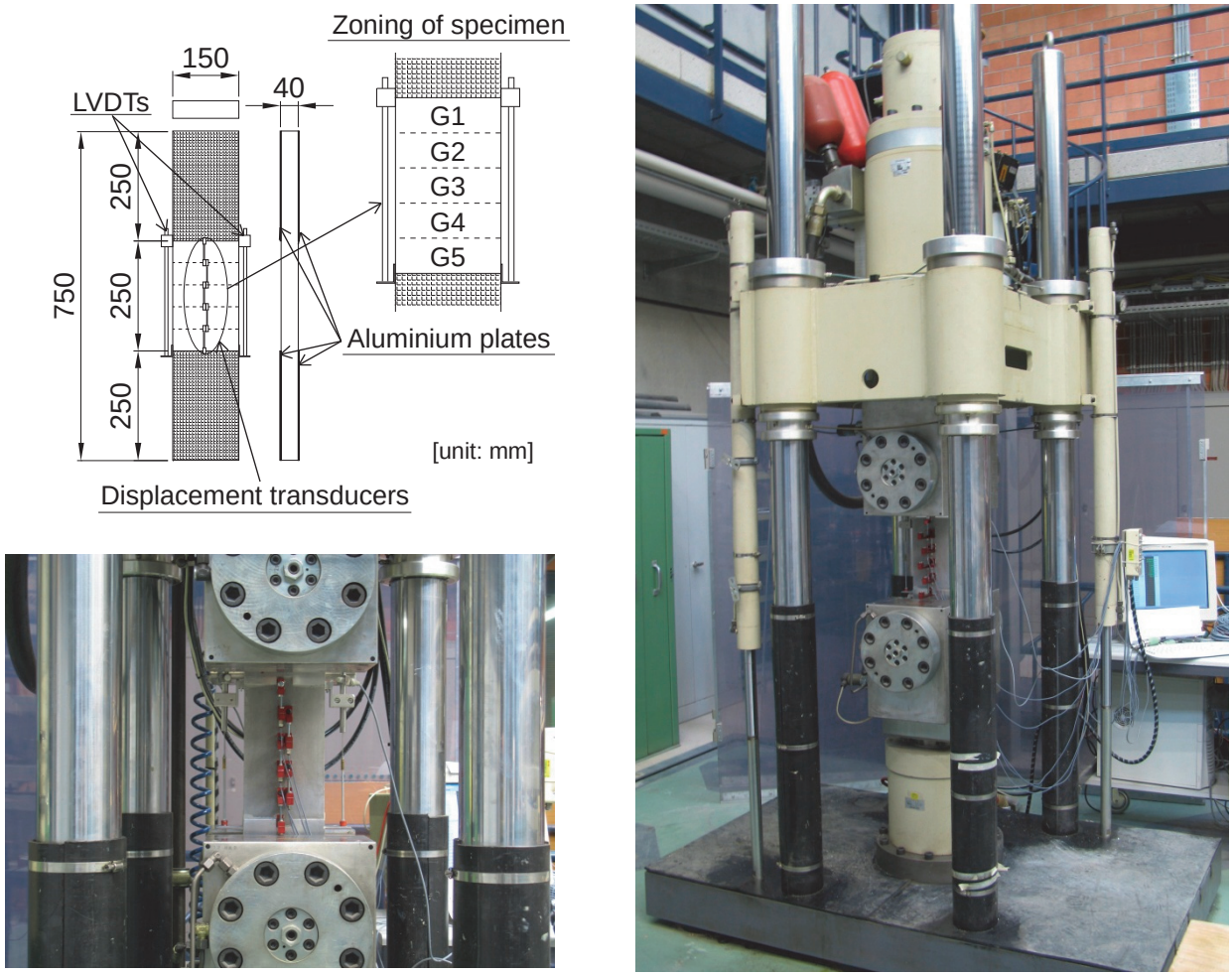


**Figure 2** Specimen geometry, measuring devices and testing set-up

## 3 Testing program

### 3.1 Quasi-static tensile test

Three quasi-static tensile tests were conducted per test parameter to determine the quasi-static specimen behaviour as well as the elastic limit and ultimate strengths. Force was applied in a displacement-controlled mode with a displacement rate of 0.02mm/min within pre-peak domain and 0.2mm/min within post-peak domain (Fig. 3). Deformation and force data were recorded continuously with a frequency of 2 Hz.

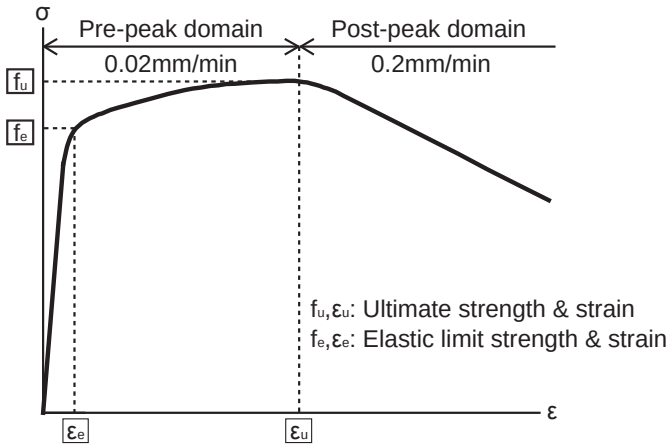


**Figure 3** Application rate of displacement-controlled force

### 3.2 Tensile fatigue test

Four series of tensile fatigue tests were planned by varying maximum stress and pre-applied deformation. Each fatigue test series is characterised referring to the quasi-static stress-strain curve following:

- S1 series: maximum stress high in the elastic domain
- S2 series: maximum stress low in the strain-hardening domain
- S2.5 series: initial application of deformation corresponding to 0.5 ‰ followed by fatigue testing
- S3 series: initial application of deformation entering into the strain-hardening domain followed by fatigue testing
- S4 series: initial application of deformation entering into the softening domain followed by fatigue testing

The objective of S1, S2 and S2.5 series was the determination of the endurance limit within the elastic domain. The comprehension of tensile fatigue behaviour beyond the elastic limit after losing the initial modulus of deformation of the specimen was the objective for the S3 and S4 series.

Determination of maximum fatigue stress of S1 and S2 series was as follows: first, the specimen was subjected to quasi-static tensile stress until one LVDT reached a target deformation (corresponding to strains of either 0.20 ‰ or 0.25 ‰ or 0.30 ‰) and unloaded. The stress that caused the target deformation was then applied as maximum stress level for the fatigue test. When the specimen sustained 10 million cycles, this result was regarded as 'run-out', and the test subsequently was continued at an increased maximum tensile fatigue stress. Maximum fatigue stress in the second fatigue test was determined in the similar way to the first fatigue test, but target deformation wasn't defined in the preceding quasi-static tensile stress application. Instead, quasi-static tensile stress was imposed on the specimen beyond maximum stress used for the preceding fatigue test. When one LVDT reached the deformation corresponding to strain of round number with one decimal place, such as 0.5 ‰ strain, quasi-static stress application was stopped and the stress causing that deformation was then applied as maximum fatigue stress. The minimum fatigue stress was always set equal to 10 % of the average elastic limit strength as determined from three quasi-static tensile tests.

Maximum fatigue stress of S2.5, S3 and S4 series was determined by using the stress-deformation curve obtained from the quasi-static tensile deformation application preceding fatigue tests. The stress causing a specific global deformation was

imposed as maximum fatigue stress, i.e. the stress corresponding to strains of either 0.10 ‰ or 0.15 ‰ or 0.20 ‰. In the second (third) fatigue tests, maximum fatigue stress was arbitrarily chosen from the stress corresponding to strains of either 0.15 ‰, 0.20 ‰ or 0.25 ‰. The minimum fatigue stress was always 10 % of maximum stress in S2.5, S3 and S4 series.

The fatigue stress application procedure was as follows. Firstly, stress was increased to the specified maximum stress under displacement control mode with a rate of 0.02 mm/min, then sinusoidal wave cyclic stress was imposed under force control mode with a frequency of 10 Hz. 10 seconds were needed for the transition period from quasi-static to the constant amplitude cyclic stress regime (Fig. 5).

Deformation and force data were recorded with a frequency of 200 Hz. The initial and final phases of the test were recorded permanently, while between these phases data was recorded for 1 second every 600 cycles (Fig. 6).

When a specimen sustained 10 million cycles, this result was regarded as 'run-out', and the test subsequently was continued at an increased maximum tensile fatigue stress.

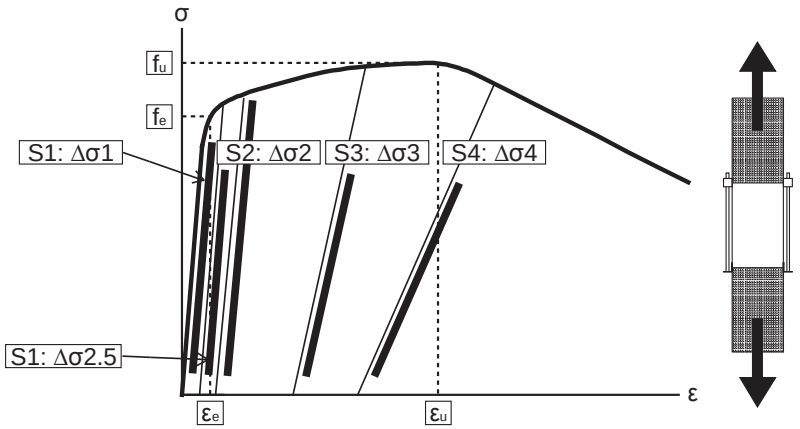


**Figure 4** Schematic representation of tensile response of UHPFRC and definition of tensile fatigue test series

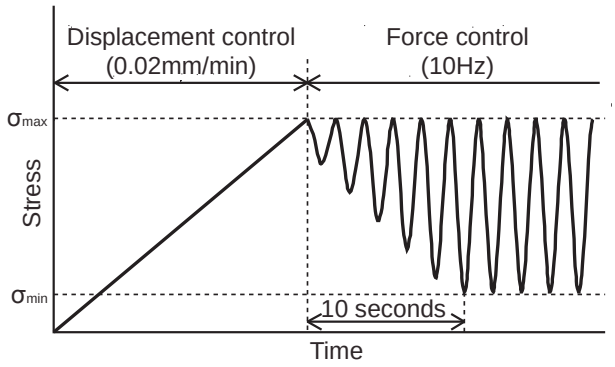


**Figure 5** Fatigue stress application procedure

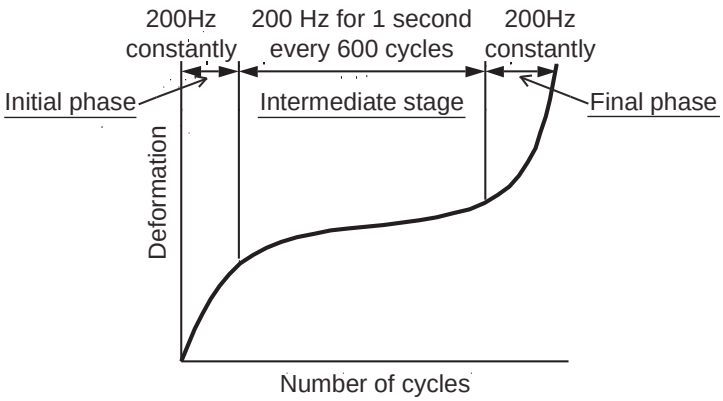


**Figure 6** Data recording rule during the fatigue test

**4 Result of quasi-static tensile test**

Age of all the specimens of quasi-static tensile tests was 70 days when the tests were done. Stress-global deformation curve was drawn for each test (Fig. 7). The stress- global deformation curve of Static test 2 was drawn only using data from one LVDT because the other LVDT didn't work properly, which was supposed to be due to microcracking under the fittings of the LVDT.

Average stress-deformation curve was drawn from the three quasi-static tensile test results. The elastic limit strength and strain was determined to be 8.2 MPa and 0.32 ‰ with the method proposed in [1]. The ultimate strength and corresponding strain was read from the curve to be 9.4 MPa and 1.64 ‰.

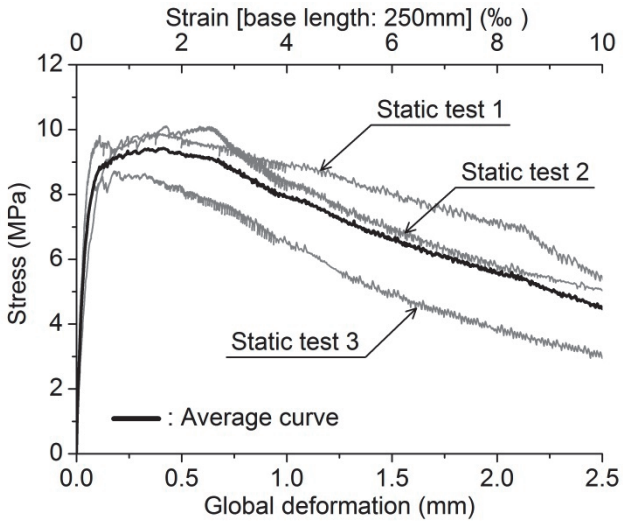


**Figure 7** Stress-global deformation curve of the quasi-static tensile tests

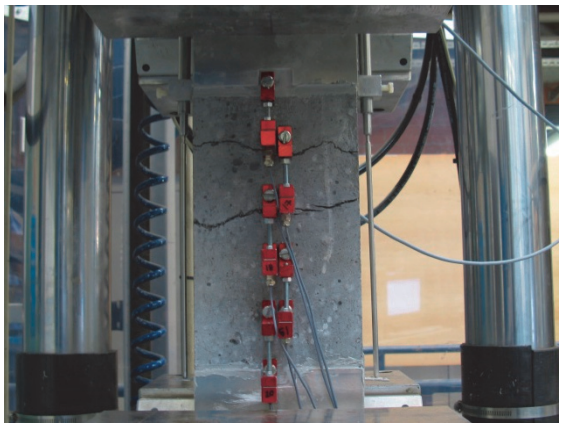

(a)

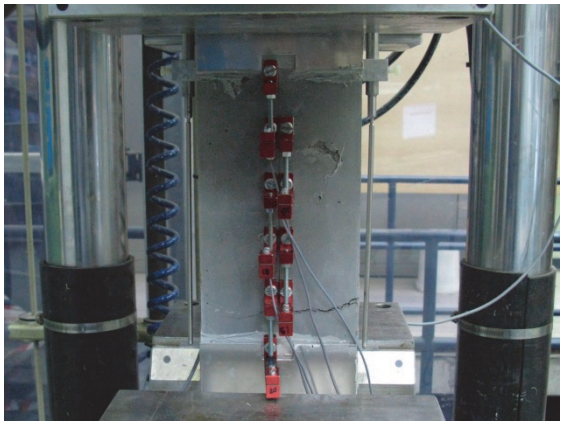

(b)

(c)

**Figure 8** Fractured specimens (a) Static test 1, (b) Static test 2 and (c) Static test 3

***Fracture surface of quasi-static tensile test specimens***

All part of the fracture surfaces was rough and pull-out fibres are clearly observed (Fig. 9). On the fracture surface of Static test 2 specimen, an area with few fibres was identified, which is enclosed with a line in Fig. 9a.

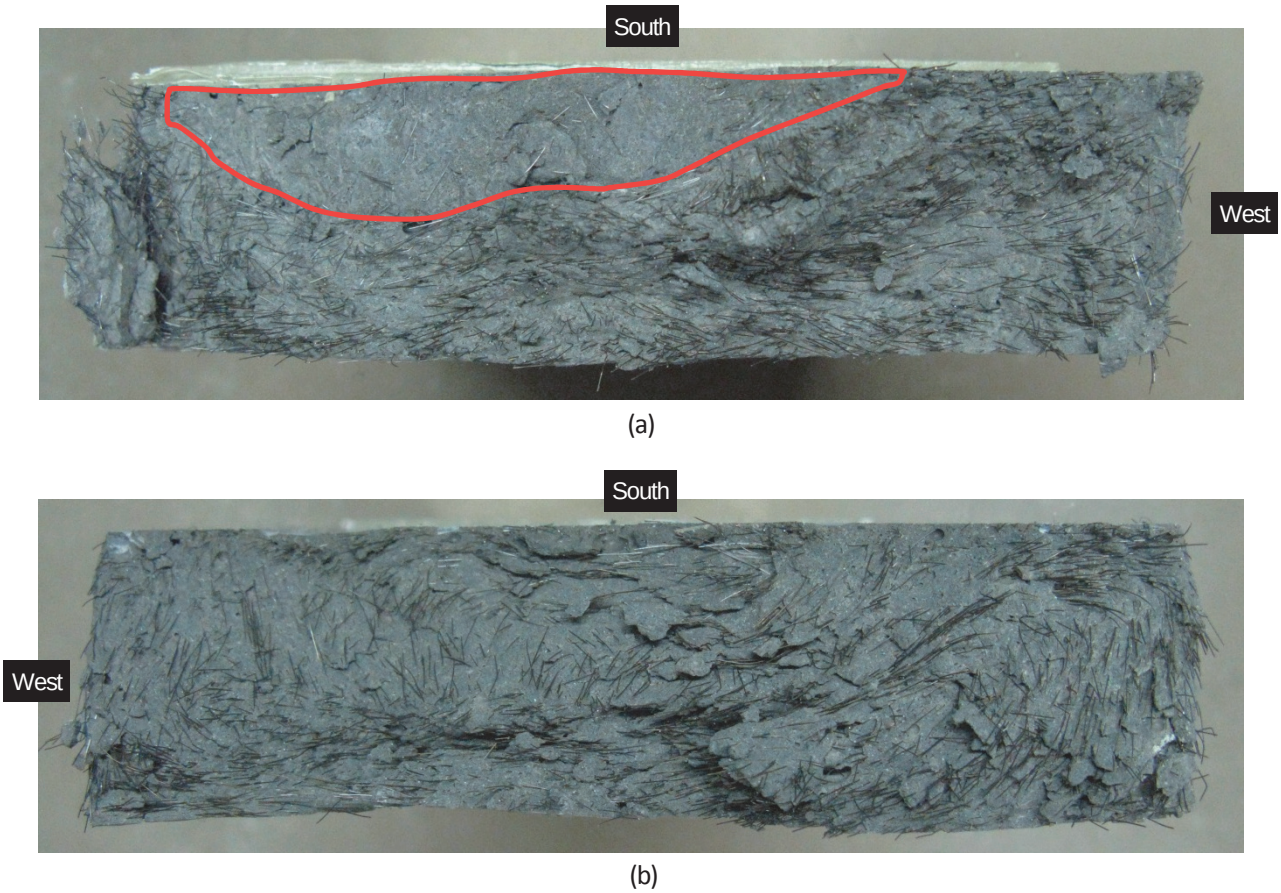


**Figure 9** Fracture surface of (a) Static test 2 specimen (lower half of the fractured specimen) and (b) Static test 3 specimen (upper half of the fractured specimen)

**5 Results of tensile fatigue tests**

Specimens were regarded as failed when the global deformation reading reached2.5 mm, corresponding to 10 ‰ of strain. For each test, maximum global deformation corresponding to maximum fatigue stress, global deformation range, maximum local deformation of five consecutive zones corresponding to maximum fatigue stress and local deformation range were plotted against the number of cycles. Since recorded data for each test was huge, reduced number of data (approximately 500 points of data) was plotted for each measurement. In the following, test results are explained one by one.

**5.1 Results of Preliminary tests**

Table 5 lists the summary of Preliminary test results.

**Table 5** Results of Preliminary tensile fatigue tests of UHPFRC

| Test No. | | $\sigma_{max}$ [MPa] | $\sigma_{min}$ [MPa] | $\sigma_{max}/f_e$ | $N$ | Remarks |
|---|---|---|---|---|---|---|
| 1 | i | 7.20 | 0.82 | 0.88 | 10,000,416 | run-out |
| | ii | 8.50 | 0.82 | 1.04 | 10,002,977 | run-out |
| | iii | 10.00 | 0.82 | 1.22 | 7,450,396 | |
| 2 | | 8.50 | 0.82 | 1.04 | 145,704 | |

$\sigma_{max(min)}$: applied maximum (minimum) fatigue stress

$N$: sustained number of fatigue cycles

$f_e$: average elastic limit strength of UHPFRC determined from three quasi-static tensile tests (= 8.2 MPa)

### 5.1.1 Preliminary test 1

**First fatigue test**

***Test parameters and results***

| $\sigma_{max}$ [MPa] | $\sigma_{min}$ [MPa] | $N$ | Deformation localisation |
|---|---|---|---|
| 7.20 | 0.82 | 10,000,416 | run-out |

Comment: Maximum fatigue stress was determined arbitrarily. Because data recording program could not work continuously more than 24 hours, stop and restart of the test was repeated about every 800,000 cycles.

***Behaviour of Preliminary test 1 specimen during the first fatigue test***

Maximum global deformation, global deformation range, maximum local deformation and local deformation range kept approximately constant. Variations were observed on local deformation readings.

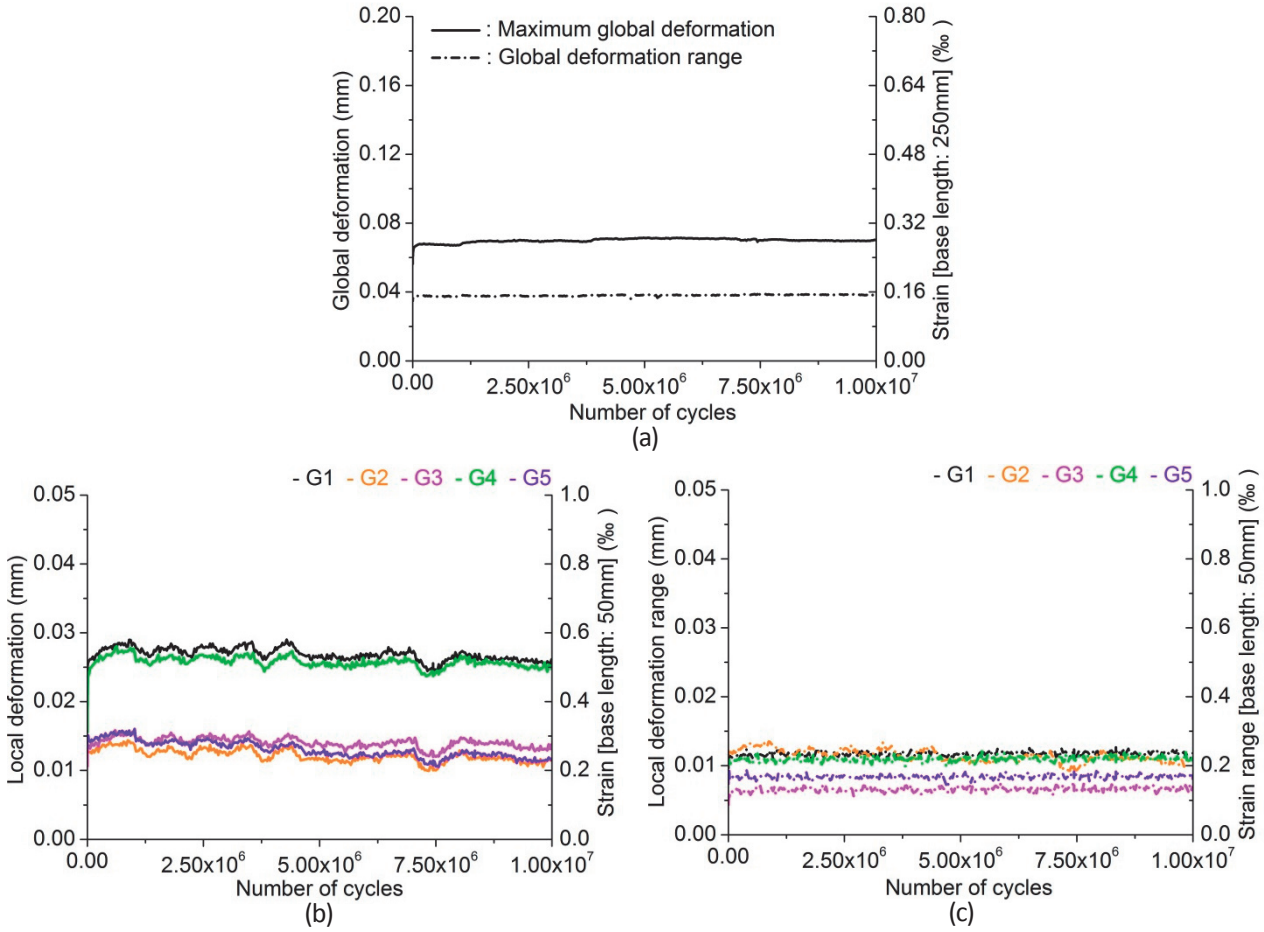


**Figure 10** Preliminary test 1-i: growth curves of (a) maximum global deformation and global deformation range, (b) maximum local deformation and (c) local deformation range

**Second fatigue test**

***Test parameters and results***

| $\sigma_{max}$ [MPa] | $\sigma_{min}$ [MPa] | *N* | Deformation localisation |
|---|---|---|---|
| 8.50 | 0.82 | 10,002,977 | run-out |

Comment: Maximum fatigue stress was determined arbitrarily. Because data recording program could not work continuously more than 24 hours, stop and restart of the test was repeated about every 800,000 cycles.

***Behaviour of Preliminary test 1 specimen during the second fatigue test***

Maximum global deformation and global deformation range kept approximately constant.

Maximum local deformation at G1 and G4 zones increased slightly, whereas maximum local deformation at G2, G3 and G5 zones kept approximately constant. Local deformation range at all local zones except G1 zone kept almost constant, while local deformation range at G1 zone increased slightly.

Variations were left on local deformation readings.

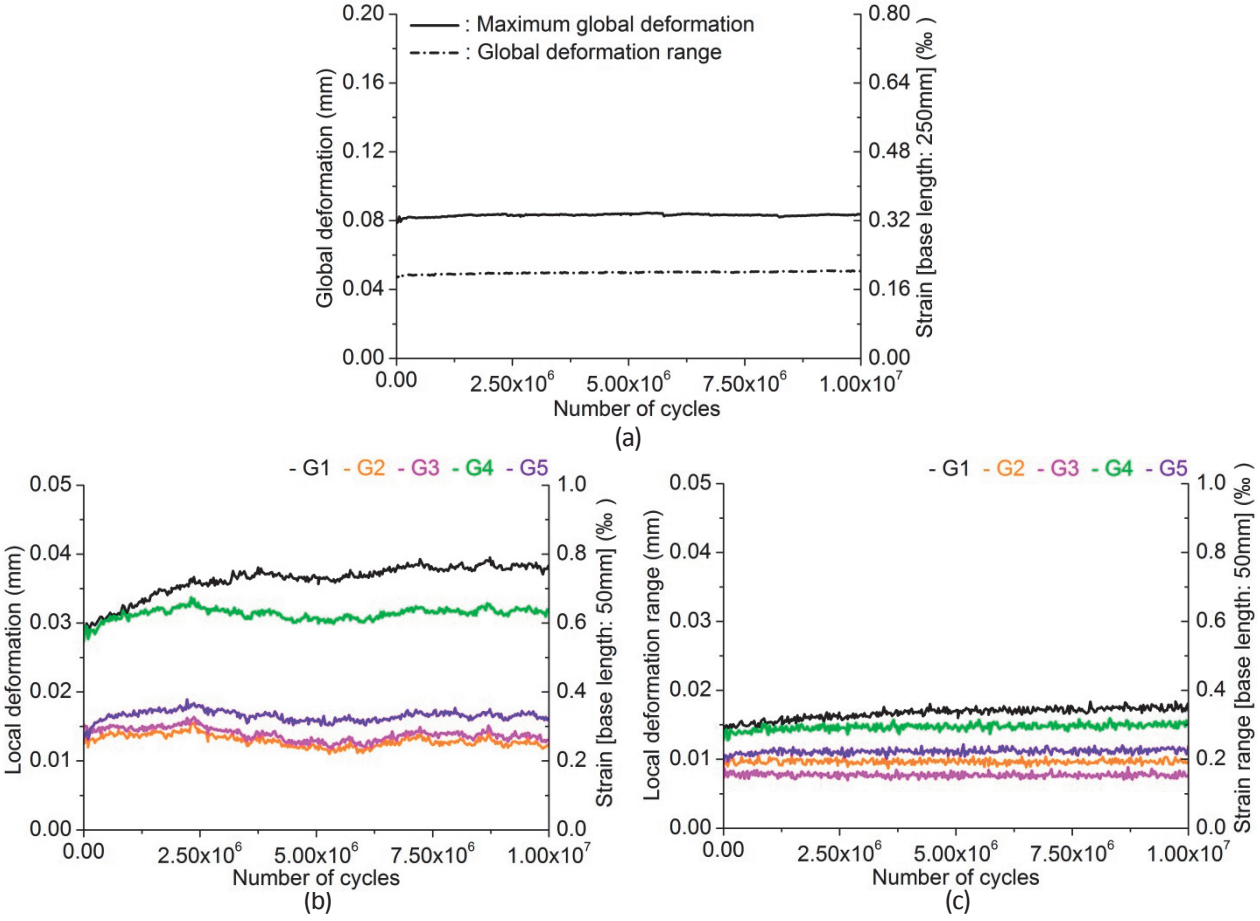


**Figure 11** Preliminary test 1-ii: growth curves of (a) maximum global deformation and global deformation range, (b) maximum local deformation and (c) local deformation range

**Third fatigue test**

***Test parameters and results***

| $\sigma_{max}$ [MPa] | $\sigma_{min}$ [MPa] | *N* | Deformation localisation |
|---|---|---|---|
| 10.00 MPa | 0.82 MPa | 7,450,396 | G4 zone |

Comment: Maximum fatigue stress was determined arbitrarily. Because data recording program could not work continuously more than 24 hours, stop and restart of the test was repeated about every 800,000 cycles.

***Behaviour of Preliminary test 1 specimen during the third fatigue test***

Maximum global deformation gradually increased, and when maximum global strain reached about 1.2 ‰ at about 6,519,700 cycles, redistribution of localised deformation occurred. After sustaining additional about 930,700 cycles, the specimen fractured. Behaviour of global deformation range was quite similar to that of maximum global deformation.

Maximum local deformation at all local zones except G2 zone increased with various growth rates, whereas maximum local deformation at G2 zone kept approximately constant. When redistribution of localised deformation occurred at about 6,519,700 cycles, all maximum local deformation readings quickly rose. Deformation localisation occurred at G4 zone despite the fact that its deformation reading was the second largest of all local deformation readings. Behaviour of local deformation range was approximately similar to that of maximum local deformation.

Variations were left on local deformation readings.

In the eastern part of the specimen, fracture crack propagated in a path inclined from horizontal axis with an angle of 20˚, while in the western part of the specimen which including fatigue cracked area, fracture crack propagated in a path approximately perpendicular to fatigue force direction.

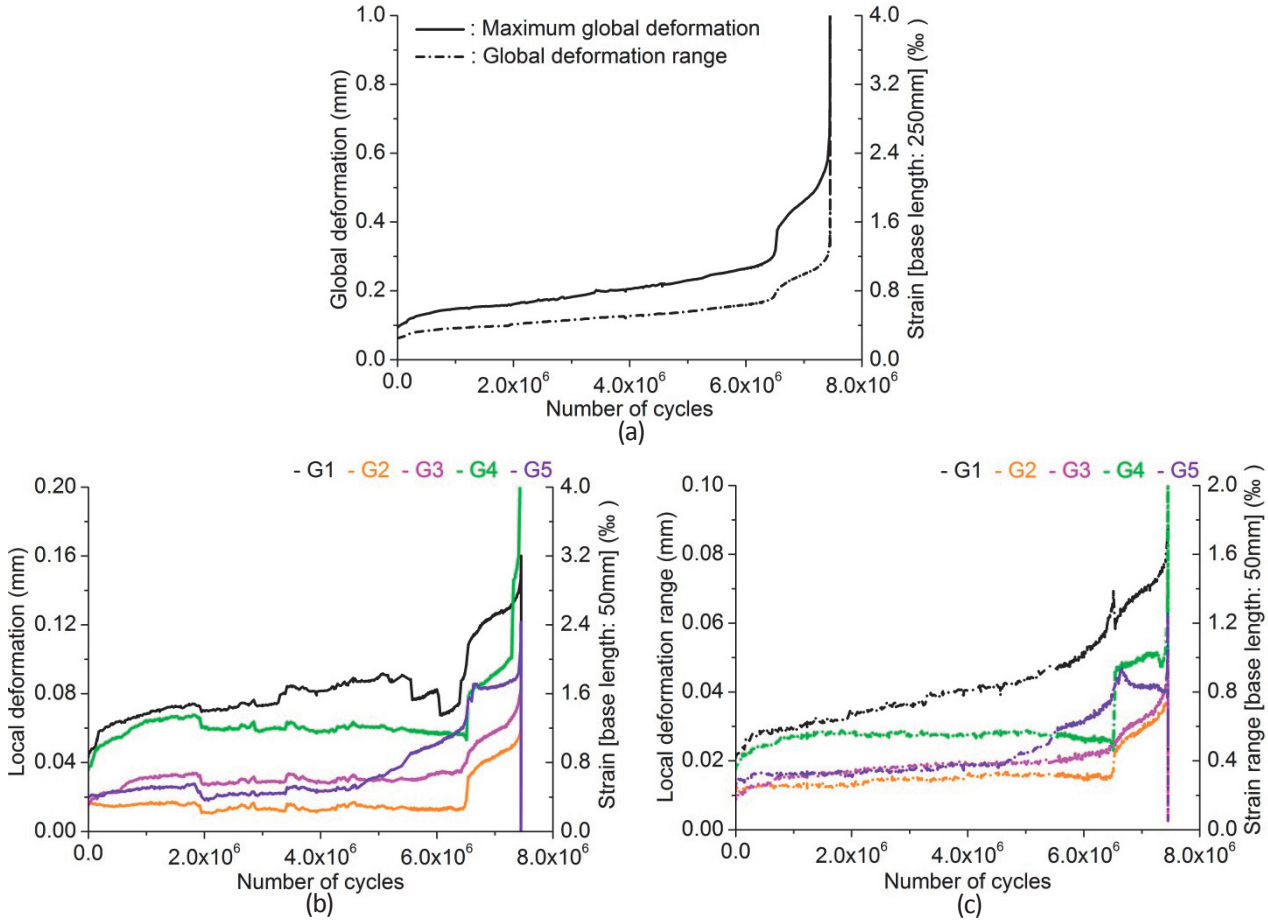


**Figure 12** Preliminary test 1-iii: growth curves of (a) maximum global deformation and global deformation range, (b) maximum local deformation and (c) local deformation range

(a)

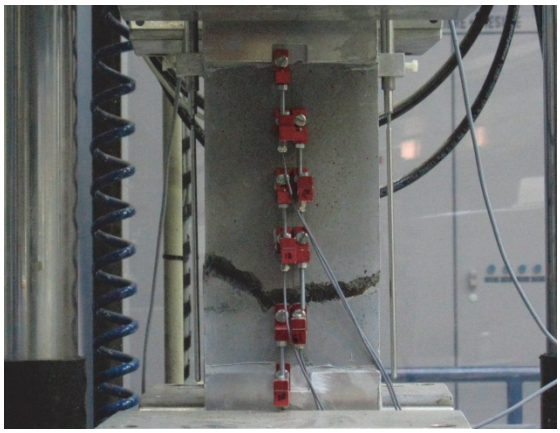

(b)

**Figure 13** (a) Macrocrack opening of 0.1 mm at about 6,519,700 cycles and (b) fractured Preliminary test 1 specimen

***Fatigue fracture surface of Preliminary test 1 specimen:***

Fatigue cracked area was smooth and covered with rust-coloured powdery products (enclosed with a line in Fig. 14). Direction of fatigue crack propagation was extrapolated from a macrocrack of 0.1 mm opening observed at about 6,519,700 cycles (Fig. 13a) and indicated with arrows in Fig. 14.

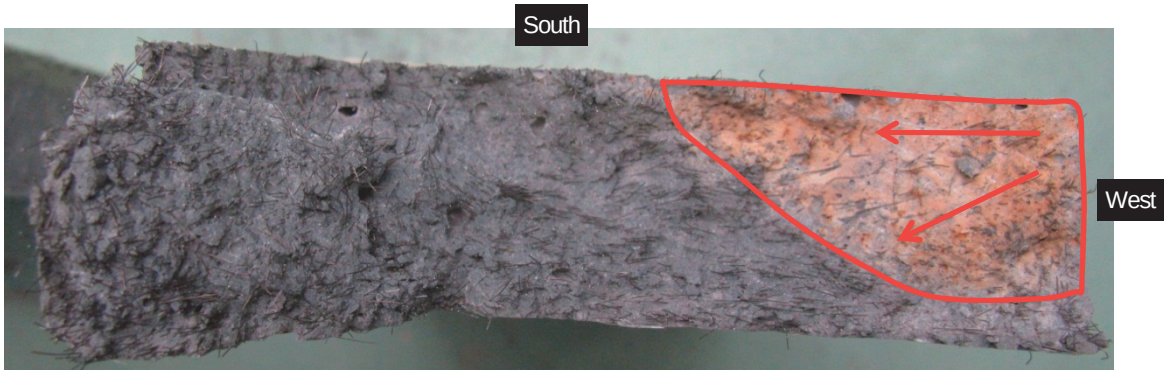


**Figure 14** Fatigue fracture surface of Preliminary test 1 specimen (lower half of the fractured specimen)

### 5.1.2 Preliminary test 2

***Test parameters and results***

| $\sigma_{max}$ [MPa] | $\sigma_{min}$ [MPa] | *N* | Deformation localisation |
|---|---|---|---|
| 8.50 | 0.82 | 145,704 | G3 zone |

Comment: Maximum fatigue stress was determined arbitrarily.

***Behaviour of Preliminary test 2 specimen***

Maximum global deformation increased slightly until about 44,200 cycles, at which redistribution of localised deformation occurred. Subsequently, growth rate of maximum global deformation increased. When maximum global strain reached 1.2 ‰, growth rate of maximum global deformation started to increase gradually, and eventually the specimen fractured. Behaviour of global deformation range was approximately similar to that of maximum global deformation, while growth rate of global deformation range was always smaller than that of maximum global deformation.

Maximum local deformation at G4 zone was excessively larger than the other local zones and increased unstably. Redistribution of localised deformation occurred at about 44,200 cycles leading to an increase of local deformation readings at G4 zone. Maximum local deformation at G3 zone started to grow at about 73,600 cycles and deformation localisation occurred at G3 zone. Behaviour of local deformation range was similar to that of maximum local deformation.

Variations were observed on local deformation readings.

Fracture crack propagated in a path inclined from horizontal axis with an angle of 15˚.

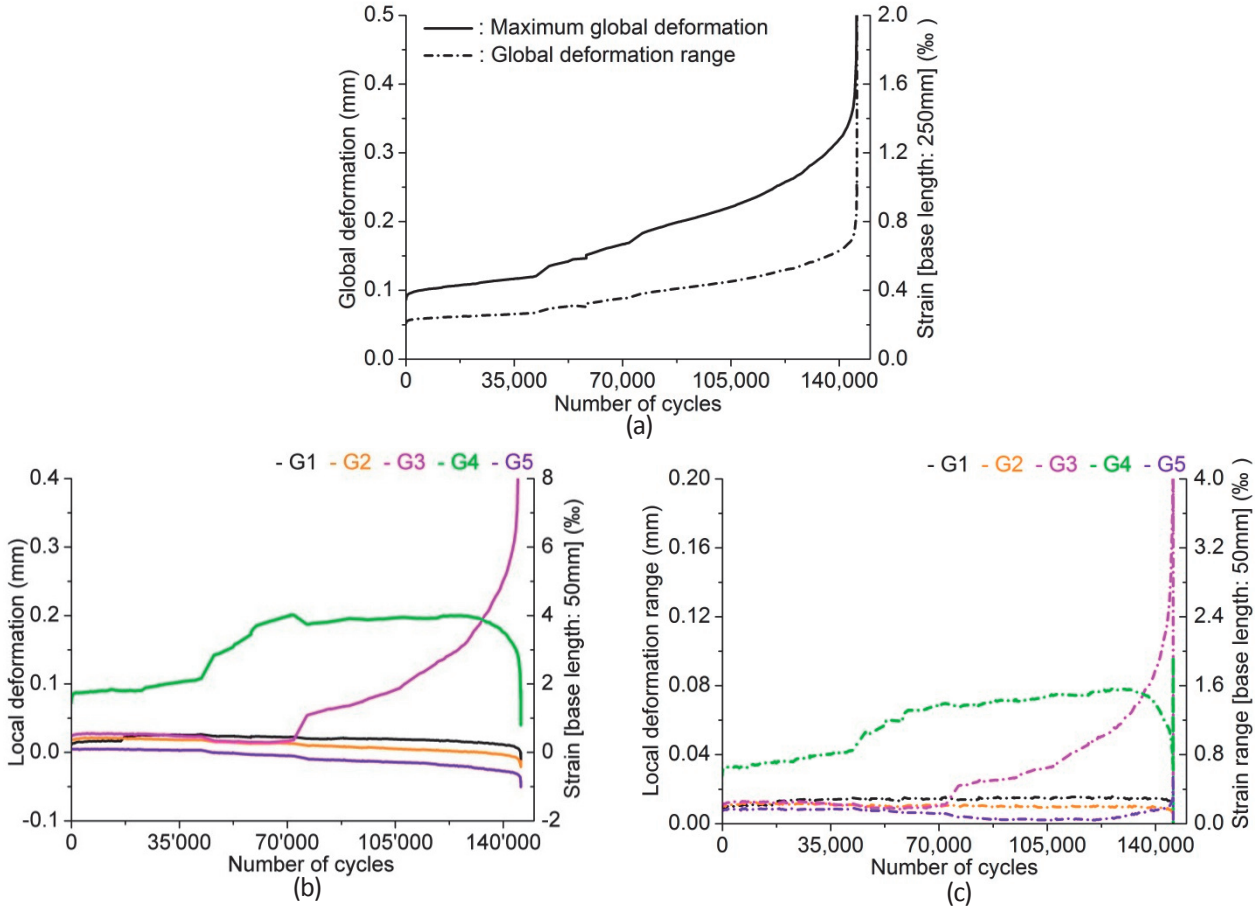


**Figure 15** Preliminary test 2: growth curves of (a) maximum global deformation and global deformation range, (b) maximum local deformation and (c) local deformation range

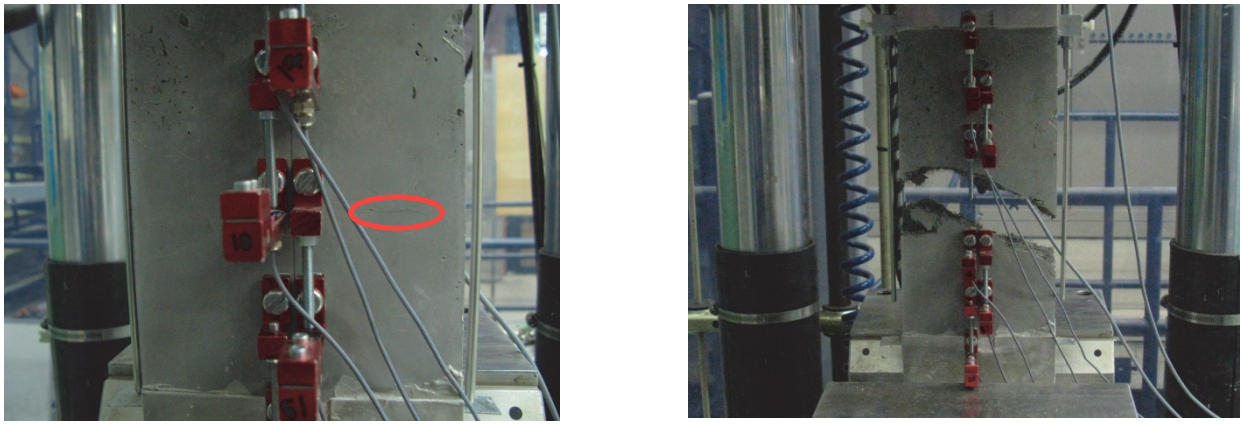

(a) (b)

**Figure 16** (a) Macrocrack opening of 0.1 mm at about 44,200 cycles and (b) fractured Preliminary test 2 specimen

***Fatigue fracture surface of Preliminary test 2 specimen:***

The whole fatigue fracture surface is rough. It is similar to the fracture surface of the specimen subjected to quasi-static tensile stress. This is because sustained number of fatigue cycles was small.


**Figure 17** Fatigue fracture surface of Preliminary test 2 specimen (lower half of the fractured specimen)

### 5.2 Results of S1 series

Table 6 lists the summary of S1 series test results.

**Table 6** Results of S1 series tensile fatigue tests of UHPFRC

| Test No. | | $\sigma_{max}$ [MPa] | $\sigma_{min}$ [MPa] | $\sigma_{max}/f_e$ | $N$ | Remarks |
|---|---|---|---|---|---|---|
| 1 | i | 5.00 | 0.82 | 0.61 | 5,000,002 | run-out |
| | ii | 6.60 | 0.82 | 0.80 | 352,358 | |
| 2 | i | 7.80 | 0.82 | 0.95 | 20,003,232 | run-out |
| | ii | 8.70 | 0.82 | 1.06 | 428,072 | |
| 3 | | 6.10 | 0.00 | 0.74 | 285,261 | |
| 4 | | 8.10 | 0.82 | 0.99 | 280,022 | |
| 5 | i | 8.20 | 0.82 | 1.00 | 10,002,698 | run-out |
| | ii | 10.80 | 0.82 | 1.32 | 61,108 | |
| 6 | | 8.20 | 0.82 | 1.00 | 288,341 | |
| 7 | | 9.40 | 0.82 | 1.15 | 157,199 | |

### 5.2.1 S1-1 test

**First fatigue test**

***Test parameters and results***

| $\sigma_{max}$ [MPa] | $\sigma_{min}$ [MPa] | *N* | Deformation localisation |
|---|---|---|---|
| 5.00 | 0.82 | 5,000,002 | run-out |

Comment: For the logistics reason, the first fatigue test was stopped at 5 million cycles. Stress causing 0.2 ‰ global strain was determined as maximum fatigue stress (Fig. 18a).

***Behaviour of S1-1 test specimen during the first fatigue test***

Maximum global deformation rapidly increased during the first 60,000 cycles, followed by modest increase. Global deformation range kept approximately constant.

Maximum local deformation and local deformation range at all local zones remained quite small.

Small variations were observed on local deformation readings.

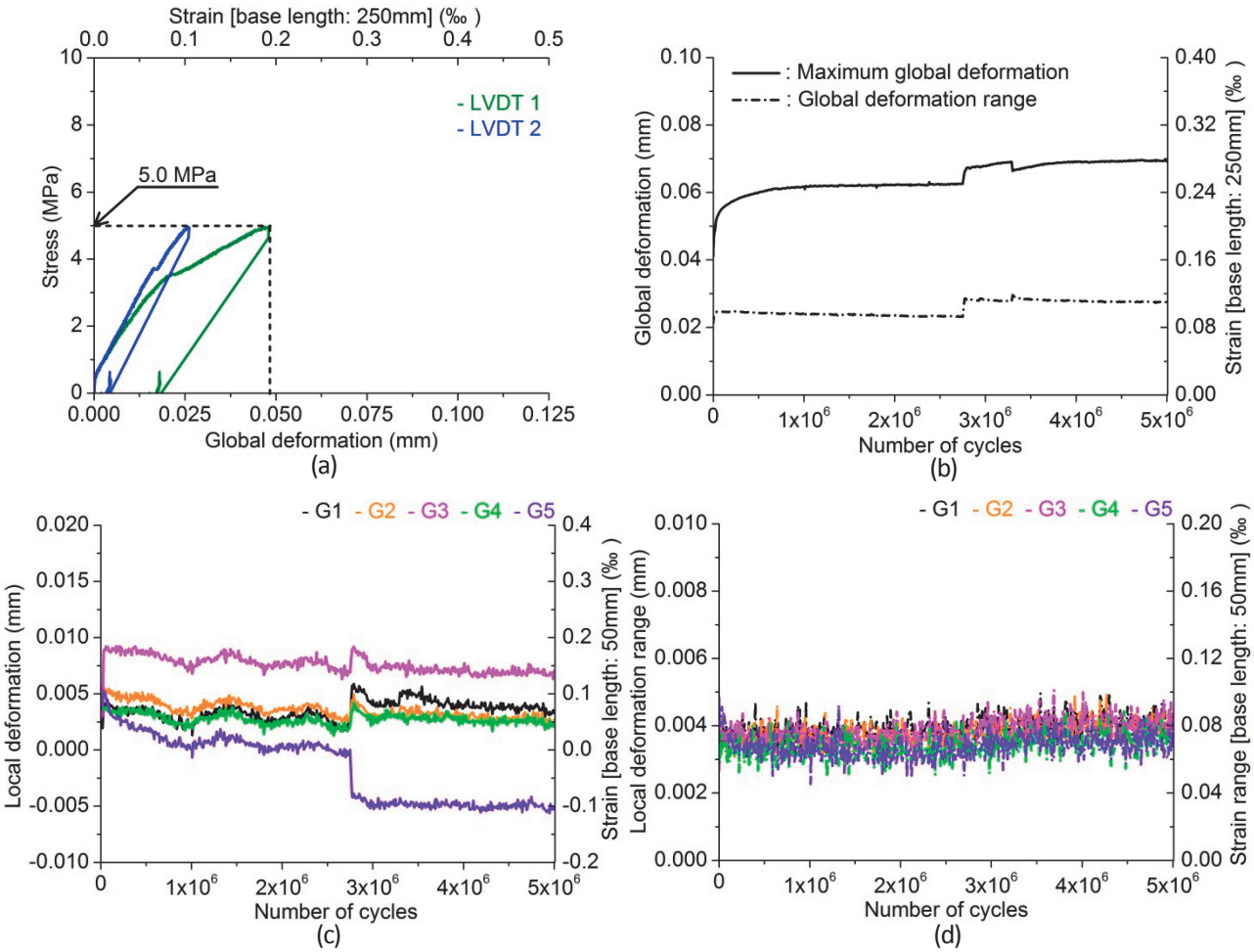


**Figure 18** S1-1_i test: (a) stress-deformation curve obtained from quasi-static tensile preloading to determine the maximum fatigue stress, growth curves of (b) maximum global deformation and global deformation range, (c) maximum local deformation and (d) local deformation range

**Second fatigue test**

***Test parameters and results***

| $\sigma_{max}$ [MPa] | $\sigma_{min}$ [MPa] | *N* | Deformation localisation |
|---|---|---|---|
| 6.60 | 0.82 | 352,358 | G5 zone |

Comment: Stress causing 0.6 ‰ global strain was determined as maximum fatigue stress (Fig. 19a).

***Behaviour of S1-1 test specimen during the second fatigue test***

Maximum global deformation grew steadily. When maximum global strain reached about 1.4 ‰ at about 330,500 cycles, redistribution of localised deformation occurred. After sustaining additional about 21,800 cycles, the specimen fractured. Behaviour of global deformation range was similar to that of maximum global deformation, while growth rate of global deformation range was always smaller than that of maximum global deformation.

Although maximum local deformation at G1 zone kept the largest among all local zones, deformation localised at G5 zone, not G1 zone. Deformation reading of G5 zone was negative (compression), which might be due to micro- and macrocracks under the base of displacement transducers until just before fracture of the specimen. Behaviour of local deformation range at all local zones except G5 zone was similar to that of maximum local deformation. Local deformation range at G5 zone decreased during the first 60,000 cycles and then started to increase.

Variations in local deformation readings became larger than the first fatigue test.

Fracture crack propagated in a path perpendicular to fatigue force direction.

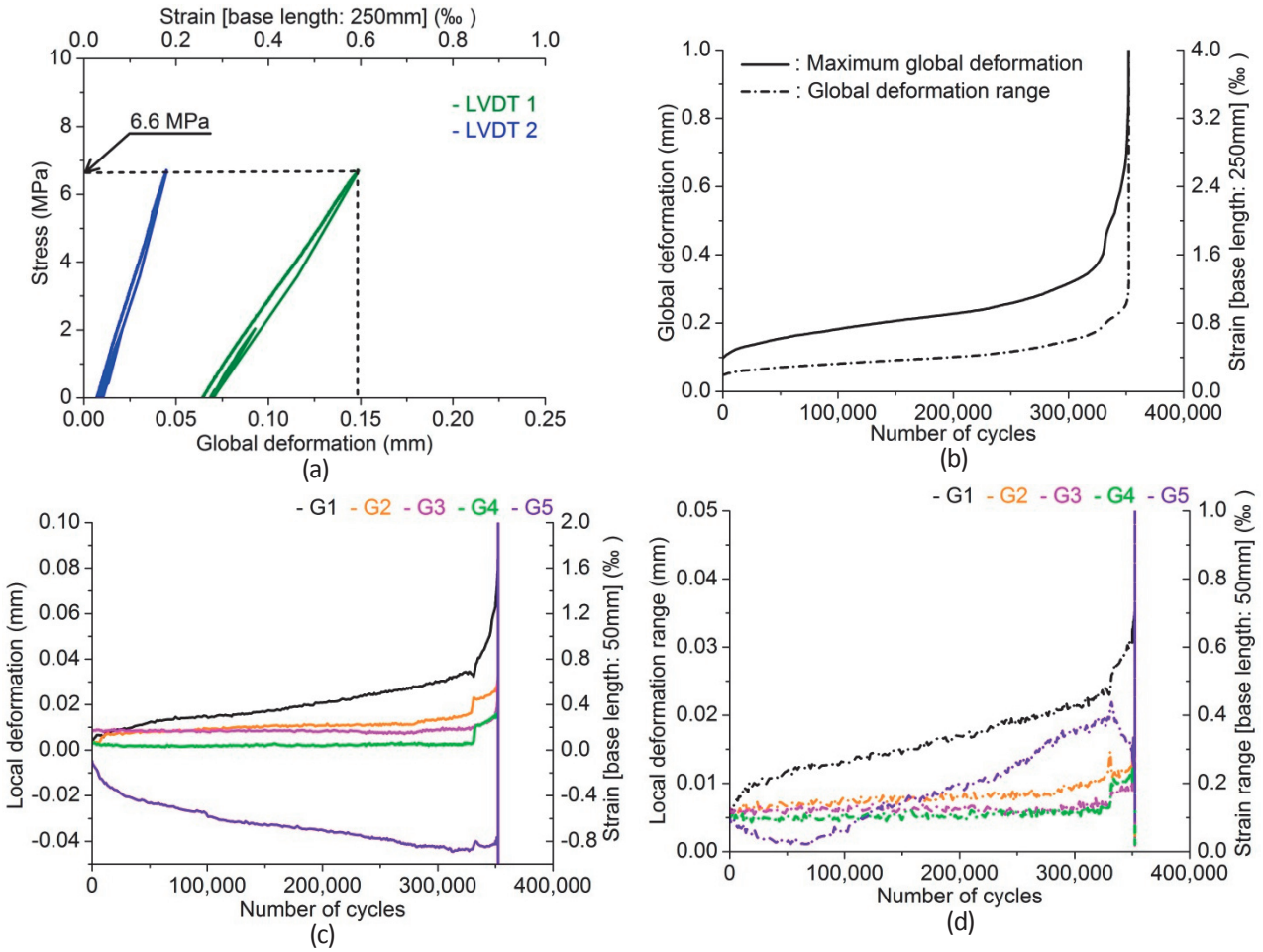


**Figure 19** S1-1_ii test: (a) stress-deformation curve obtained from quasi-static tensile preloading to determine the maximum fatigue stress, growth curves of (b) maximum global deformation and global deformation range, (c) maximum local deformation and (d) local deformation range

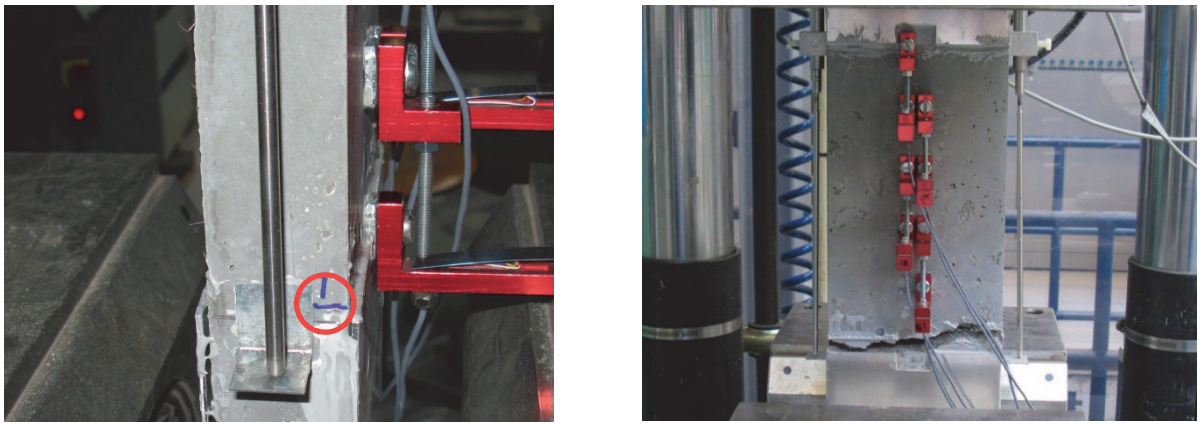

(a) (b)

**Figure 20** (a) Macrocrack opening observed during S1-1_ii test and (b) fractured S1-1 test specimen

***Fatigue fracture surface of S1-1 test specimen:***

Eastern part of the fracture surface was covered with rust-coloured powdery products and smoother than the other area (enclosed with a line in Fig. 21). That is understood as a fatigue cracked area. The fatigue fracture crack propagation started from the north-eastern corner of the fatigue cracked area (propagation direction is indicated by two arrows in Fig. 21), which was extrapolated from a macrocrack opening observed during the S1-1_ii test (Fig. 20a).

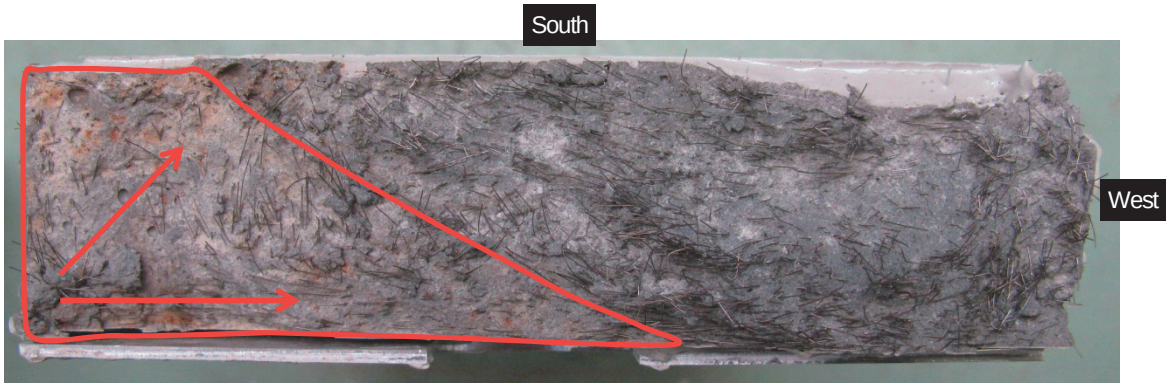


**Figure 21** Fatigue fracture surface of S1-1 test specimen (lower half of the fractured specimen)

### 5.2.2 S1-2 test

**First fatigue test**

***Test parameters and results***

| $\sigma_{max}$ [MPa] | $\sigma_{min}$ [MPa] | $N$ | Deformation localisation |
|---|---|---|---|
| 7.80 | 0.82 | 20,003,232 | run-out |

Comment: Stress causing 0.2 ‰ global strain was determined as maximum fatigue stress (Fig. 22a).

***Behaviour of S1-2 test specimen during the first fatigue test***

After rapid growth during the first 2 million cycles, maximum global deformation grew with smaller growth rate. Global deformation range also rapidly increased during the first 2 million cycles, followed by modest increase with smaller growth rate than maximum global deformation.

Maximum local deformation at G1 zone gradually increased. At about 9,166,400 cycles, redistribution of localised deformation occurred at G1 zone and maximum local deformation at G1 zone rose by about 0.2 mm suddenly, after which growth rate of maximum local deformation at G1 zone became smaller than before. Maximum local deformation at the other local zones kept approximately constant or slightly increased. Although rather unstable, behaviour of local deformation range was approximately similar to that of maximum local deformation.

Variations were observed on local deformation readings.

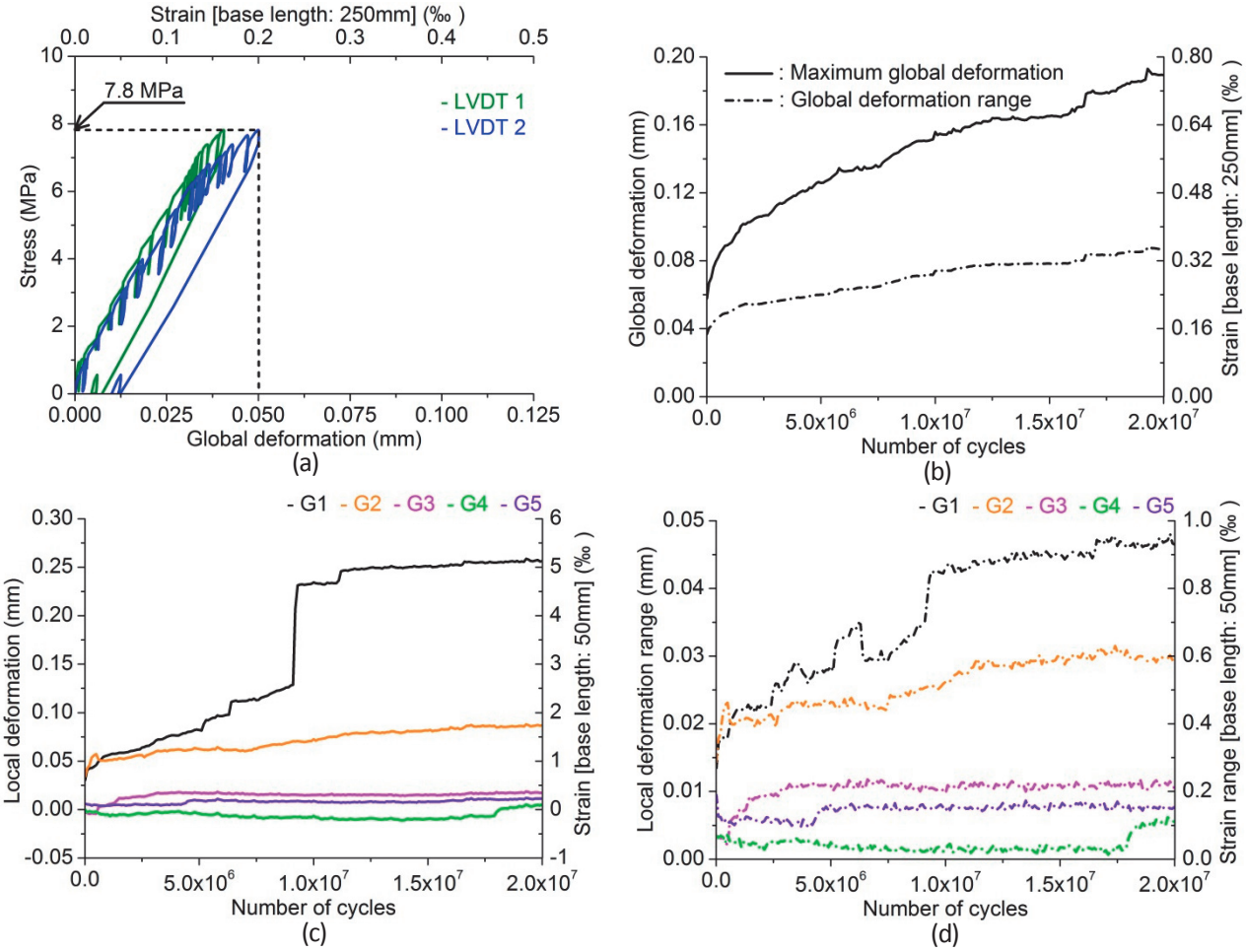


**Figure 22** S1-2_i test: (a) stress-deformation curve obtained from quasi-static tensile preloading to determine the maximum fatigue stress, growth curves of (b) maximum global deformation and global deformation range, (c) maximum local deformation and (d) local deformation range

**Second fatigue test**

***Test parameters and results***

| $\sigma_{max}$ [MPa] | $\sigma_{min}$ [MPa] | *N* | Deformation localisation |
|---|---|---|---|
| 8.70 | 0.82 | 428,072 | G2 zone |

Comment: Stress causing 1.0 ‰ global strain was determined as maximum fatigue stress (Fig. 23a).

***Behaviour of S1-2 test specimen during the second fatigue test***

Maximum global deformation gradually increased and redistribution of localised deformation occurred at about 274,300 cycles, causing maximum global deformation to rise by about 0.1 mm suddenly. After that, growth rate of maximum global deformation increased, and when maximum global strain reached about 2.6 ‰, the growth rate started to increase gradually and eventually the specimen fractured.

Maximum local deformation at all local zones gradually increased. When redistribution of localised deformation occurred at about 274,300 cycles, maximum local deformation at G2 and G3 zone rose by about 0.15 mm suddenly. After that, growth rate of maximum local deformation at G2 zone gradually increased and eventually deformation localisation occurred at G2 zone, while growth rate of maximum local deformation at G3 zone decreased. As for local deformation range, sudden rise of its reading was caused at G1 and G2 zone when redistribution of localised deformation occurred, except which behaviour of local deformation range was generally similar to that of maximum local deformation.

Variations remained on local deformation readings.

Fracture crack propagated in a path inclined from horizontal axis with an angle of 10˚.

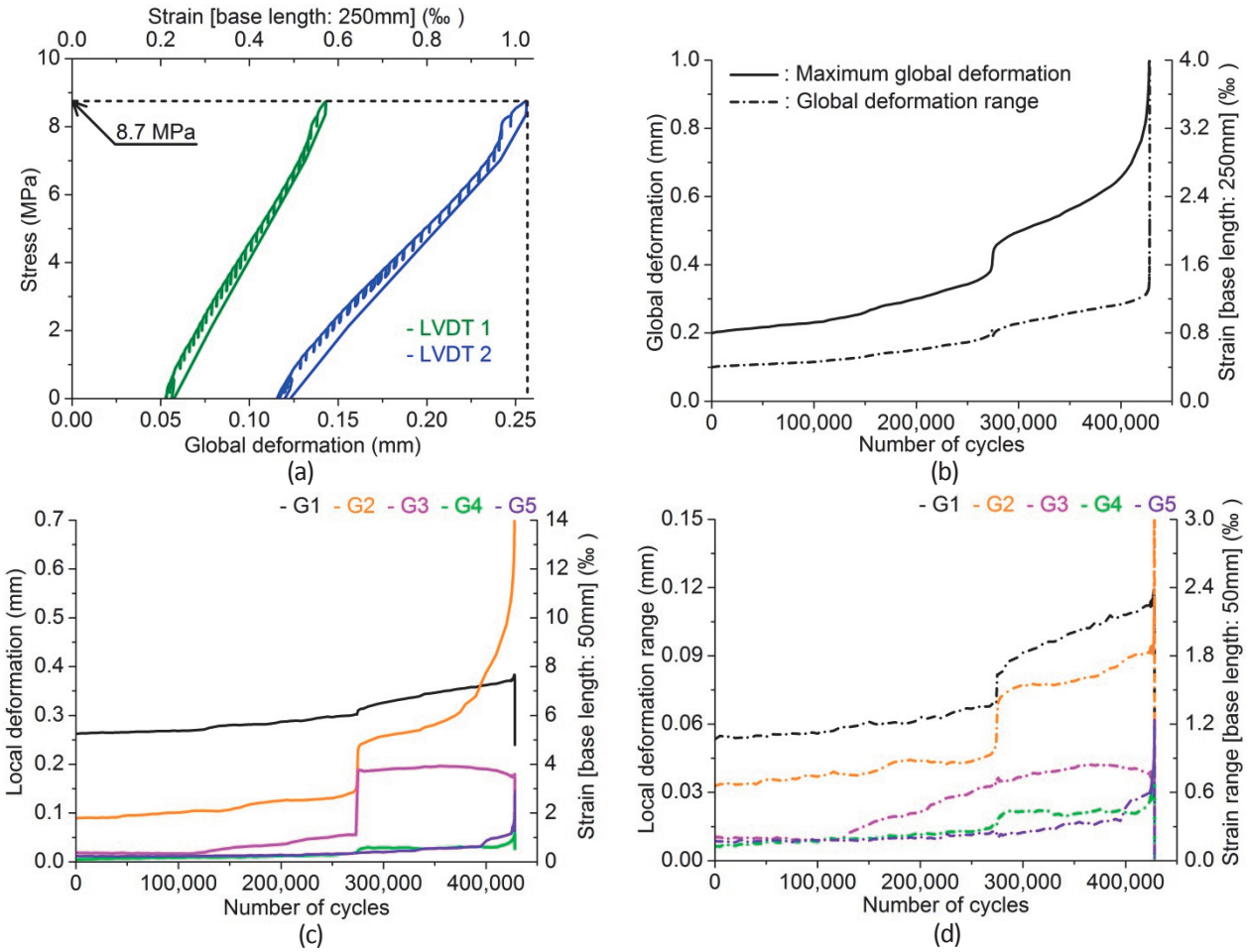


**Figure 23** S1-2_ii test: (a) stress-deformation curve obtained from quasi-static tensile preloading to determine the maximum fatigue stress, growth curves of (b) maximum global deformation and global deformation range, (c) maximum local deformation and (d) local deformation range

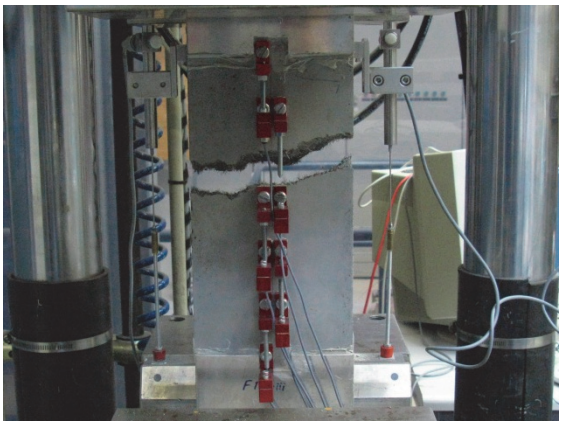

**Figure 24** Fractured S1-2 test specimen

***Fatigue fracture surface of S1-2 test specimen:***

At the south-western corner of the fatigue fracture surface, the area void of fibres covered with rust-coloured powdery products was observed (enclosed with a line in Fig. 25). That is understood as fatigue cracked area. Extrapolated direction of fatigue fracture crack propagation is indicated with an arrow in Fig. 25.


**Figure 25** Fatigue fracture surface of S1-2 test specimen (upper half of the fractured specimen)

### 5.2.3 S1-3 test

***Test parameters and results***

| $\sigma_{max}$ [MPa] | $\sigma_{min}$ [MPa] | *N* | Deformation localisation |
|---|---|---|---|
| 6.10 | 0.00 | 285,261 | G5 zone |

Comment: Stress causing 0.20 ‰ global strain was determined as maximum fatigue stress (Fig. 26a). Due to programing mistake of testing machine, minimum fatigue stress was set to be 0.00 MPa.

***Behaviour of S1-3 test specimen***

Maximum global deformation increased slightly. At about 44,100 cycles, maximum global deformation suddenly rose by about 0.02 mm, after which maximum global deformation continued to increase with slightly higher growth rate than before. When maximum global strain reached about 0.8 ‰, its growth rate started to increase and eventually the specimen fractured. Behaviour of global deformation range was similar to that of maximum global deformation, while its growth rate was smaller than growth rate of maximum global deformation.

Only maximum local deformation at G5 zone increased. Its behaviour was similar to the behaviour of maximum global deformation. Deformation localisation occurred at G5 zone. Behaviour of local deformation range was almost identical to that of maximum local deformation.

Local deformation readings at all local zones except G5 zone was approximately the same.

Fracture crack propagated in a path approximately perpendicular to fatigue force direction.

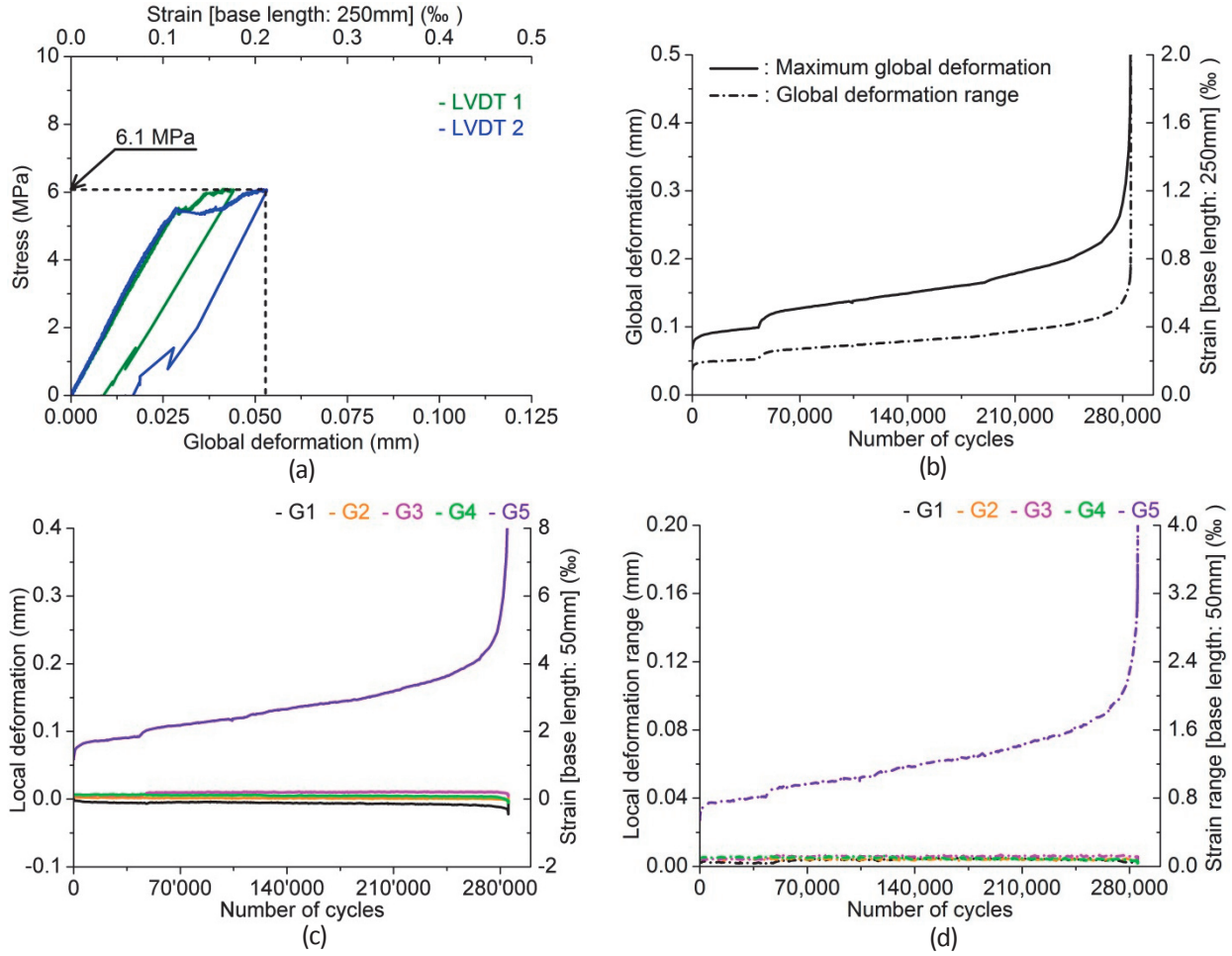


**Figure 26** S1-3 test: (a) stress-deformation curve obtained from quasi-static tensile preloading to determine the maximum fatigue stress, growth curves of (b) maximum global deformation and global deformation range, (c) maximum local deformation and (d) local deformation range

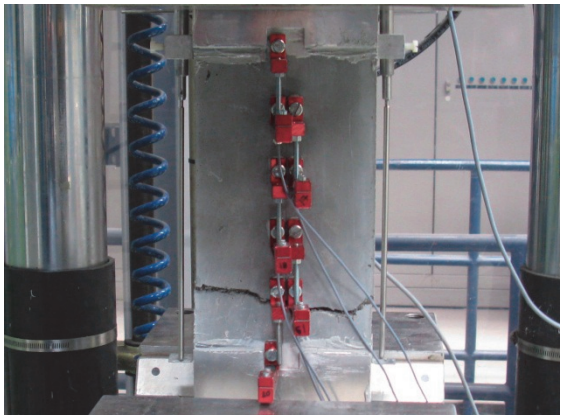

**Figure 27** Fractured S1-3 test specimen

***Fatigue fracture surface of S1-3 test specimen:***

Although large macrocrack opening wasn't observed during the fatigue test, an area at north-west part of the fracture surface seemed to be subjected to repeating crack open and closure movements (enclosed with a line in Fig. 28) because rust-coloured products were observed around the steel fibres in the area.


**Figure 28** Fatigue fracture surface of S1-3 test specimen (lower half of the fractured specimen)

### 5.2.4 S1-4 test

***Test parameters and results***

| $\sigma_{max}$ [MPa] | $\sigma_{min}$ [MPa] | $N$ | Deformation localisation |
|---|---|---|---|
| 8.10 | 0.82 | 280,022 | G1 zone |

Comment: Stress causing 0.25 ‰ global strain was determined as maximum fatigue stress (Fig. 29a).

***Behaviour of S1-4 test specimen***

Maximum global deformation rapidly increased until about 25,000 cycles, followed by steady increase with smaller growth rate. When maximum global strain reached about 1.1 ‰, its growth rate started to increase and eventually the specimen fractured. Behaviour of global deformation range was similar to that of maximum global deformation, while its growth rate was smaller than growth rate of maximum global deformation.

In the beginning of the test, maximum local deformation at all local zones was quite small. At about 57,500 cycles, maximum local deformation at G1 zone suddenly rose by about 0.2 mm and then started to increase. Eventually, deformation localised at G1 zone, while UHPFRC at the other local zones softened. Behaviour of local deformation range was quite similar to that of maximum local deformation.

Local deformation readings at all local zones except G1 zone was approximately the same.

Fracture crack propagated in a path approximately perpendicular to fatigue force direction.

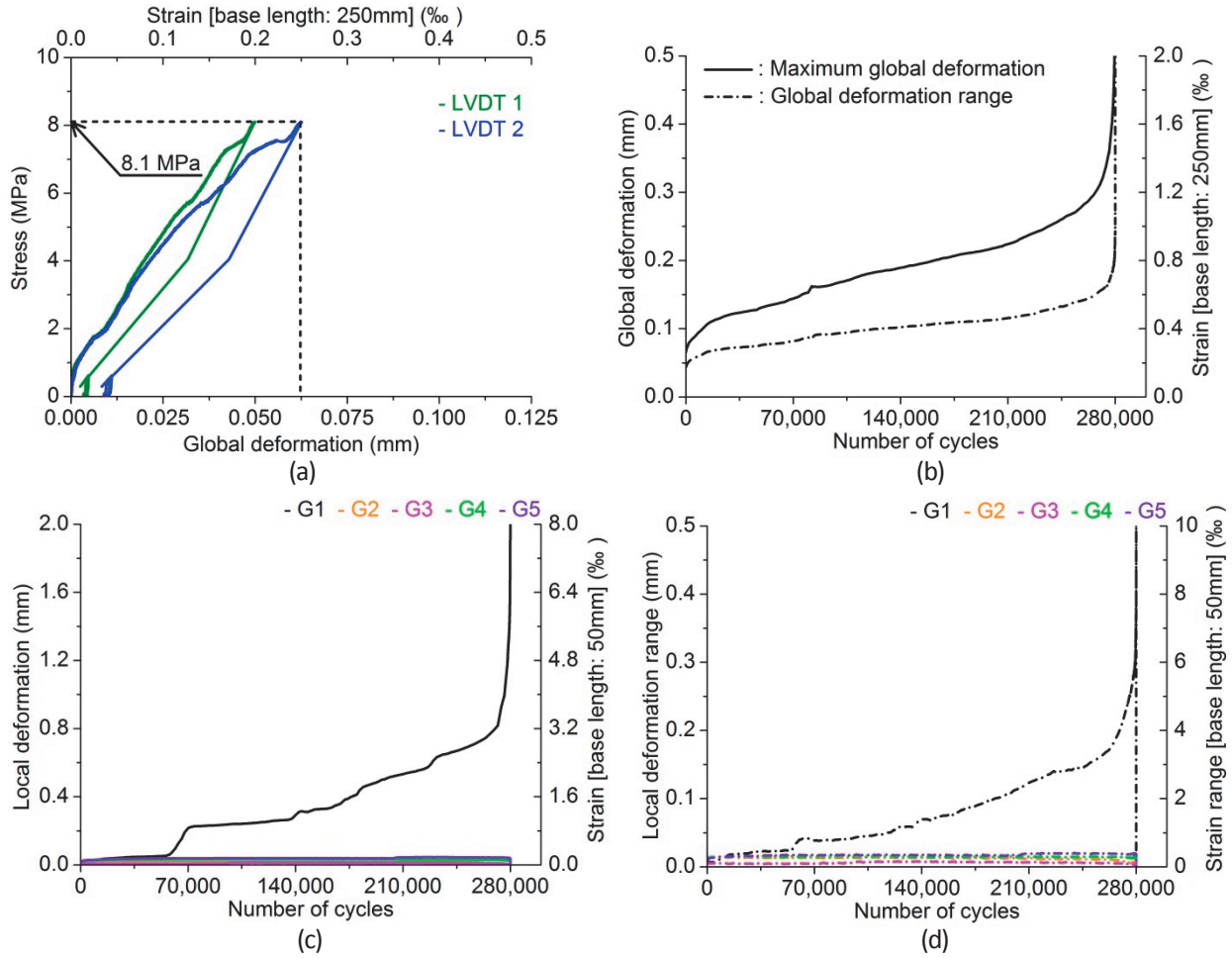


**Figure 29** S1-4 test: (a) stress-deformation curve obtained from quasi-static tensile preloading to determine the maximum fatigue stress, growth curves of (b) maximum global deformation and global deformation range, (c) maximum local deformation and (d) local deformation range

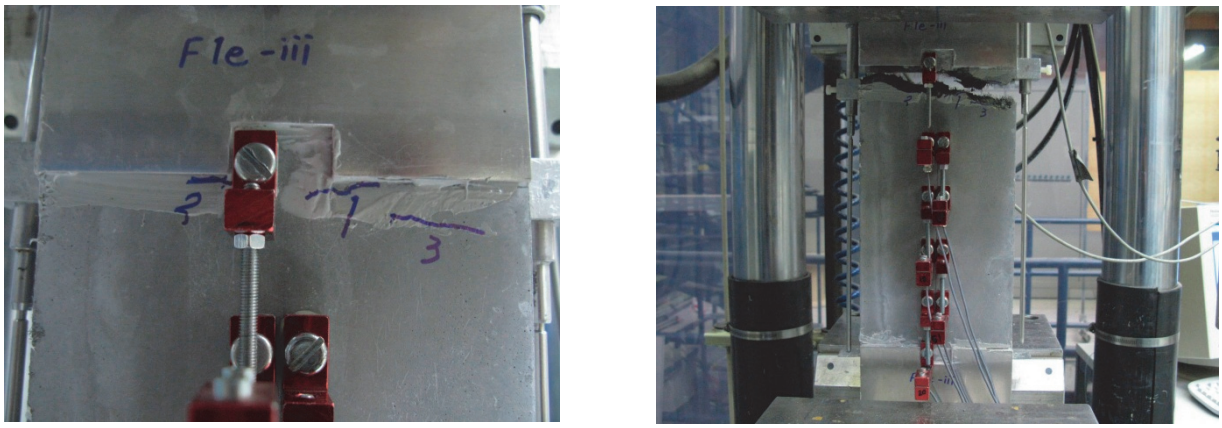


(a) (b)

**Figure 30** (a) macrocrack opening during S1-4 test and (b) fractured S1-4 test specimen

***Fatigue fracture surface of S1-4 test specimen:***

Fatigue cracked area was identified by the smooth surface and rust-coloured products (enclosed with a line in Fig. 31). Extrapolated direction of the fatigue fracture crack propagation is indicated with an arrow in Fig. 31.

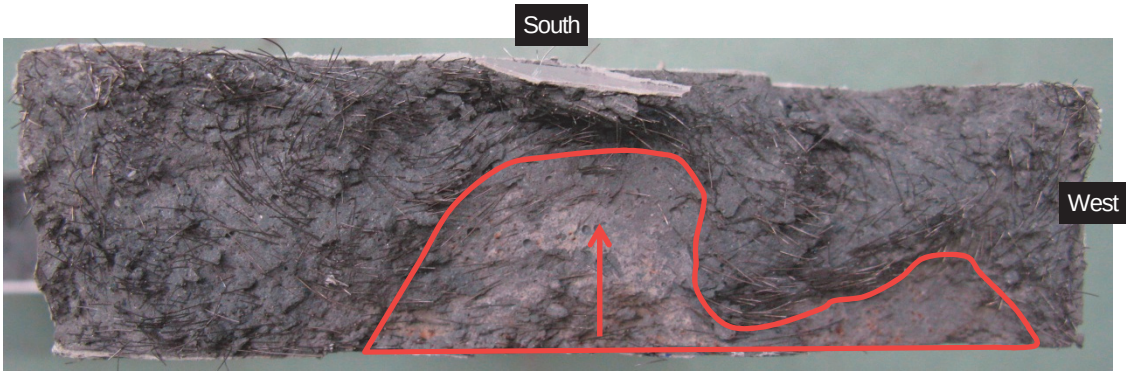


**Figure 31** Fatigue fracture surface of S1-4 test specimen (lower half of the fractured specimen)

### 5.2.5 S1-5 test

**First fatigue test**

***Test parameters and results***

| $\sigma_{max}$ [MPa] | $\sigma_{min}$ [MPa] | $N$ | Deformation localisation |
|---|---|---|---|
| 8.20 | 0.82 | 10,002,698 | run-out |

Comment: Stress causing 0.25 ‰ global strain was determined as maximum fatigue stress (Fig. 32a).

***Behaviour of S1-5 test specimen during the first fatigue test***

Maximum global deformation rapidly increased during the first 1 million cycles and then kept approximately constant. Global deformation range kept almost constant.

Maximum local deformation and local deformation range at all local zones increased slightly and those readings remained quite small.

Variations were observed on local deformation readings.

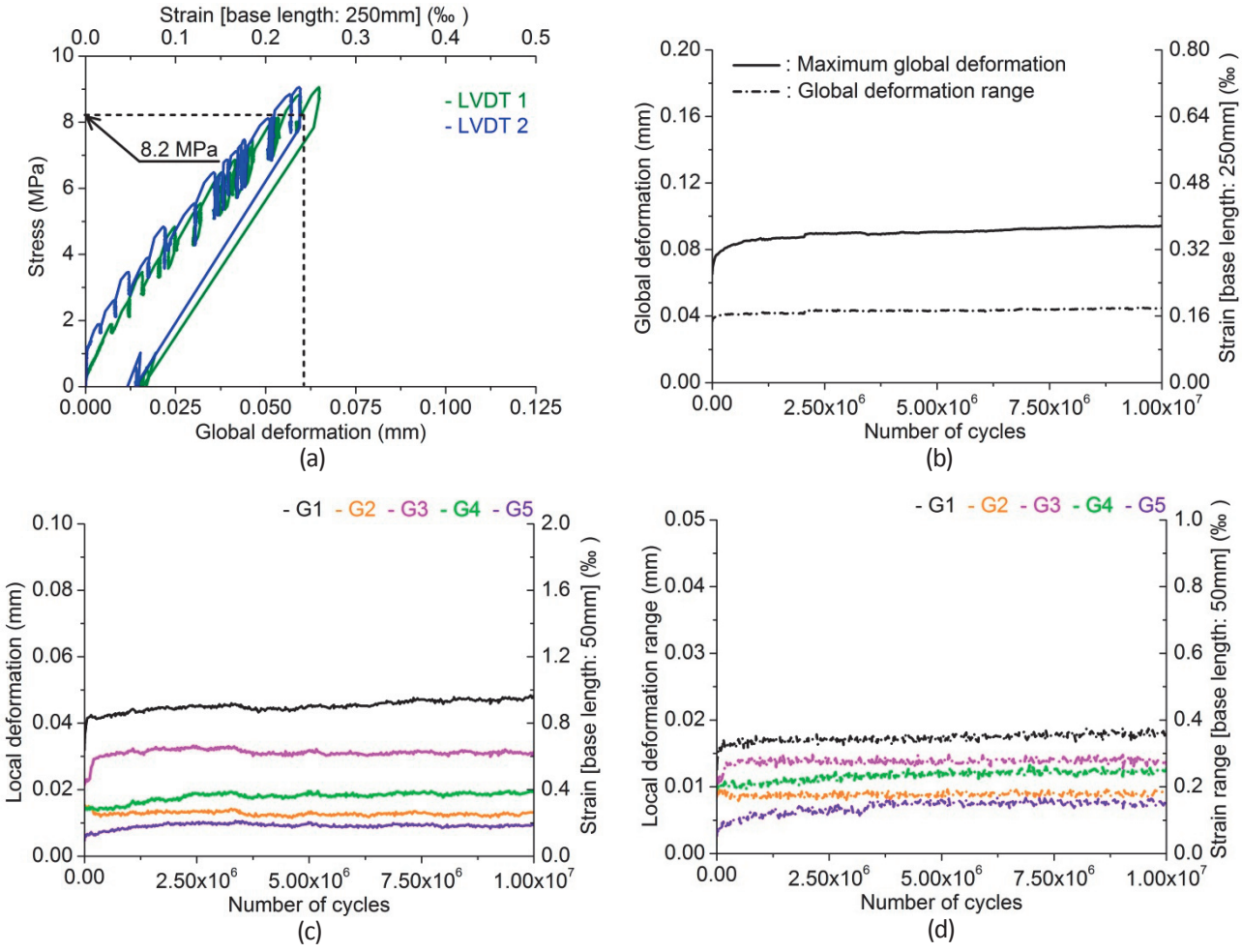


**Figure 32** S1-5_i test: (a) stress-deformation curve obtained from quasi-static tensile preloading to determine the maximum fatigue stress, growth curves of (b) maximum global deformation and global deformation range, (c) maximum local deformation and (d) local deformation range

**Second fatigue test**

***Test parameters and results***

| $\sigma_{max}$ [MPa] | $\sigma_{min}$ [MPa] | *N* | Deformation localisation |
|---|---|---|---|
| 10.80 | 0.82 MPa | 61,108 | G4 zone |

Comment: Stress causing 0.5 ‰ global strain was determined as maximum fatigue stress (Fig. 33a).

***Behaviour of S1-5 test specimen during the second fatigue test***

Maximum global deformation rapidly increased during the early stage of the test, and at about 8,700 cycles, redistribution of localised deformation occurred. Maximum global deformation increased with lower growth rate than before, and when maximum global deformation reached about 4.2 ‰, its growth rate started to increase and eventually the specimen fractured. Global deformation range showed similar behaviour to maximum global deformation, while its growth rate was smaller than growth rate of maximum global deformation.

Maximum local deformation at G3 to G5 zones rapidly increased during the early stage of the test, and after redistribution of localised deformation at G4 zone, those growth rates became smaller than before. Local maximum deformation at G1 and G2 zones constantly increased. Deformation localised at G4 zone whose maximum deformation reading was the largest, while UHPFRC at the other local zones softened. Behaviour of local deformation range was similar to that of maximum local deformation.

Variations were left on local deformation readings.

Fracture crack propagated in a path inclined from horizontal axis with an angle of 20˚.

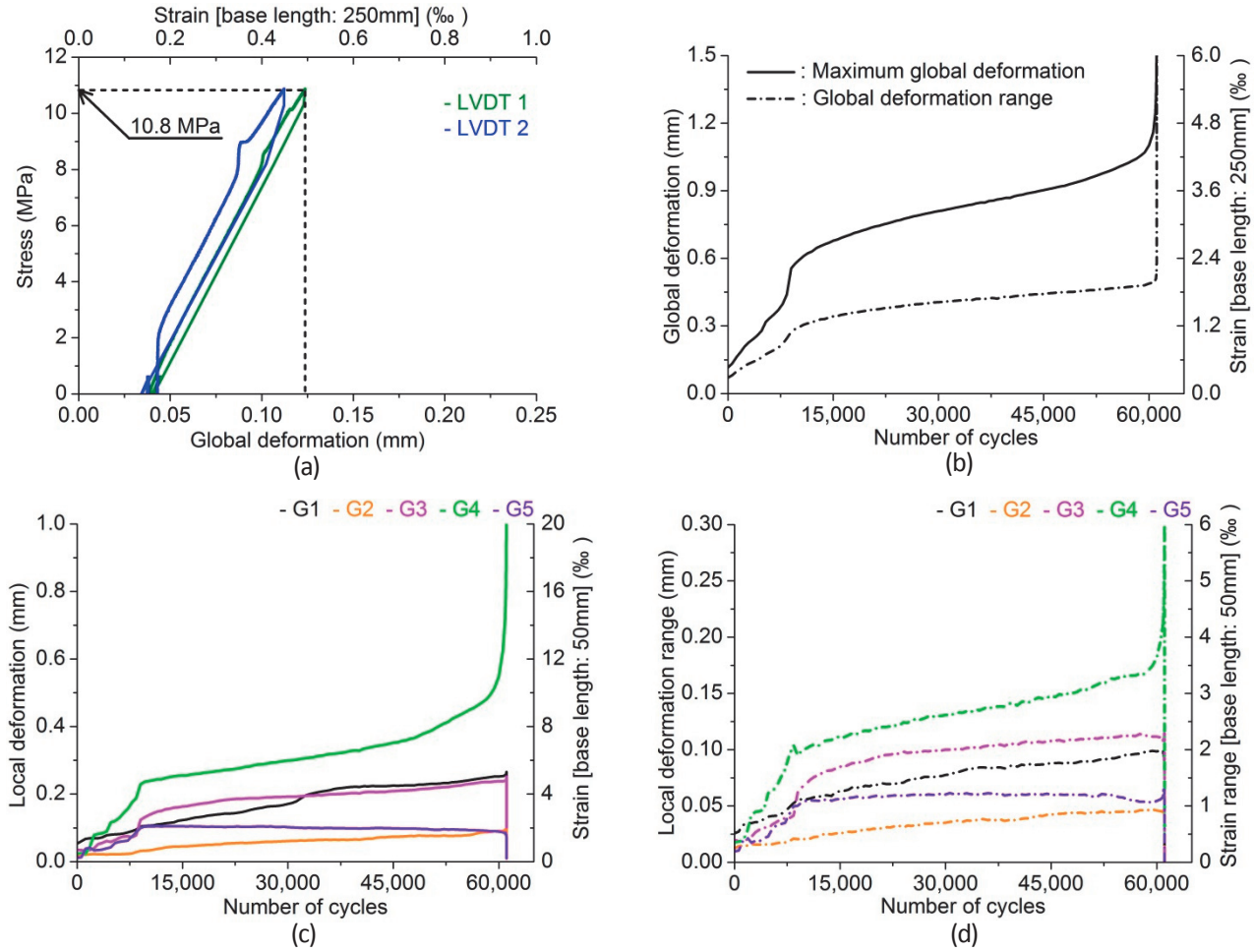


**Figure 33** S1-5_ii test: (a) stress-deformation curve obtained from quasi-static tensile preloading to determine the maximum fatigue stress, growth curves of (b) maximum global deformation and global deformation range, (c) maximum local deformation and (d) local deformation range

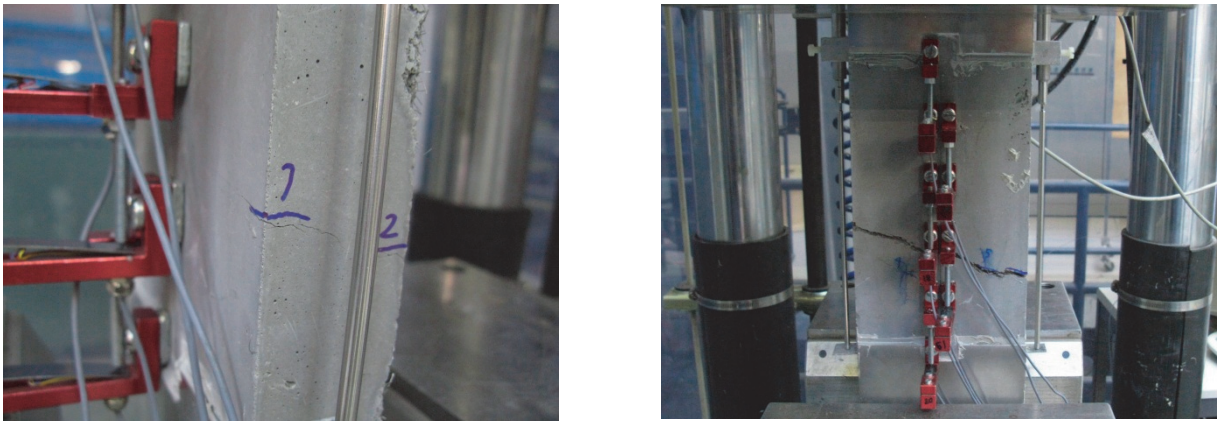


(a) (b)

**Figure 34** (a) Macrocrack opening during S1-5_ii test and (b) fractured S1-5 test specimen

***Fatigue fracture surface of S1-5 test specimen:***

Fatigue cracked area was identified by rust-coloured powdery products on the western corner of the fracture surface (enclosed with a line in Fig. 35). Extrapolated direction of the fatigue fracture crack propagation is indicated with an arrow in Fig. 35.


**Figure 35** Fatigue fracture surface of S1-5 test specimen (lower half of the fractured specimen)

### 5.2.6 S1-6 test

***Test parameters and results***

| $\sigma_{max}$ [MPa] | $\sigma_{min}$ [MPa] | $N$ | Deformation localisation |
|---|---|---|---|
| 9.40 | 0.82 | 157,199 | G3 zone |

Comment: Stress causing 0.30 ‰ global strain was determined as maximum fatigue stress (Fig. 36a).

***Behaviour of S1-6 test specimen***

Maximum global deformation rapidly increased during the early stage of the test, and at about 26,300 cycles, redistribution of localised deformation occurred. Maximum global deformation increased with lower growth rate than before, and when maximum global deformation reached about 2.8 ‰, its growth rate started to increase and eventually the specimen fractured. Global deformation range showed similar behaviour to maximum global deformation, while its growth rate was smaller than growth rate of maximum global deformation.

Maximum local deformation at G2, G3 and G5 zones rapidly increased during the early stage of the test. When redistribution of localised deformation occurred at G2 zone at about 26,300 cycles, maximum local deformation at G1, G2 and G4 zones suddenly rose. After that, growth rate of maximum deformation of all local zones became lower than before. Although maximum local deformation at G3 zone was the third largest among all local zones after redistribution of localised deformation, deformation localised at G3 zone. Behaviour of local deformation range was similar to that of maximum local deformation. Significant variations were observed on local deformation readings.

Fracture crack propagated in a path approximately perpendicular to fatigue force direction.

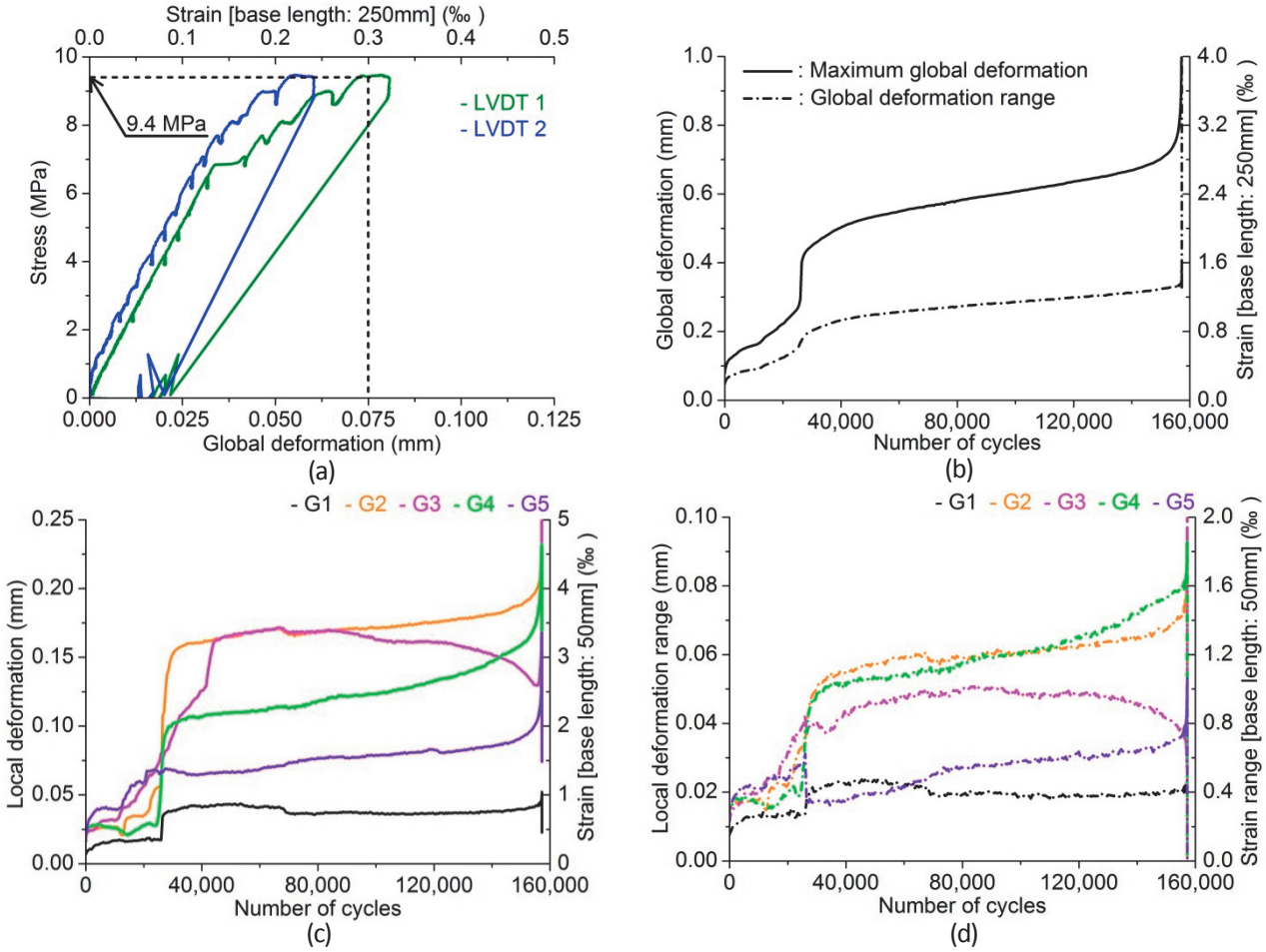


**Figure 36** S1-6 test: (a) stress-deformation curve obtained from quasi-static tensile preloading to determine the maximum fatigue stress, growth curves of (b) maximum global deformation and global deformation range, (c) maximum local deformation and (d) local deformation range

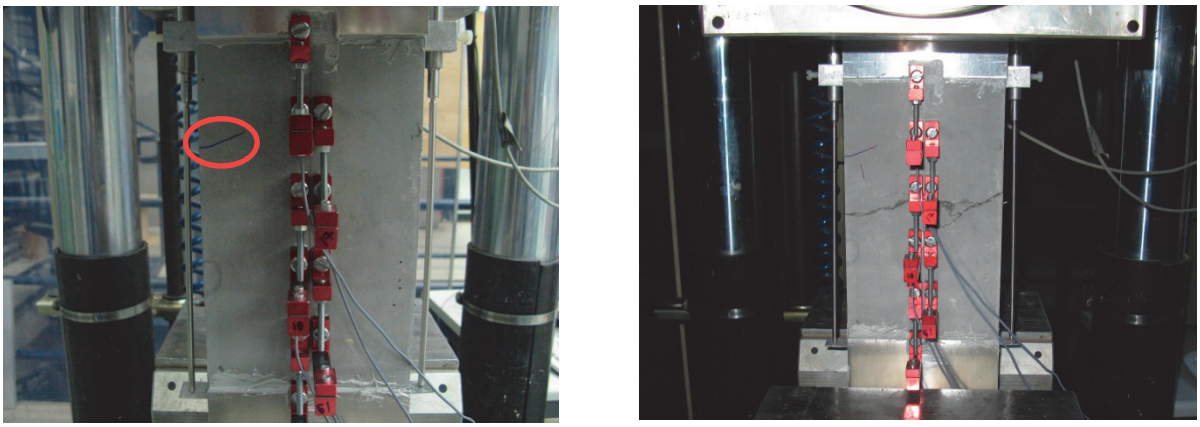

(a) (b)

**Figure 37** (a) Macrocrack opening during S1-6 test and (b) fractured S1-6 test specimen

***Fatigue fracture surface of S1-6 test specimen:***

Two separated areas void of fibres were observed on the fracture surface (enclosed with a lines in Fig. 38). One of the areas was covered with rust-coloured powdery products. The other area might have had few fibres initially. Propagation direction of the fatigue fracture crack wasn't understood.

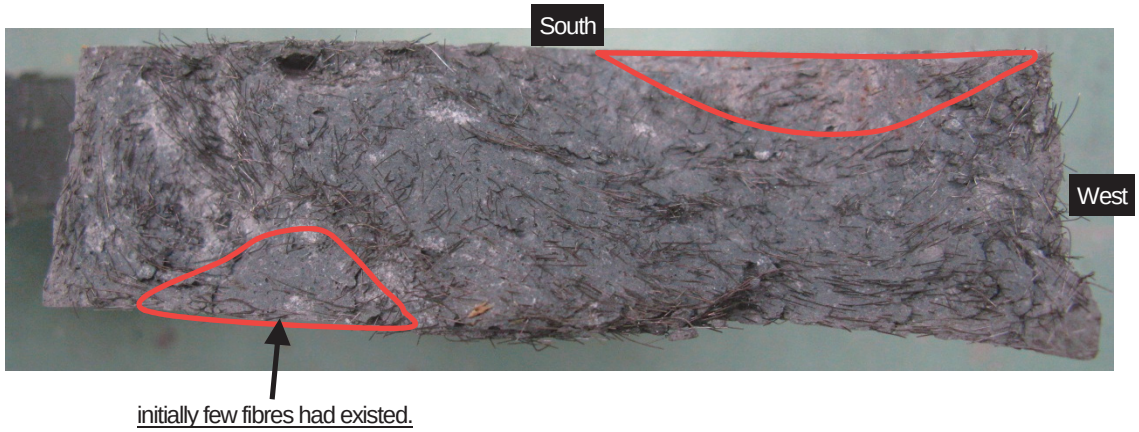


**Figure 38** Fatigue fracture surface of S1-6 test specimen (lower half of the fractured specimen)

### 5.2.7 S1-7 test

***Test parameters and results***

| $\sigma_{max}$ [MPa] | $\sigma_{min}$ [MPa] | *N* | Deformation localisation |
|---|---|---|---|
| 8.20 | 0.82 | 288,341 | G4 zone |

Comment: Stress causing 0.30 ‰ global strain was determined as maximum fatigue stress (Fig. 39a).

***Behaviour of S1-7 test specimen***

Maximum global deformation steadily increased. When maximum global strain reached about 1.5 ‰, its growth rate started to increase and eventually the specimen fractured. Behaviour of global deformation range was similar to that of maximum global deformation, while its growth rate was smaller than growth rate of maximum global deformation.

Maximum local deformation at G4 zone rapidly increased during the first 20,000 cycles and became excessively larger than the other local zones. It continued to increase and eventually deformation localised at G4 zone. Maximum local deformation at G1 and G3 zones slightly increased, while maximum local deformation at G2 and G5 zones kept approximately constant. Behaviour of local deformation range was quite similar to that of maximum local deformation.

Small variations were observed on local deformation readings.

Fracture crack propagated in a path approximately perpendicular to fatigue force direction.

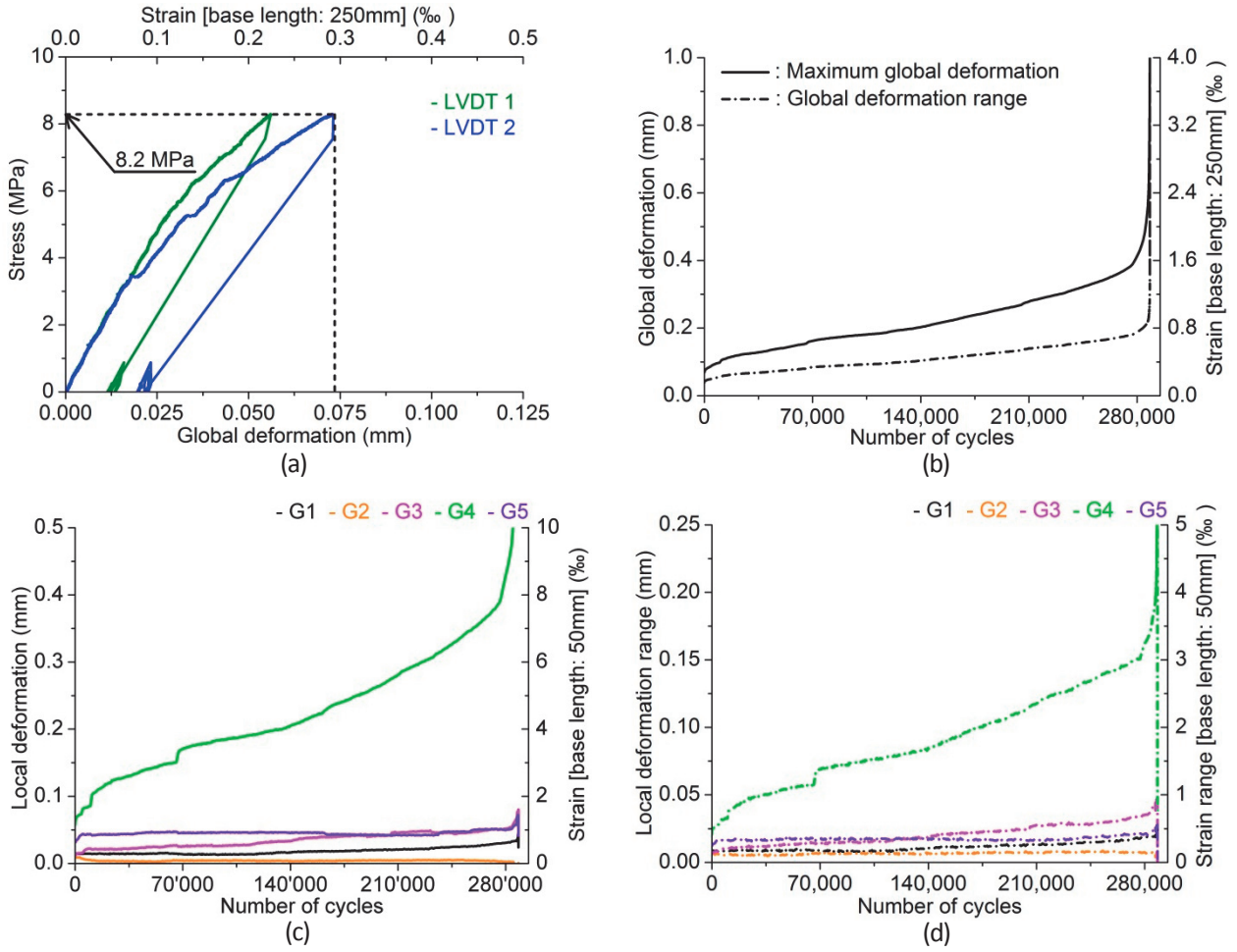


**Figure 39** S1-7 test: (a) stress-deformation curve obtained from quasi-static tensile preloading to determine the maximum fatigue stress, growth curves of (b) maximum global deformation and global deformation range, (c) maximum local deformation and (d) local deformation range

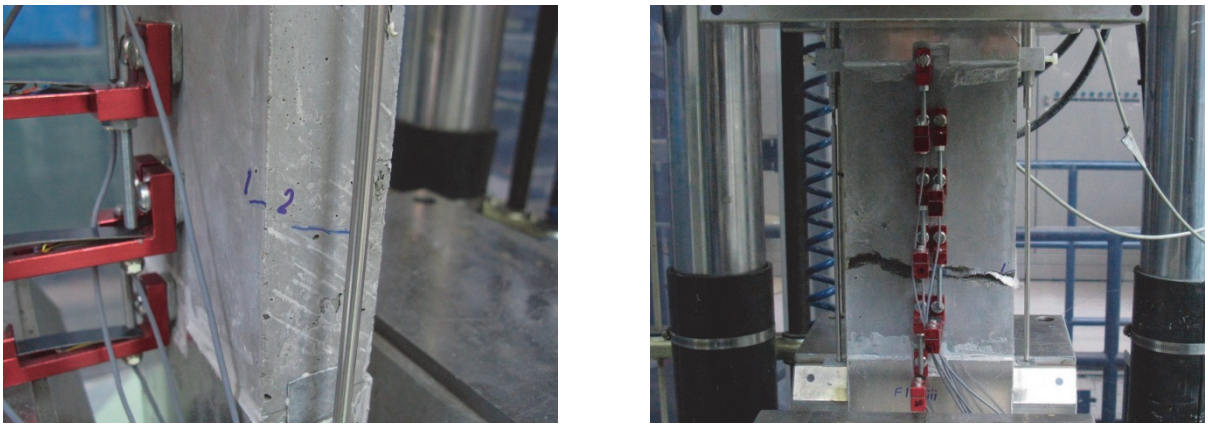

(a) (b)

**Figure 40** (a) Macrocrack openings during S1-7 test and (b) fractured S1-7 test specimen

***Fatigue fracture surface of S1-7 test specimen:***

Two separated areas void of fibres were observed on the fracture surface (enclosed with lines in Fig. 41). One of the areas was covered with rust-coloured powdery products. The other area might have few fibres initially. Propagation direction of the fatigue fracture crack was extrapolated from the macrocrack openings during the fatigue test (Fig. 40a) and indicated with two arrows in Fig. 41.


**Figure 41** Fatigue fracture surface of S1-7 test specimen (lower half of the fractured specimen)

### 5.3 Results of S2 series

Table 7 lists the summary of S2 series test results. S2 series test was conducted only for one specimen because it was difficult to correctly determine maximum stress being low in the strain-hardening domain.

**Table 7** Results of S2 series tensile fatigue tests of UHPFRC

| Test No. | $\sigma_{max}$ [MPa] | $\sigma_{min}$ [MPa] | $\sigma_{max}/f_{e,i}$ | $N$ | Remarks |
|---|---|---|---|---|---|
| 1 | 9.60 | 0.82 | 1.02 | 797 | |

$f_{e,i}$: elastic limit strength of each UHPFRC specimen

### 5.3.1 S2-1 test

***Test parameters and results***

| $\sigma_{max}$ [MPa] | $\sigma_{min}$ [MPa] | *N* | Deformation localisation |
|---|---|---|---|
| 9.60 MPa | 0.82 MPa | 797 | G1 zone |

Comment: Quasi-static tensile force wasn't stopped properly when either of LVDTs' readings reached 0.075 mm corresponding to 0.30 ‰ strain because of the sudden rise of UHPFRC deformation. Therefore, stress causing 0.32 ‰ global strain was determined as maximum fatigue stress.

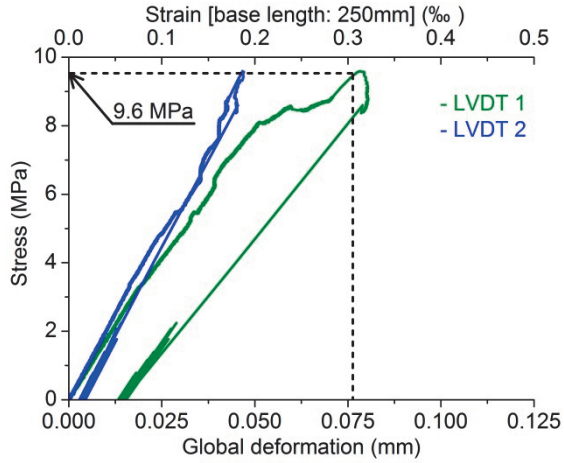


**Figure 42** Stress-deformation curves obtained from quasi-static tensile preloading to determine the maximum fatigue stress of S2-1 test

***The reason why this test is categorised into S2 series:***

Fig. 43a shows stress-deformation curves obtained from quasi-static tensile stress application before fatigue stress application. Change of slope of the curve is clearly observed at around 8.8 MPa and this change indicates that the UHPFRC specimen entered into the strain-hardening domain. The elastic limit strength and the corresponding strain were determined to be 9.4 MPa and 0.34 ‰, respectively. Imposed maximum fatigue stress of 9.6 MPa was within the strain-hardening domain, so this test is categorised into S2 series.

***Behaviour of S2-1 test specimen***

Maximum global deformation gradually increased and redistribution of localised deformation occurred at 658 cycles, after which the specimen soon fractured. Behaviour of global deformation range was similar to that of maximum global deformation, while its growth rate was smaller than growth rate of maximum global deformation.

Maximum local deformation at all local zones except G2 zone gradually increased with various growth rates, while maximum local deformation at G2 zone kept almost constant. Behaviour of maximum local deformation at G1 zone was similar to that of maximum global deformation. Deformation localised at G1 zone whose maximum deformation reading kept the largest among all local zones during the test.

Variations were observed on local deformation readings.

Fracture crack propagated in a path perpendicular to fatigue force direction.

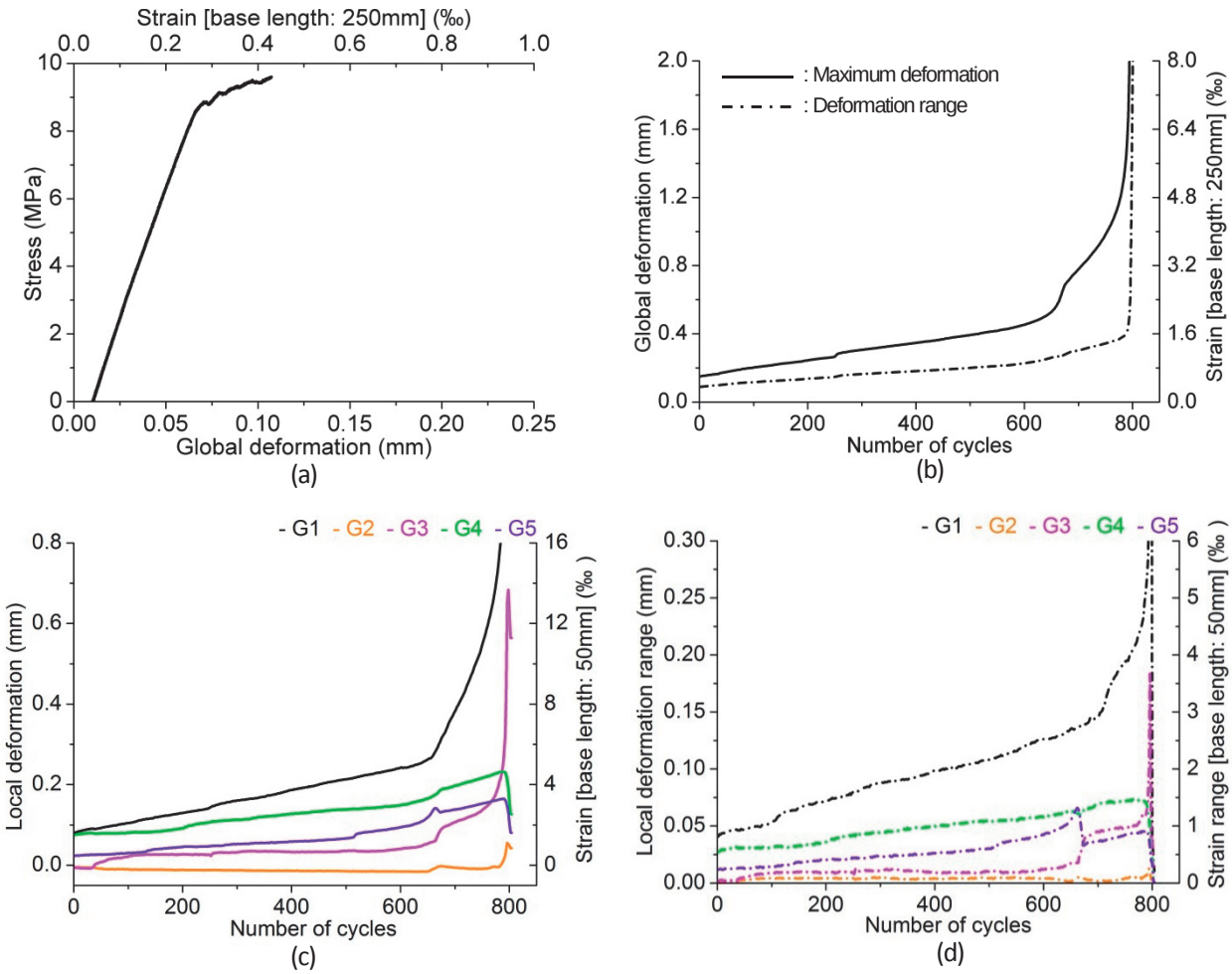


**Figure 43** S2-1 test: (a) stress-deformation curves obtained from quasi-static tensile stress application before fatigue stress application, growth curves of (b) maximum global deformation and global deformation range, (c) maximum local deformation and (d) local deformation range

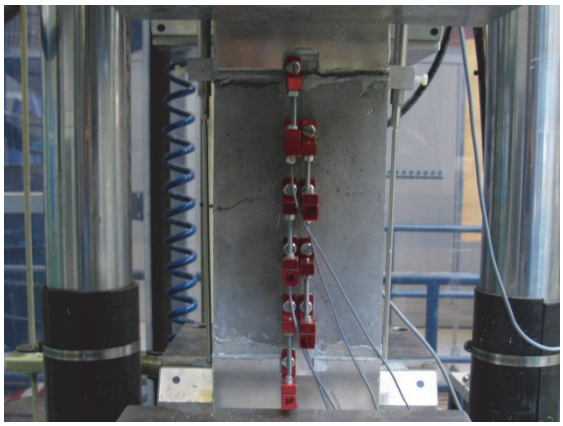

**Figure 44** Fractured S2-1 test specimen

***Fatigue fracture surface of S2-1 test specimen:***

Most part of the fracture surface was rough and it was very similar to fracture surface of specimens subjected to quasi-static tensile test.

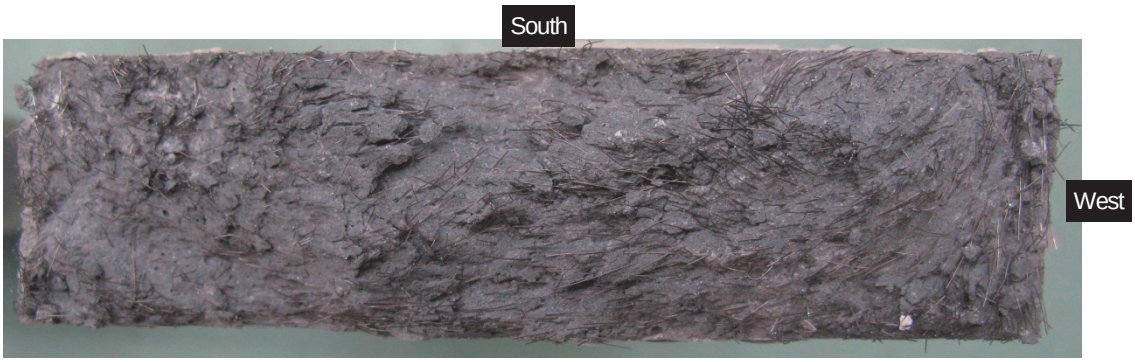


**Figure 45** Fatigue fracture surface of S2-1 test specimen (lower half of the fractured specimen)

### 5.4 Results of S2.5 series

Table 8 lists the summary of S2.5 series test results.

**Table 8** Results of S2.5 series tensile fatigue tests of UHPFRC

| Test No. | | $\sigma_{max}$ [MPa] | $\sigma_{min}$ [MPa] | $\sigma_{max}/f_{e,i}$ | $N$ | Remarks |
|---|---|---|---|---|---|---|
| 1 | | 5.7 | 0.57 | 0.84 | 389,598 | |
| 2 | | 6.4 | 0.64 | 1.00 | 19,836 | |
| 3 | | 6.4 | 0.64 | 0.80 | 43,573 | |
| 4 | | 7.8 | 0.78 | 0.89 | 1,948,128 | |
| 5 | | 8.3 | 0.83 | 0.84 | 825,513 | |
| 6 | i | 8.9 | 0.89 | 0.79 | 11,142,037 | run-out |
| | ii | 11.0 | 1.10 | 0.97 | 69,066 | |

$f_{e,i}$: elastic limit strength of each UHPFRC specimen

### 5.4.1 S2.5-1 test

***Mechanical properties of the specimen***

| $f_{e,i}$ [MPa] | $\varepsilon_{e,i}$ [‰] | $E$ [GPa] |
|---|---|---|
| 6.8 | 0.45 | 13.5 |

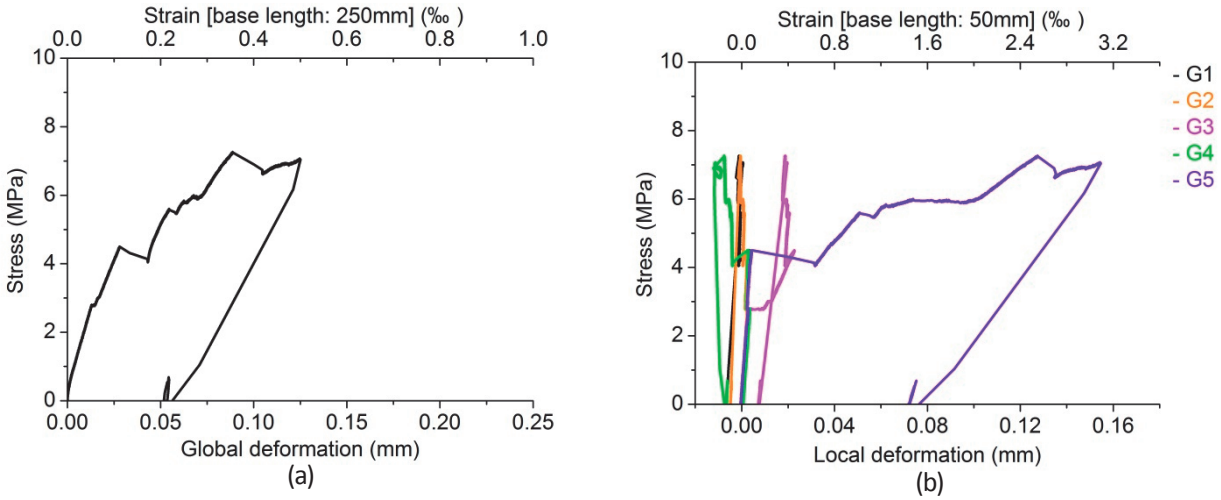


**Figure 46** Stress-deformation curves obtained from quasi-static tensile preloading preceding the S2.5-1 test (a) global deformation and (b) local deformation

***Test parameters and results***

| $\sigma_{max}$ [MPa] | $\sigma_{min}$ [MPa] | $\varepsilon_{pre}$ [‰] | $\sigma_{max}/f_{e,i}$ | $N$ | Deformation localisation |
|---|---|---|---|---|---|
| 5.7 | 0.57 | 0.50 | 0.84 | 389,598 | G4 zone |

Comment: Stress causing 0.25 ‰ global strain was determined as maximum fatigue stress from the stress-deformation curve obtained from quasi-static tensile preloading.

***Behaviour of S2.5-1 test specimen***

Maximum global deformation steadily increased. At about 343,000 cycles, redistribution of localised deformation occurred at G5 zone. Maximum global deformation suddenly rose and its growth rate became significantly large. After sustaining additional about 46,600 cycles, the specimen fractured. Behaviour of global deformation range was similar to that of maximum global deformation, while its growth rate was smaller than growth rate of maximum global deformation and its sudden rise on the redistribution of localised deformation was much smaller than that of maximum global deformation.

Maximum local deformation at all local zones except G5 zone was quite small and approximately constant. Behaviour of maximum local deformation at G5 zone was similar to that of maximum global deformation. Eventually deformation localised at G4 zone. Behaviour of local deformation range was almost similar to that of maximum local deformation.

Although slightly curved, fracture crack propagated in a path almost perpendicular to fatigue force direction.

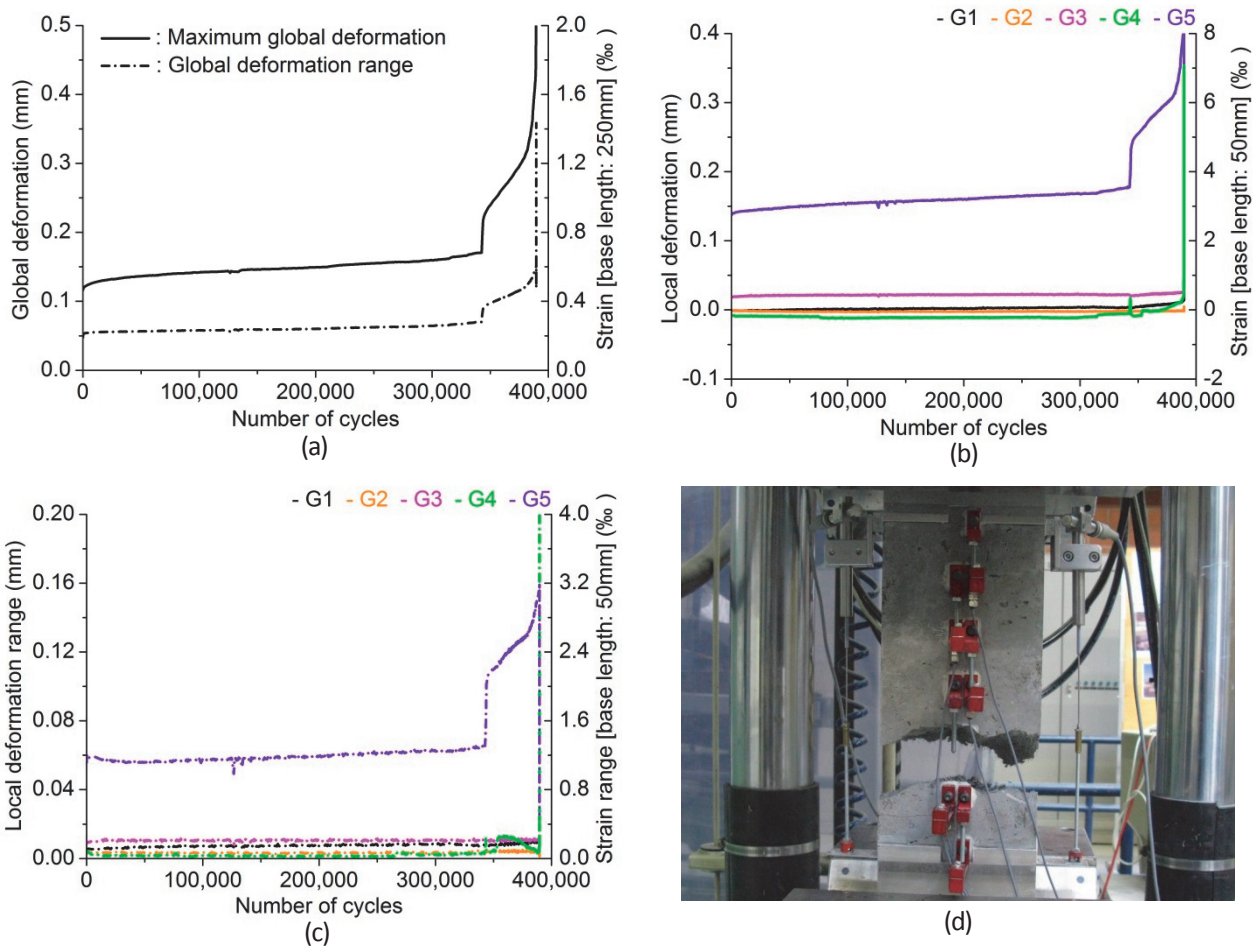


**Figure 47** S2.5-1 test: growth curves of (a) maximum global deformation and global deformation range, (b) maximum local deformation and (c) local deformation range and (d) fractured specimen

***Fatigue fracture surface of S2.5-1 test specimen:***

An area void of fibres was identified at north-western part of the fracture surface (enclosed with a line in Fig. 48). Since powdery products covering that area wasn't rust-coloured, there seemed to be initially few fibres in that area.

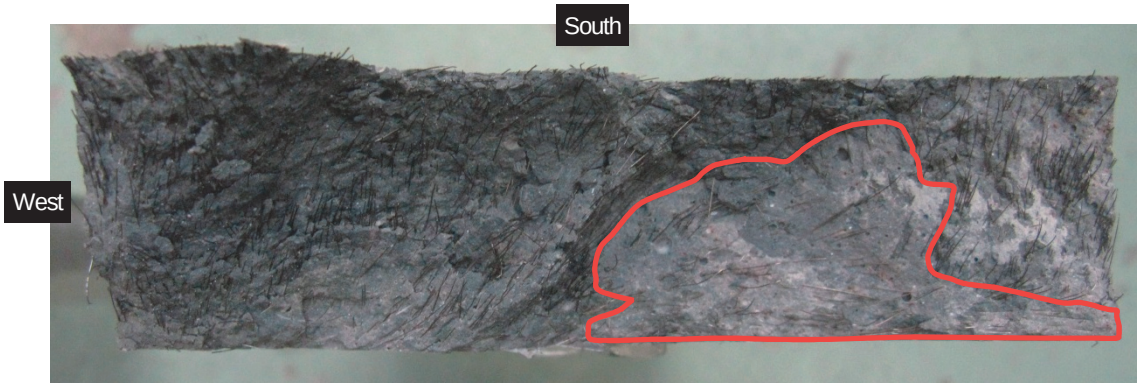


**Figure 48** Fatigue fracture surface of S2.5-1 test specimen (upper half of the fractured specimen)

### 5.4.2 S2.5-2 test

***Mechanical properties of the specimen***

| $f_{e,i}$ [MPa] | $\varepsilon_{e,i}$ [‰] | $E$ [GPa] |
|---|---|---|
| 6.8 | 0.38 | 39.5 |

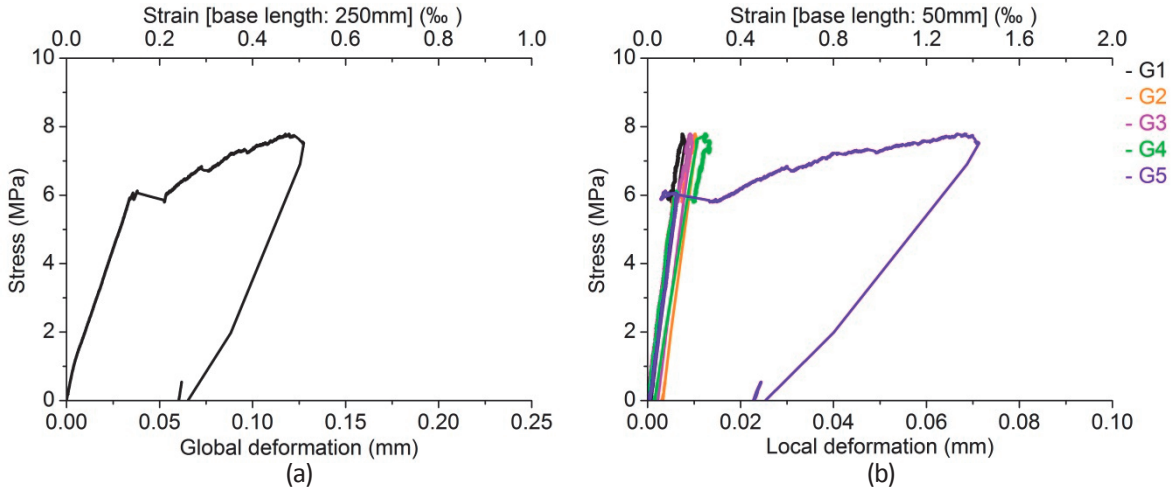


**Figure 49** Stress-deformation curves obtained from quasi-static tensile preloading preceding the S2.5-2 test (a) global deformation and (b) local deformation

***Test parameters and results***

| $\sigma_{max}$ [MPa] | $\sigma_{min}$ [MPa] | $\varepsilon_{pre}$ [‰] | $\sigma_{max}/f_{e,i}$ | $N$ | Deformation localisation |
|---|---|---|---|---|---|
| 6.4 | 0.64 | 0.50 | 1.00 | 19,836 | G5 zone |

Comment: Stress causing 0.25 ‰ global strain was determined as maximum fatigue stress from the stress-deformation curve obtained from quasi-static tensile preloading.

***Behaviour of S2.5-2 test specimen***

During the first 300 cycles, maximum global deformation rapidly increased, followed by steady increase. Reaching about 0.8 ‰, it started to increase significantly and soon the specimen fractured. Behaviour of global deformation range was similar to that of maximum global deformation, while its growth rate was smaller than growth rate of maximum global deformation.

Maximum local deformation at all local zones except G5 zone was quite small and unchanged. Behaviour of maximum local deformation at G5 zone was similar to that of maximum global deformation. Eventually deformation localised at G5 zone. Behaviour of local deformation range was almost similar to that of maximum local deformation.

Although slightly curved, fracture crack propagated in a path almost perpendicular to fatigue force direction.

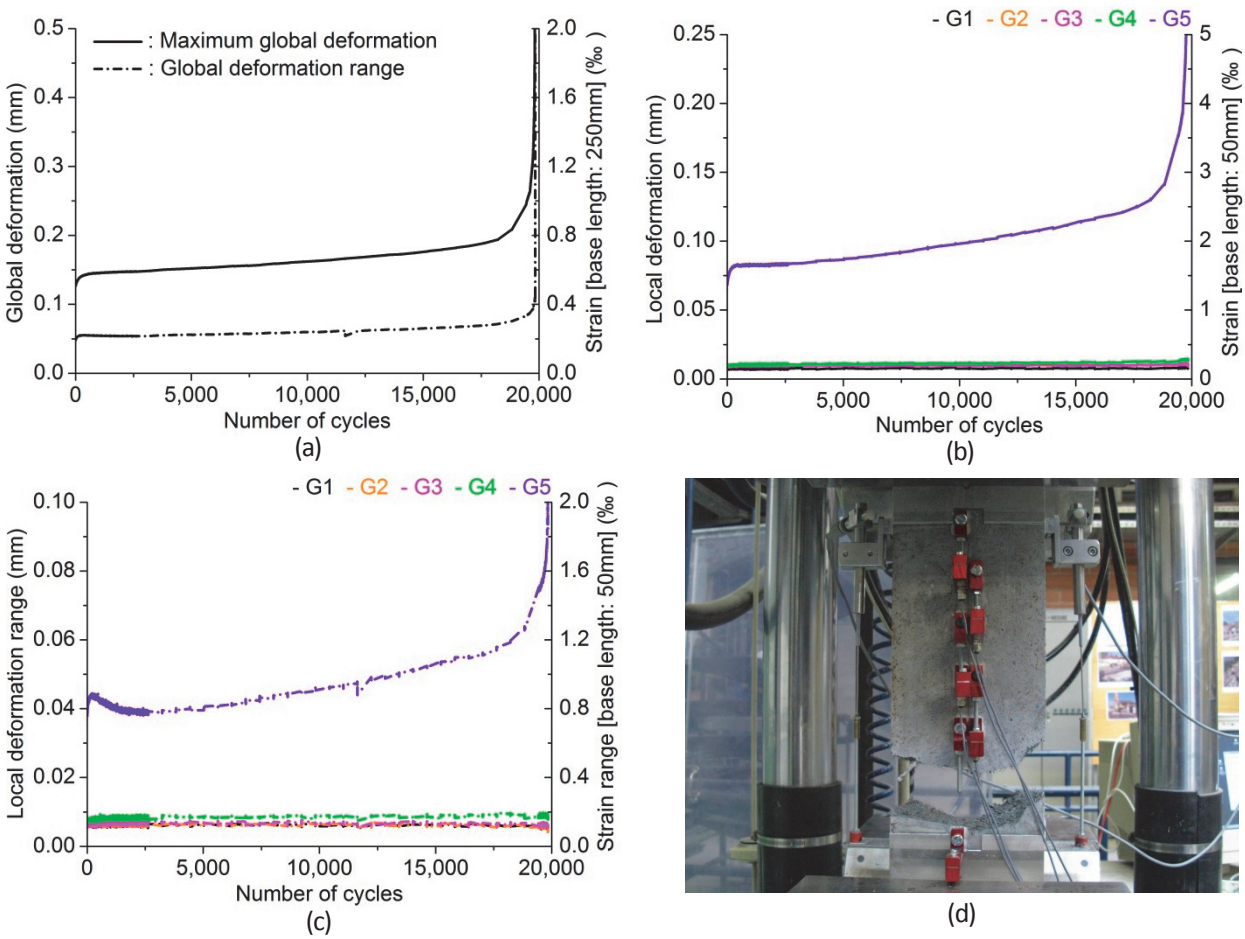


**Figure 50** S2.5-2 test: growth curves of (a) maximum global deformation and global deformation range, (b) maximum local deformation and (c) local deformation range and (d) fractured specimen

***Fatigue fracture surface of S2.5-2 test specimen:***

The fracture surface was quite similar to that of specimen subjected to quasi-static tensile test. At almost 50 % of the fracture surface, orientation of fibre was approximately horizontal to fatigue force direction.

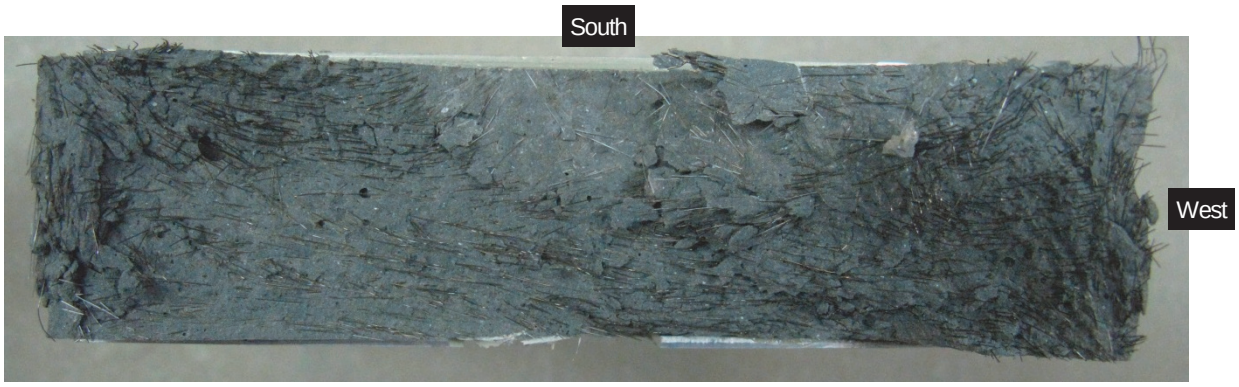


**Figure 51** Fatigue fracture surface of S2.5-2 test specimen (lower half of the fractured specimen)

### 5.4.3 S2.5-3 test

Sum of local deformation was adopted as global deformation.

***Mechanical properties of the specimen***

| $f_{e,i}$ [MPa] | $\varepsilon_{e,i}$ [‰] | $E$ [GPa] |
|---|---|---|
| 8.0 | 0.28 | 44.7 |

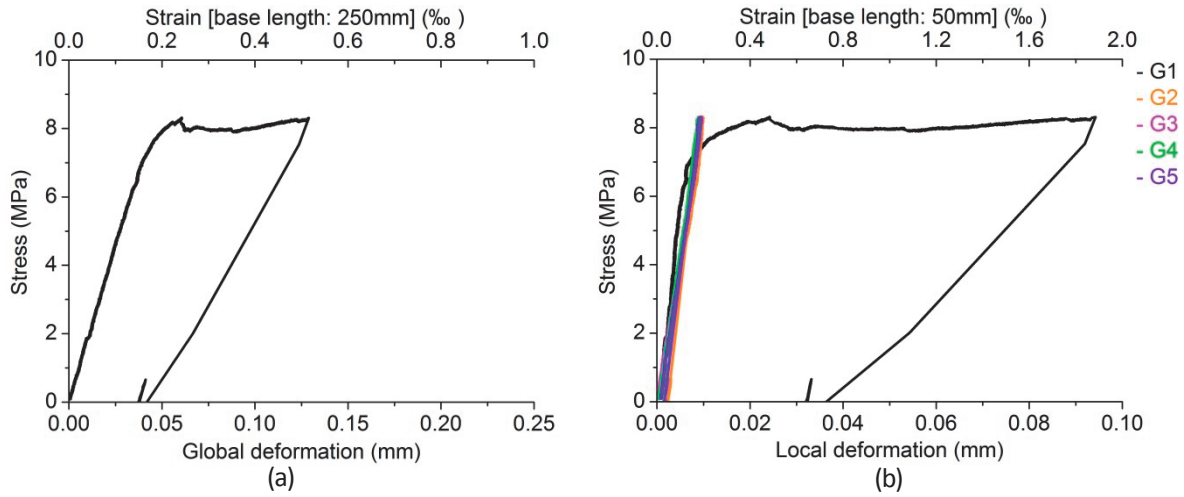


**Figure 52** Stress-deformation curves obtained from quasi-static tensile preloading preceding the S2.5-3 test (a) global deformation and (b) local deformation

***Test parameters and results***

| $\sigma_{max}$ [MPa] | $\sigma_{min}$ [MPa] | $\varepsilon_{pre}$ [‰] | $\sigma_{max}/f_{e,i}$ | $N$ | Deformation localisation |
|---|---|---|---|---|---|
| 6.4 | 0.64 | 0.50 | 0.80 | 43,573 | G1 zone |

Comment: 80 % of the elastic limit strength was determined as maximum fatigue stress.

***Behaviour of S2.5-3 test specimen***

Maximum global deformation steadily increased. Reaching at 0.9 ‰, it started to increase significantly and soon the specimen fractured. Global deformation range kept approximately constant, and when the specimen fractured, it suddenly rose.

Maximum local deformation and local deformation range at all local zones except G1 zone was quite small and unchanged. Behaviour of maximum local deformation at G5 zone was similar to that of maximum global deformation.

Fracture crack propagated in a path almost perpendicular to fatigue force direction.

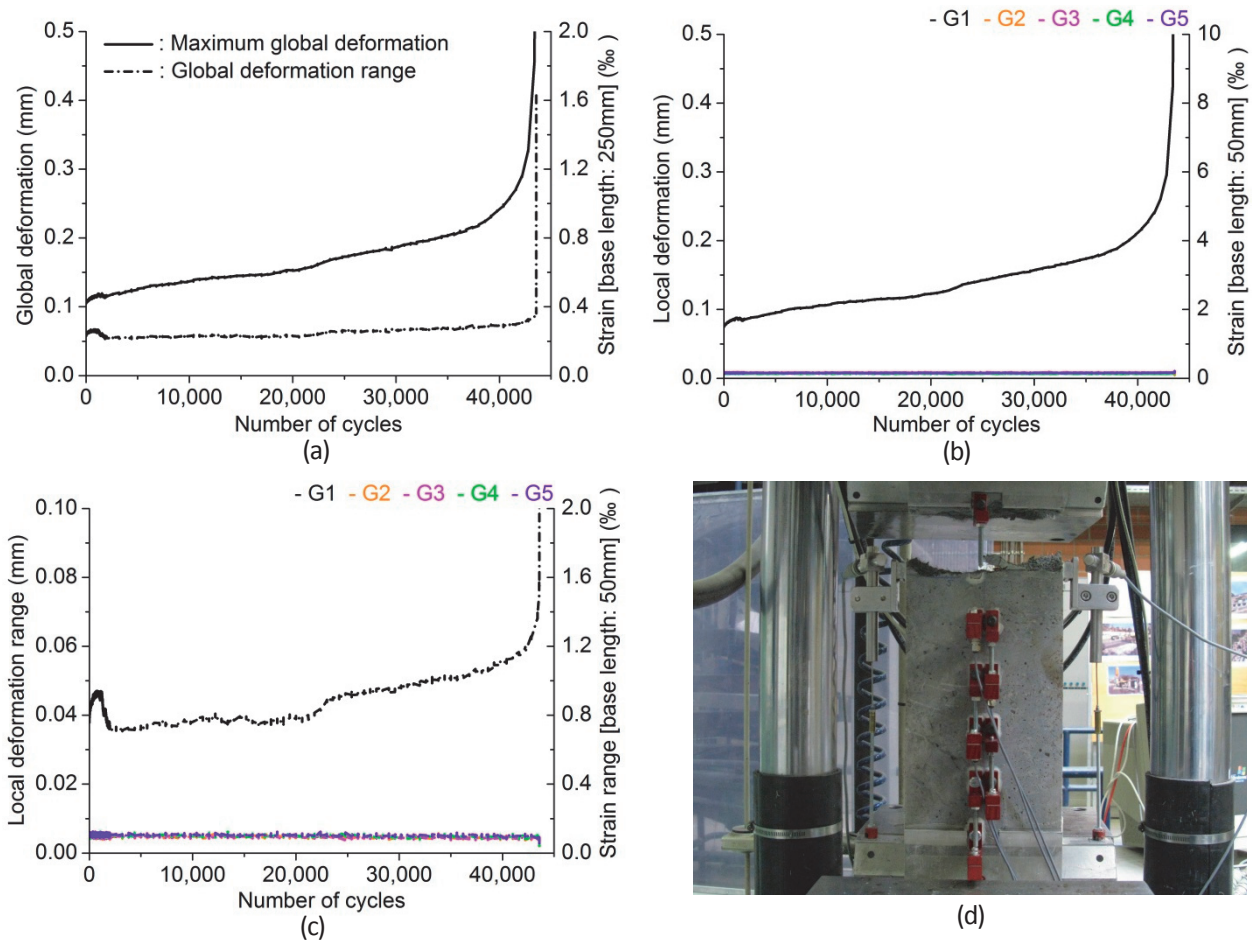


**Figure 53** S2.5-3 test: growth curves of (a) maximum global deformation and global deformation range, (b) maximum local deformation and (c) local deformation range and (d) fractured specimen

***Fatigue fracture surface of S2.5-3 test specimen:***

The fracture surface was quite similar to that of specimen subjected to quasi-static tensile test.


**Figure 54** Fatigue fracture surface of S2.5-3 test specimen (lower half of the fractured specimen)

### 5.4.4 S2.5-4 test

***Mechanical properties of the specimen***

| $f_{e,i}$ [MPa] | $\varepsilon_{e,i}$ [‰] | $E$ [GPa] |
|---|---|---|
| 8.8 | 0.35 | 32.4 |

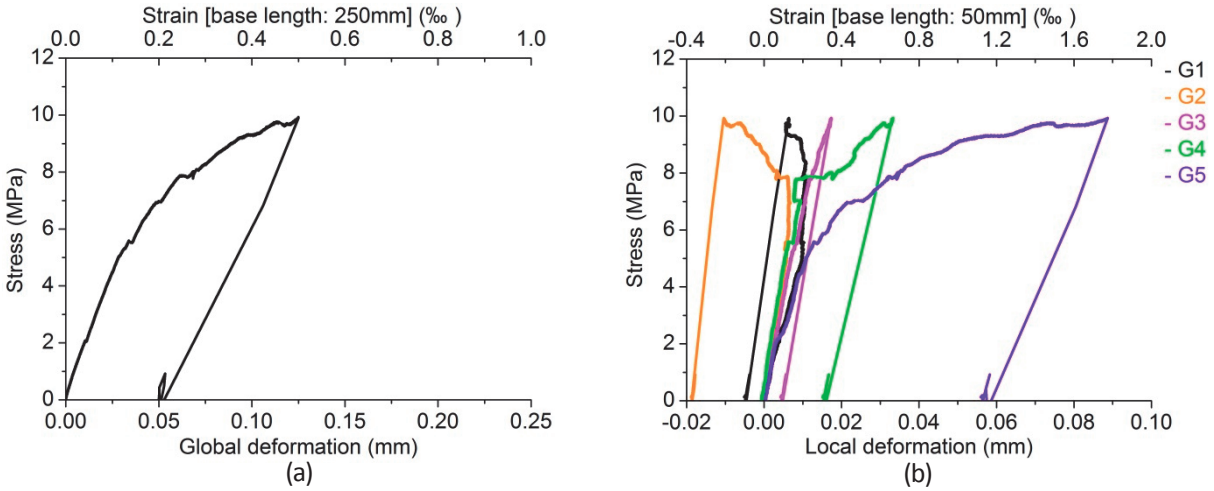


**Figure 55** Stress-deformation curves obtained from quasi-static tensile preloading preceding the S2.5-4 test (a) global deformation and (b) local deformation

***Test parameters and results***

| $\sigma_{max}$ [MPa] | $\sigma_{min}$ [MPa] | $\varepsilon_{pre}$ [‰] | $\sigma_{max}/f_{e,i}$ | $N$ | Deformation localisation |
|---|---|---|---|---|---|
| 7.8 | 0.78 | 0.50 | 0.89 | 1,948,128 | G3 zone |

Comment: Stress causing 0.25 ‰ global strain was determined as maximum fatigue stress from the stress-deformation curve obtained from quasi-static tensile preloading.

***Behaviour of S2.5-4 test specimen***

Maximum global deformation increased with modest growth rate until about 400,000 cycles after which its growth rate became smaller. At about 1,489,600 cycles, maximum global deformation suddenly rose by 0.01 mm and then its growth rate started to increase. When maximum global deformation reached 1.3 ‰, deformation localisation started and eventually the specimen fractured. Behaviour of global deformation range was approximately similar to that of maximum global deformation, while growth rate of global deformation range was always smaller than that of maximum global deformation.

Behaviour of maximum local deformation at G3 zone was similar to that of maximum global deformation. Maximum local deformation at G1, G2 and G4 zone kept approximately constant, while maximum local deformation at G5 zone rapidly increased until about 69,000 cycles and then kept approximately constant. When deformation localised at G3 zone, UHPFRC at G2, G4 and G5 zone softened. Behaviour of local deformation range at all local zones was more or less similar to that of maximum local deformation.

Variations were observed in local deformation readings.

In the western half of the specimen including fatigue cracked part, fracture crack propagated in a path perpendicular to fatigue force direction. In the eastern half of the specimen, fracture crack propagated in a path inclined from horizontal axis with an angle of 35˚.

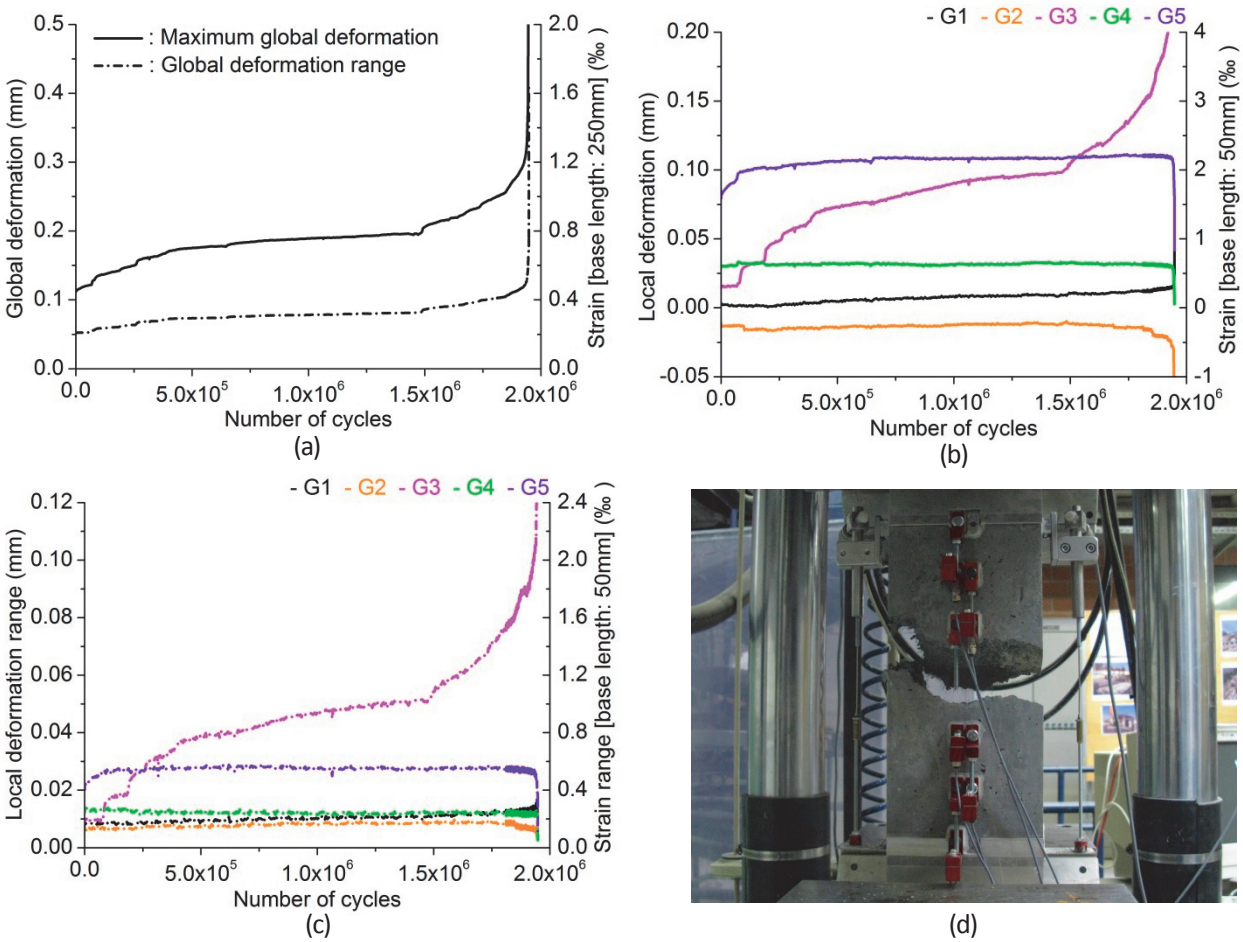


**Figure 56** S2.5-4 test: growth curves of (a) maximum global deformation and global deformation range, (b) maximum local deformation and (c) local deformation range and (d) fractured specimen

***Fatigue fracture surface of S2.5-4 test specimen:***

Western part of the fracture surface was smooth and covered with rust-coloured powdery products, from which fatigue cracked area was understood (enclosed with a line in Fig. 57). Direction of fracture crack propagation was extrapolated from the depth of rust-colour of powdery products (indicated with an arrow in Fig. 57).

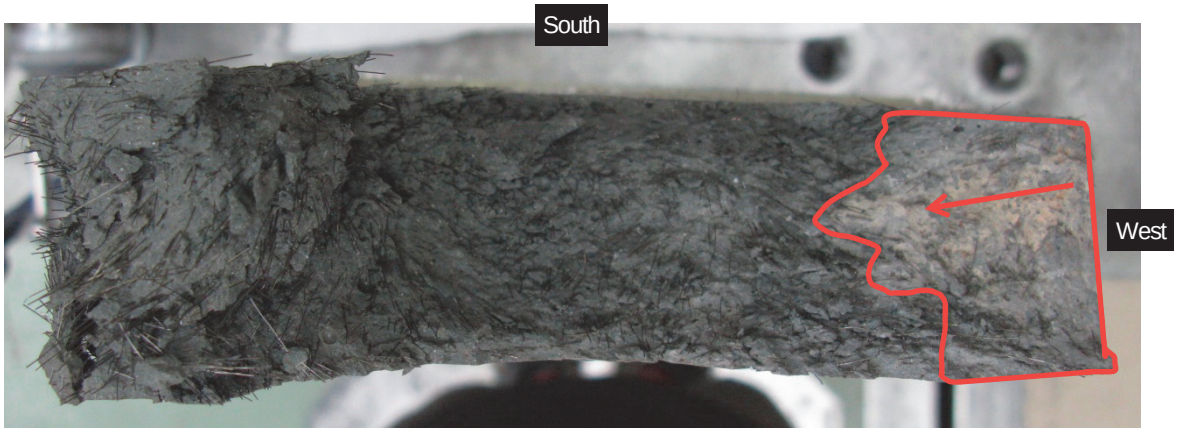


**Figure 57** Fatigue fracture surface of S2.5-4 test specimen (lower half of the fractured specimen)

### 5.4.5 S2.5-5 test

***Mechanical properties of the specimen***

| $f_{e,i}$ [MPa] | $\varepsilon_{e,i}$ [‰] | $E$ [GPa] |
|---|---|---|
| 9.9 | 0.34 | 41.7 |

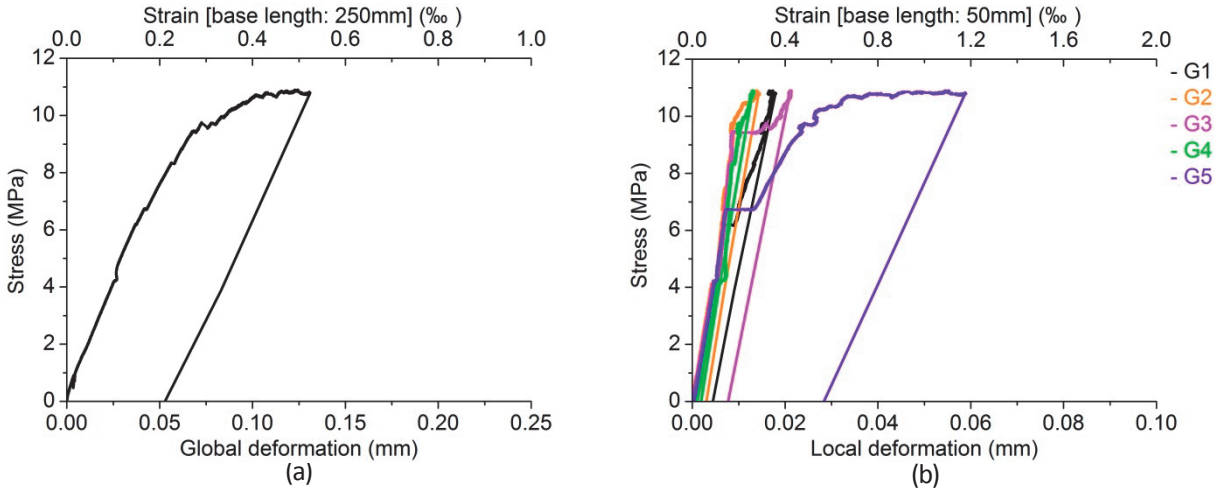


**Figure 58** Stress-deformation curves obtained from quasi-static tensile preloading preceding the S2.5-5 test (a) global deformation and (b) local deformation

***Test parameters and results***

| $\sigma_{max}$ [MPa] | $\sigma_{min}$ [MPa] | $\varepsilon_{pre}$ [‰] | $\sigma_{max}/f_{e,i}$ | $N$ | Deformation localisation |
|---|---|---|---|---|---|
| 8.3 | 0.83 | 0.50 | 0.84 | 825,513 | G5 zone |

Comment: Stress causing 0.225 ‰ global strain was determined as maximum fatigue stress from the stress-deformation curve obtained from quasi-static tensile preloading.

***Behaviour of S2.5-5 test specimen***

Maximum global deformation gradually increased. When maximum global strain reached about 0.9 ‰, its growth rate started to increase and then the specimen fractured. Global deformation range increased with lower growth rate than maximum global deformation. When the specimen fractured, its reading significantly increased.

Behaviour of maximum local deformation at G5 zone was similar to that of maximum global deformation. Maximum local deformation at the other local zones kept roughly constant. Behaviour of local deformation range at all local zones was almost similar to that of maximum local deformation.

Variations were observed in local deformation readings.

Fracture crack propagated in a path approximately perpendicular to fatigue force direction.

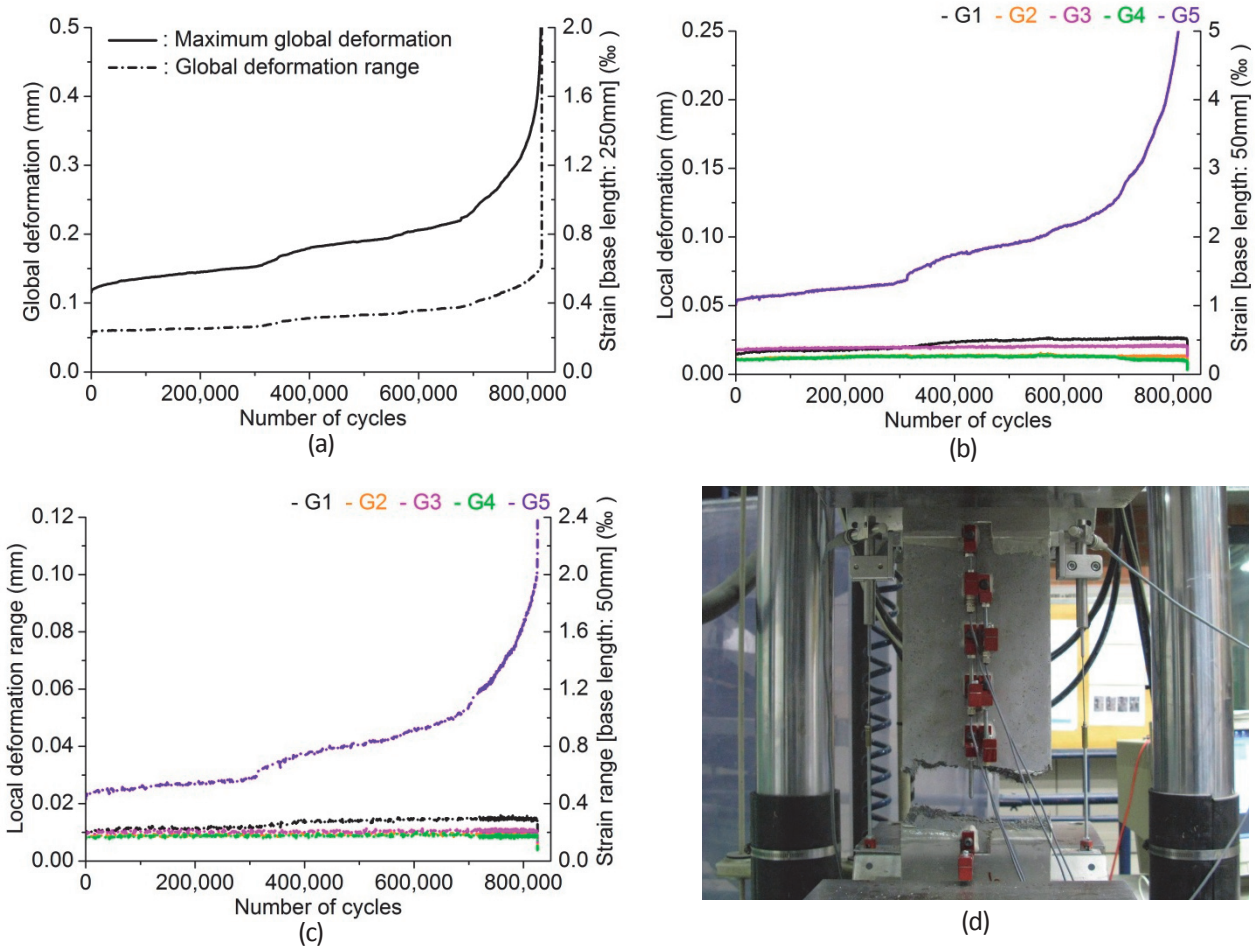


**Figure 59** S2.5-5 test: growth curves of (a) maximum global deformation and global deformation range, (b) maximum local deformation and (c) local deformation range and (d) fractured specimen

***Fatigue fracture surface of S2.5-5 test specimen:***

In the centre of the fracture surface, a smooth surface area covered with rust-coloured powdery products was observed. It is identified to be fatigue cracked area (enclosed with a line in Fig. 60). From the geometry of the fatigue cracked area, direction of fracture crack propagation was extrapolated (indicated with an arrow in Fig. 60).

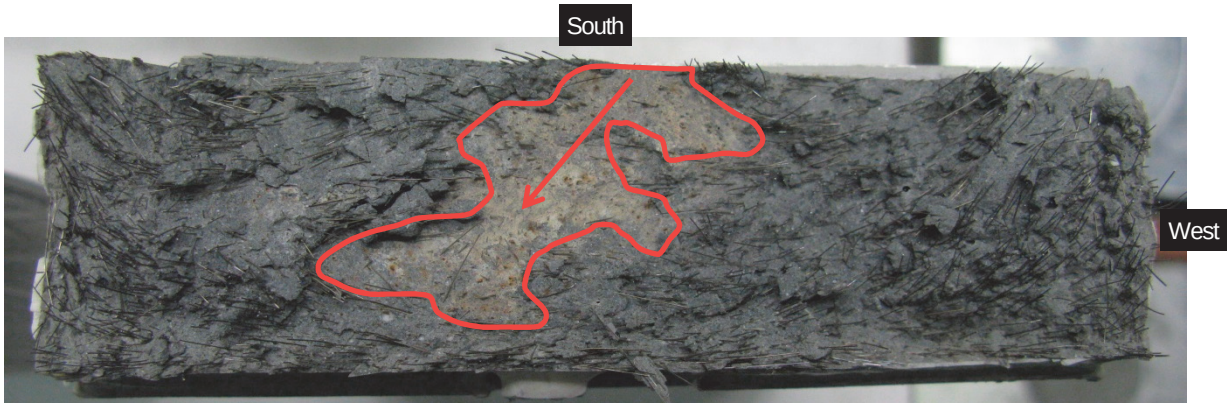


**Figure 60** Fatigue fracture surface of S2.5-5 test specimen (lower half of the fractured specimen)

### 5.4.6 S2.5-6 test

***Mechanical properties of the specimen***

| $f_{e,i}$ [MPa] | $\varepsilon_{e,i}$ [‰] | $E$ [GPa] |
|---|---|---|
| 11.3 | 0.34 | 43.2 |

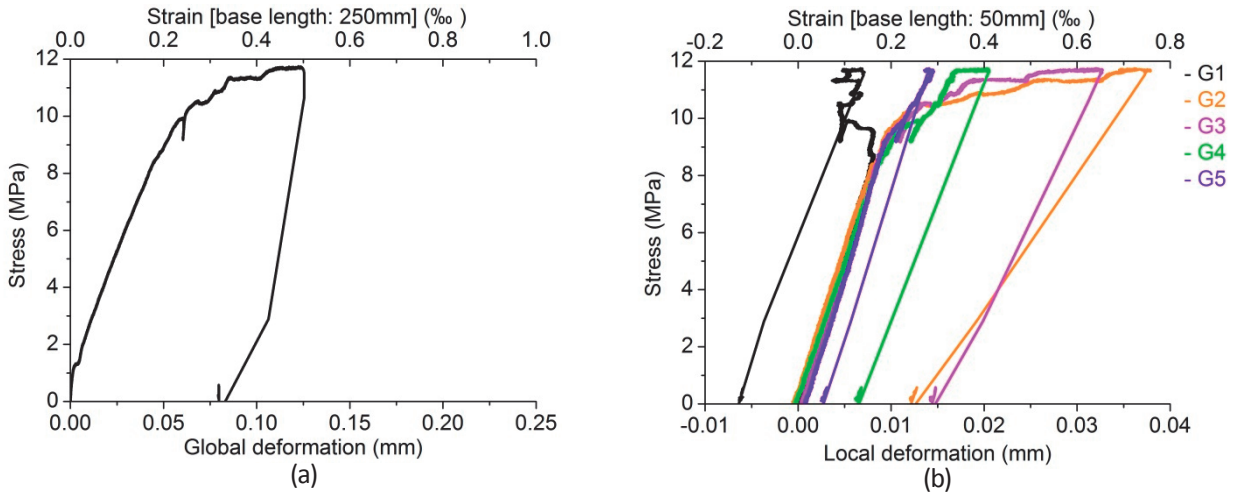


**Figure 61** Stress-deformation curves obtained from quasi-static tensile preloading preceding the S2.5-6 test (a) global deformation and (b) local deformation

**First fatigue test**

***Test parameters and results***

| $\sigma_{max}$ [MPa] | $\sigma_{min}$ [MPa] | $\varepsilon_{pre}$ [‰] | $\sigma_{max}/f_{e,i}$ | $N$ | Deformation localisation |
|---|---|---|---|---|---|
| 8.9 | 0.89 | 0.50 | 0.79 | 11,142,037 | run-out |

Comment: Stress causing 0.20 ‰ global strain was determined as maximum fatigue stress from the stress-deformation curve obtained from quasi-static tensile preloading.

***Behaviour of S2.5-6 test specimen during the first fatigue test***

Maximum global deformation rapidly increased until about 2 million cycles, followed by increase with much lower growth rate. Behaviour of global deformation range was similar to that of maximum global deformation.

Maximum local deformation at G2 and G3 showed similar behaviour to maximum global deformation, while G2 zone had larger deformation than G3 zone. Maximum local deformation at G1, G4 and G5 zones increased in unstable manner. Behaviour of local deformation range at G2 zone was approximately similar to that of maximum local deformation. Local deformation range at G1 and G3 zones increased with lower growth rate than G2 zone. Local deformation rang at G4 and G5 zones kept more almost constant.

Variations were observed in local deformation readings.

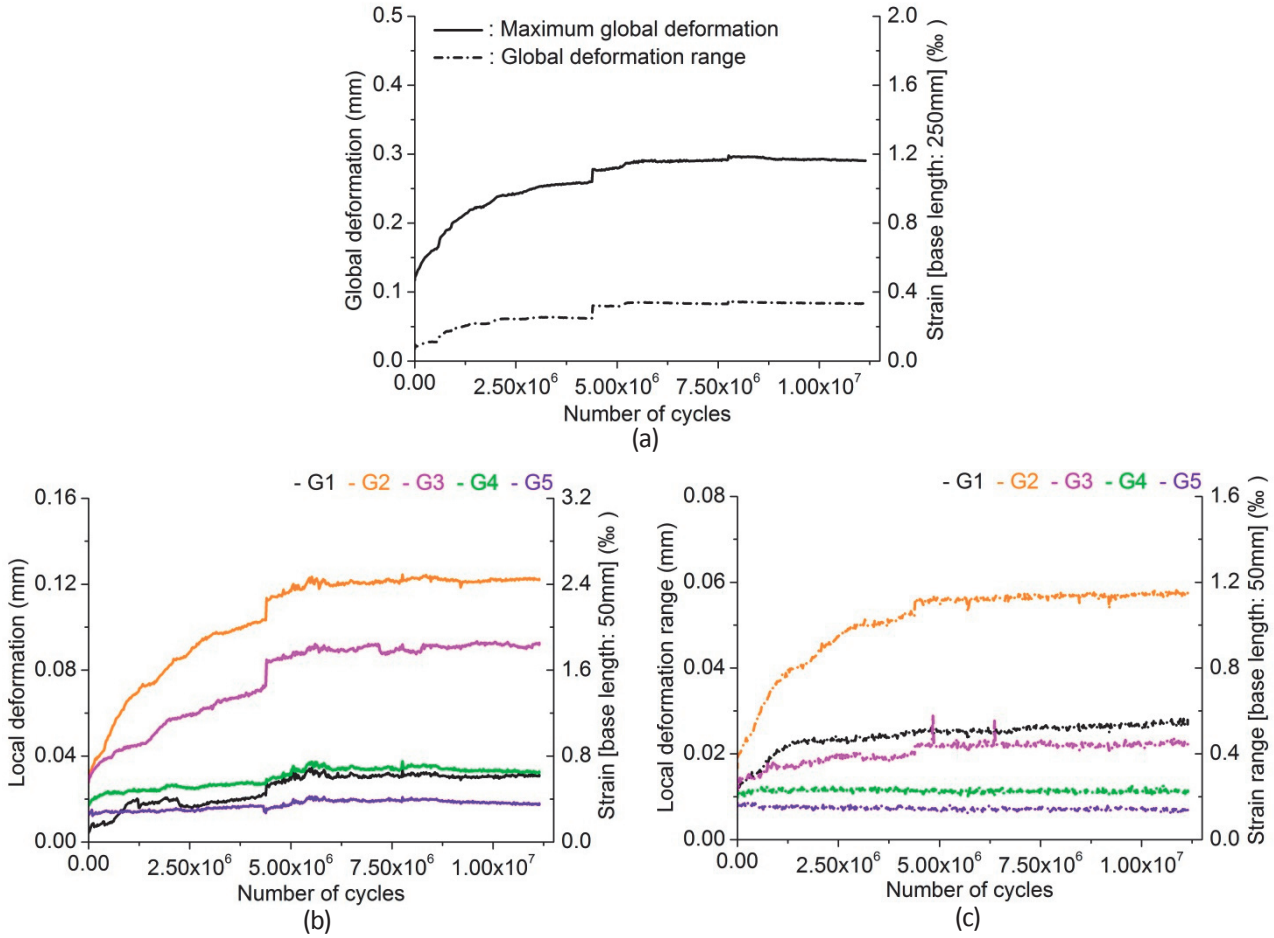


**Figure 62** S2.5-6_i test: growth curves of (a) maximum global deformation and global deformation range, (b) maximum local deformation and (c) local deformation range

**Second fatigue test**

***Test parameters and results***

| $\sigma_{max}$ [MPa] | $\sigma_{min}$ [MPa] | $\sigma_{max}/f_{e,i}$ | $N$ | Deformation localisation |
|---|---|---|---|---|
| 11.0 | 1.10 | 0.97 | 69,066 | G1 and G2 zones |

Comment: Maximum fatigue stress was arbitrarily determined.

***Behaviour of S2.5-6 test specimen during the second fatigue test***

Maximum global deformation steadily increased. When maximum global strain reached about 2.6 ‰, its growth rate started to increase and soon the specimen fractured. Global deformation range increased with approximately constant growth rate until the specimen fractured.

Behaviour of maximum local deformation at G2 zone was again similar to that of maximum global deformation. Maximum local deformation at G3 zone increased with lower growth rate than G2 zone. When deformation localised at G1 andG2 zone, UHPFRC at G3 zone softened. Maximum local deformation at G1 zone kept almost constant until about 40,000 cycles, followed by gradual decrease. Eventually, deformation localised at G1 zone. Maximum local deformation at G4 and G5 zone kept approximately constant. Behaviour of local deformation range at all local zones was roughly similar to that of maximum local deformation.

Variations were left on local deformation readings.

Two fracture cracks appeared. Both propagated in a path approximately perpendicular to fatigue force direction.

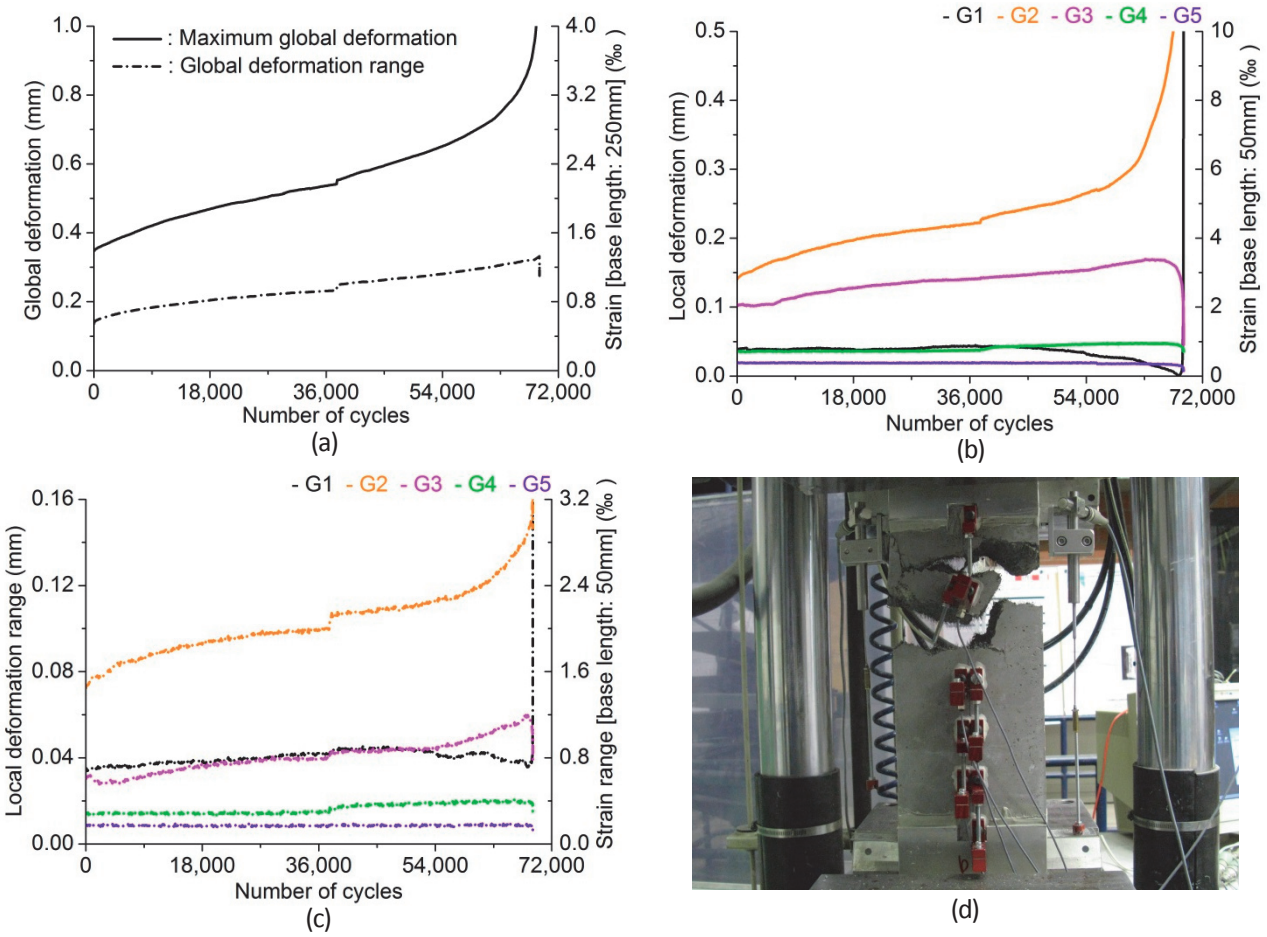


**Figure 63** S2.5-6_ii test: growth curves of (a) maximum global deformation and global deformation range, (b) maximum local deformation and (c) local deformation range and (d) fractured S2.5-6 test specimen

***Fatigue fracture surface of S2.5-6 test specimen:***

At eastern and western edges of the fracture surface, smooth surface areas covered with rust-coloured powdery products were observed. Those were identified as fatigue cracked area (enclosed with a line in Fig. 64).


**Figure 64** Fatigue fracture surface of S2.5-6 test specimen (lower half of the fractured specimen)

### 5.5 Results of S3 series

Table 9 lists the summary of S3 series test results.

**Table 9** Results of S3 series tensile fatigue tests of UHPFRC

| Test No. | | $\sigma_{max}$ [MPa] | $\sigma_{min}$ [MPa] | $\varepsilon_{pre}$ [‰] | $\sigma_{max}/f_{e,i}$ | $N$ | Remarks |
|---|---|---|---|---|---|---|---|
| 1 | | 7.4 | 0.74 | 0.48 | 0.68 | 7,776,735 | |
| 2 | i | 6.3 | 0.63 | 0.50 | 0.62 | 10,069,570 | run-out |
| | ii | 7.8 | 0.78 | | 0.77 | 10,056,789 | run-out |
| | iii | 8.8 | 0.88 | | 0.87 | 7,093,824 | |
| 3 | i | 5.9 | 0.59 | 1.13 | 0.56 | 10,000,000 | run-out |
| | ii | 8.4 | 0.84 | | 0.80 | 3,107,413 | |
| 4 | i | 6.9 | 0.69 | 1.99 | 0.64 | 5,002,373 | run-out |
| | ii | 9.0 | 0.90 | | 0.84 | 2,000,072 | run-out |
| | iii | 10.4 | 1.04 | | 0.97 | 64,717 | |
| 5 | i | 7.6 | 0.76 | 2.01 | 0.61 | 10,000,000 | run-out |
| | ii | 11.7 | 1.17 | | 0.94 | 113,500 | |
| 6 | | 5.2 | 0.52 | 2.09 | 0.58 | 7,869,999 | |
| 7 | i | 6.7 | 0.67 | 3.00 | 0.65 | 10,082,808 | run-out |
| | ii | 8.7 | 0.87 | | 0.84 | 84,075 | |
| 8 | i | 6.0 | 0.60 | 4.00 | 0.58 | 11,363,737 | run-out |
| | ii | 7.9 | 0.79 | | 0.77 | 1,602,088 | |
| 9 | | 7.2 | 0.72 | 0.50 | 0.72 | 10,000,000 | mistake |

### 5.5.1 S3-1 test

***Mechanical properties of the specimen***

| $f_{e,i}$ [MPa] | $\varepsilon_{e,i}$ [‰] | $E$ [GPa] |
|---|---|---|
| 10.9 | 0.34 | 45.0 |

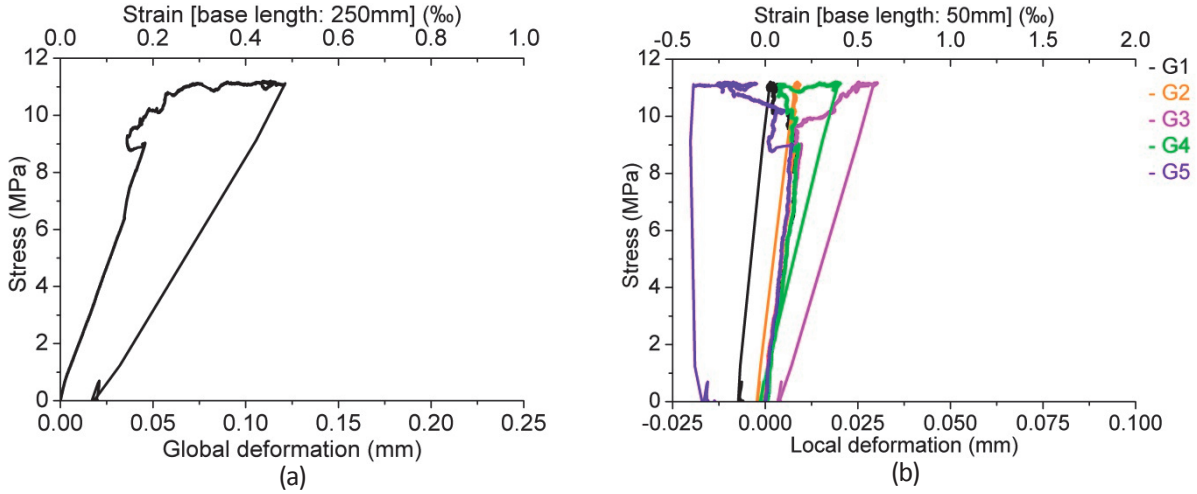


**Figure 65** Stress-deformation curves obtained from quasi-static tensile preloading preceding the S3-1 test (a) global deformation and (b) local deformation

***Test parameters and results***

| $\sigma_{max}$ [MPa] | $\sigma_{min}$ [MPa] | $\varepsilon_{pre}$ [‰] | $\sigma_{max}/f_{e,i}$ | $N$ | Deformation localisation |
|---|---|---|---|---|---|
| 7.4 | 0.74 | 0.48 | 0.68 | 7,776,735 | outside of G5 zone |

Comment: Stress causing 0.15 ‰ global strain was determined as maximum fatigue stress from the stress-deformation curve obtained from quasi-static tensile preloading.

***Behaviour of S3-1 test specimen***

Maximum global deformation gradually decreased as the number of cycles increased, which might be due to micro- and macrocracking under the base of LVDTs. Behaviour of global deformation range was similar to that of maximum global deformation until deformation localised at outside of G5 zone.

Maximum local deformation at all local zones also gradually decreased as the number of cycles increased. Local deformation range at all local zones kept approximately constant.

When deformation localised at outside of G5 zones, a part of UHPFRC covered by measuring devices softened.

Variations were observed on local deformation readings.

In the eastern part of the specimen including fatigue cracked part, fracture crack propagated in a path almost perpendicular to fatigue force direction. In the western part of the specimen where rapid fracture occurred, fracture crack propagation path curved with an angle of about 30˚ from the horizontal axis.

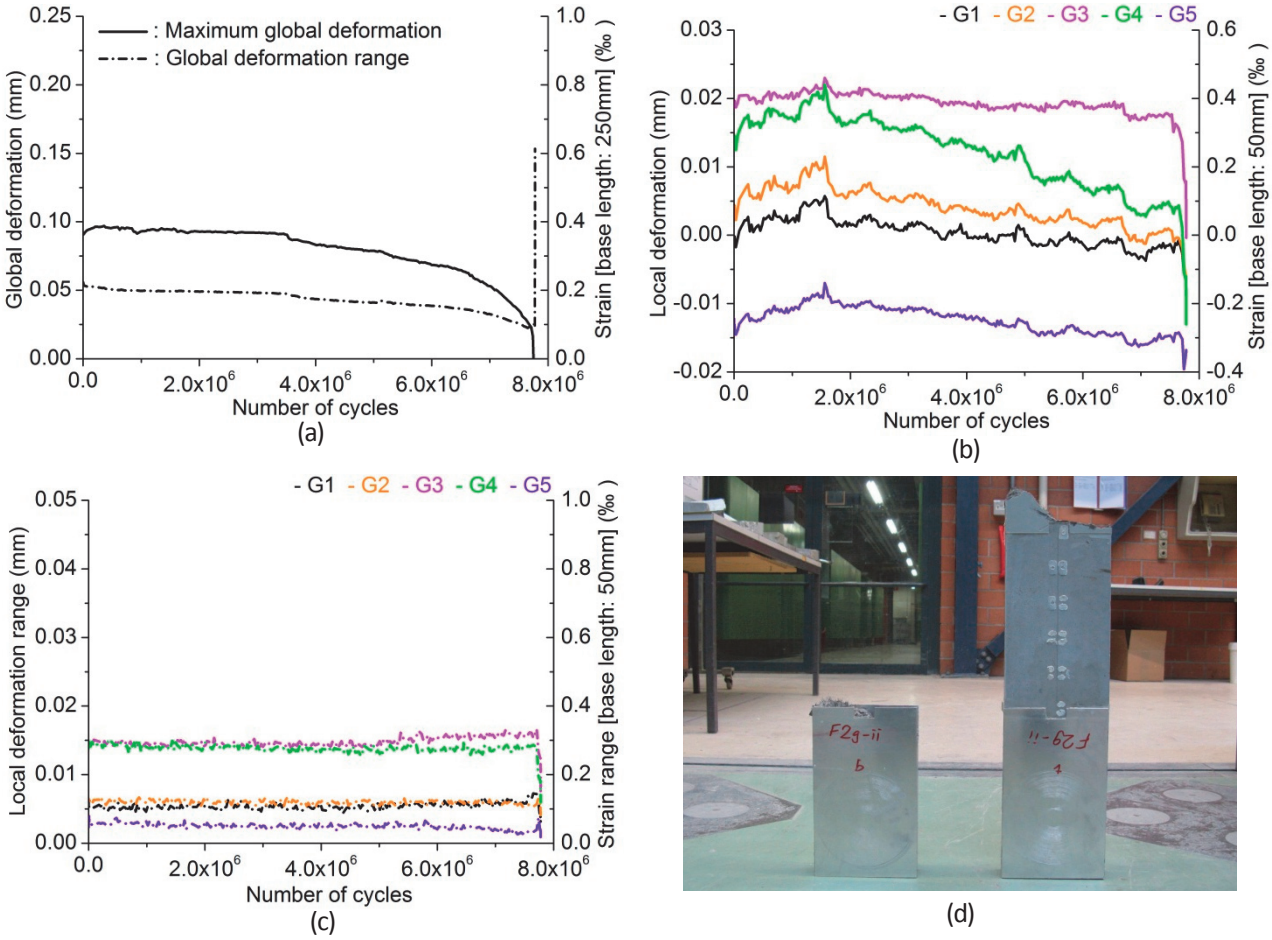


**Figure 66** S3-1 test: growth curves of (a) maximum global deformation and global deformation range, (b) maximum local deformation, (c) local deformation range and (d) fractured specimen

***Fatigue fracture surface of S3-1 test specimen:***

The area covered with rust-coloured powdery products is shown with an enclosing line in Fig. 67. Few fibres were observed in that area, which was identified as a fatigue cracked area. The other area had rough surface with fibres of moderate density. Direction of the fatigue fracture crack propagation was extrapolated and indicated with two arrows in Fig. 67.

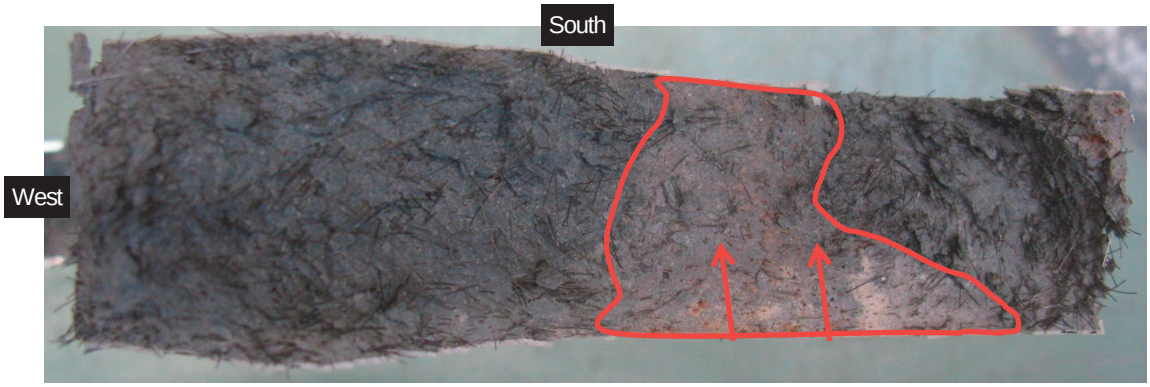


**Figure 67** Fatigue fracture surface of S3-1 test specimen (upper half of the fractured specimen)

### 5.5.2 S3-2 test

***Mechanical properties of the specimen***

| $f_{e,i}$ [MPa] | $\varepsilon_{e,i}$ [‰] | $E$ [GPa] |
|---|---|---|
| 10.1 | 0.35 | 38.2 |

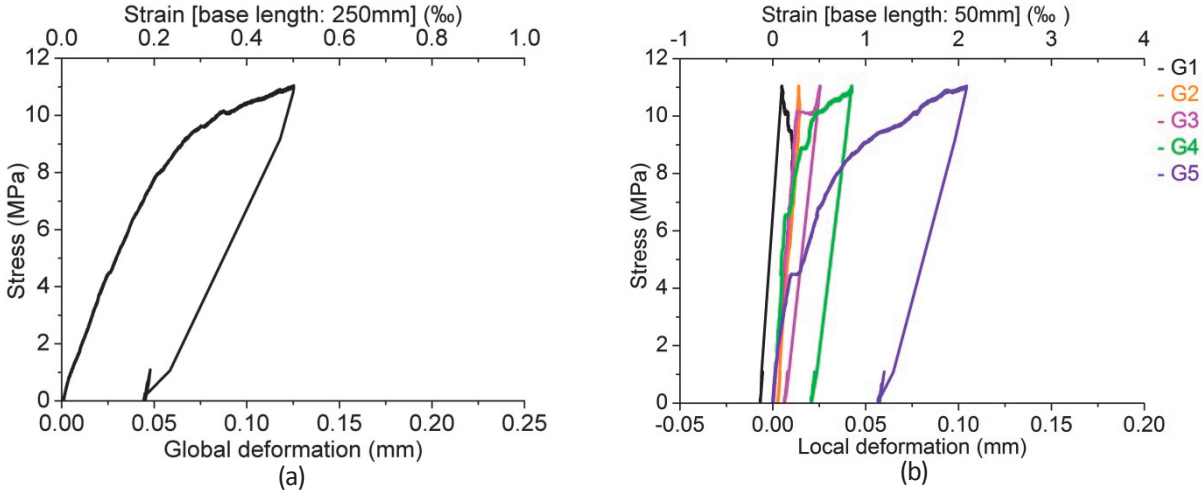


**Figure 68** Stress-deformation curves obtained from quasi-static tensile preloading preceding the S3-2 test (a) global deformation and (b) local deformation

**First fatigue test**

***Test parameters and results***

| $\sigma_{max}$ [MPa] | $\sigma_{min}$ [MPa] | $\varepsilon_{pre}$ [‰] | $\sigma_{max}/f_{e,i}$ | $N$ | Deformation localisation |
|---|---|---|---|---|---|
| 6.3 | 0.63 | 0.50 | 0.62 | 10,069,570 | run-out |

Comment: Stress causing 0.15 ‰ global strain was determined as maximum fatigue stress from the stress-deformation curve obtained from quasi-static tensile preloading.

***Behaviour of S3-2 test specimen during the first fatigue test***

Maximum global deformation and global deformation range kept approximately constant.

Maximum local deformation at all local zones kept approximately constant. At about 5,197,100 cycles it suddenly rose and then became again approximately constant soon. Local deformation range at all local zones kept approximately constant.

Variations were observed on local deformation readings.

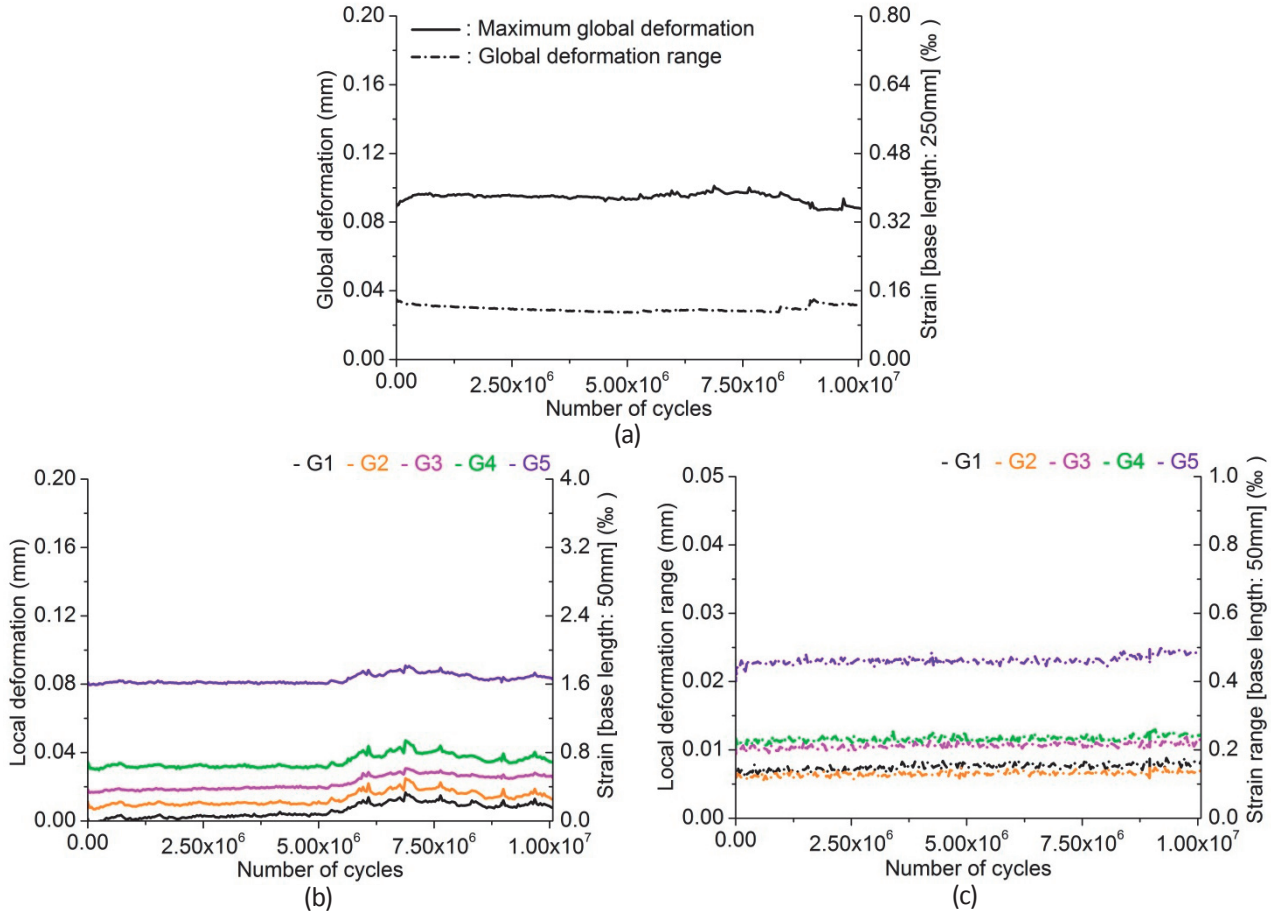


**Figure 69** S3-2_i test: growth curves of (a) maximum global deformation and global deformation range, (b) maximum local deformation and (c) local deformation range

**Second fatigue test**

***Test parameters and results***

| $\sigma_{max}$ [MPa] | $\sigma_{min}$ [MPa] | $\sigma_{max}/f_{e,i}$ | $N$ | Deformation localisation |
|---|---|---|---|---|
| 7.8 | 0.78 | 0.77 | 10,056,789 | run-out |

Comment: Stress causing 0.20 ‰ global strain was determined as maximum fatigue stress from the stress-deformation curve obtained from quasi-static tensile preloading.

***Behaviour of S3-2 test specimen during the second fatigue test***

Maximum global deformation gradually increased until about 6,170,000 cycles, after which it kept approximately constant. Global deformation range increased with lower growth rate than maximum global deformation.

Both maximum local deformation and local deformation range at all local zones except G5 zone increased with varying growth rate. Maximum local deformation and local deformation range at G5 zone kept almost constant.

Variations were left on local deformation readings.

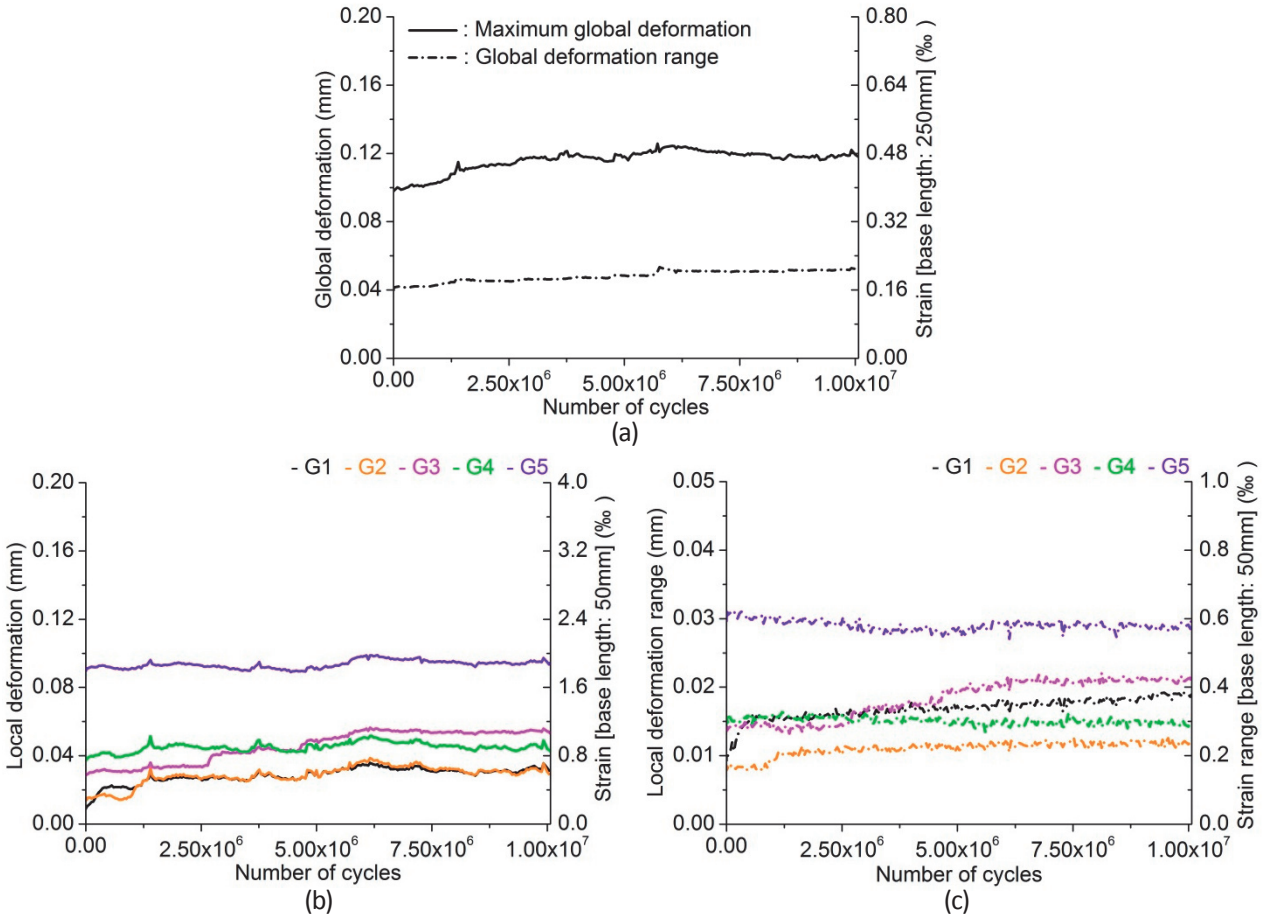


**Figure 70** S3-2_ii test: growth curves of (a) maximum global deformation and global deformation range, (b) maximum local deformation and (c) local deformation range

**Third fatigue test**

***Test parameters and results***

| $\sigma_{max}$ [MPa] | $\sigma_{min}$ [MPa] | $\sigma_{max}/f_{e,i}$ | $N$ | Deformation localisation |
|---|---|---|---|---|
| 8.8 | 0.88 | 0.87 | 7,093,824 | G3 zone |

Comment: Stress causing 0.25 ‰ global strain was determined as maximum fatigue stress from the stress-deformation curve obtained from quasi-static tensile preloading.

***Behaviour of S3-2 test specimen during the third fatigue test***

Maximum global deformation increased gradually, and at about 1,607,500 cycles, redistribution of localised deformation occurred at G3 zone and maximum deformation reading suddenly rose by about 0.15 mm. Afterwards, maximum global deformation continued to increase with the same growth rate as before, and when maximum global strain reached about 2.4 ‰, its growth rate started to increase significantly and eventually the specimen fractured. Behaviour of global deformation range was similar to that of maximum global deformation, while its growth rate was smaller than growth rate of maximum global deformation.

Maximum local deformation at G3 zone showed similar behaviour to maximum global deformation. Eventually, Deformation localised at G3 zone. Maximum local deformation readings at G1, G2 and G5 suddenly rose slightly when redistribution of localised deformation occurred at G3 zone, after which those kept nearly constant. Maximum local deformation at G4 zone gradually increased until redistribution of localised deformation at G3 zone, after which it gradually decreased. UHPFRC at all local zones except G3 zone softened when deformation localised at G3 zone.

Variations remained on local deformation readings.

Fracture crack propagated in a path inclined from horizontal axis with an angle of about 20˚.

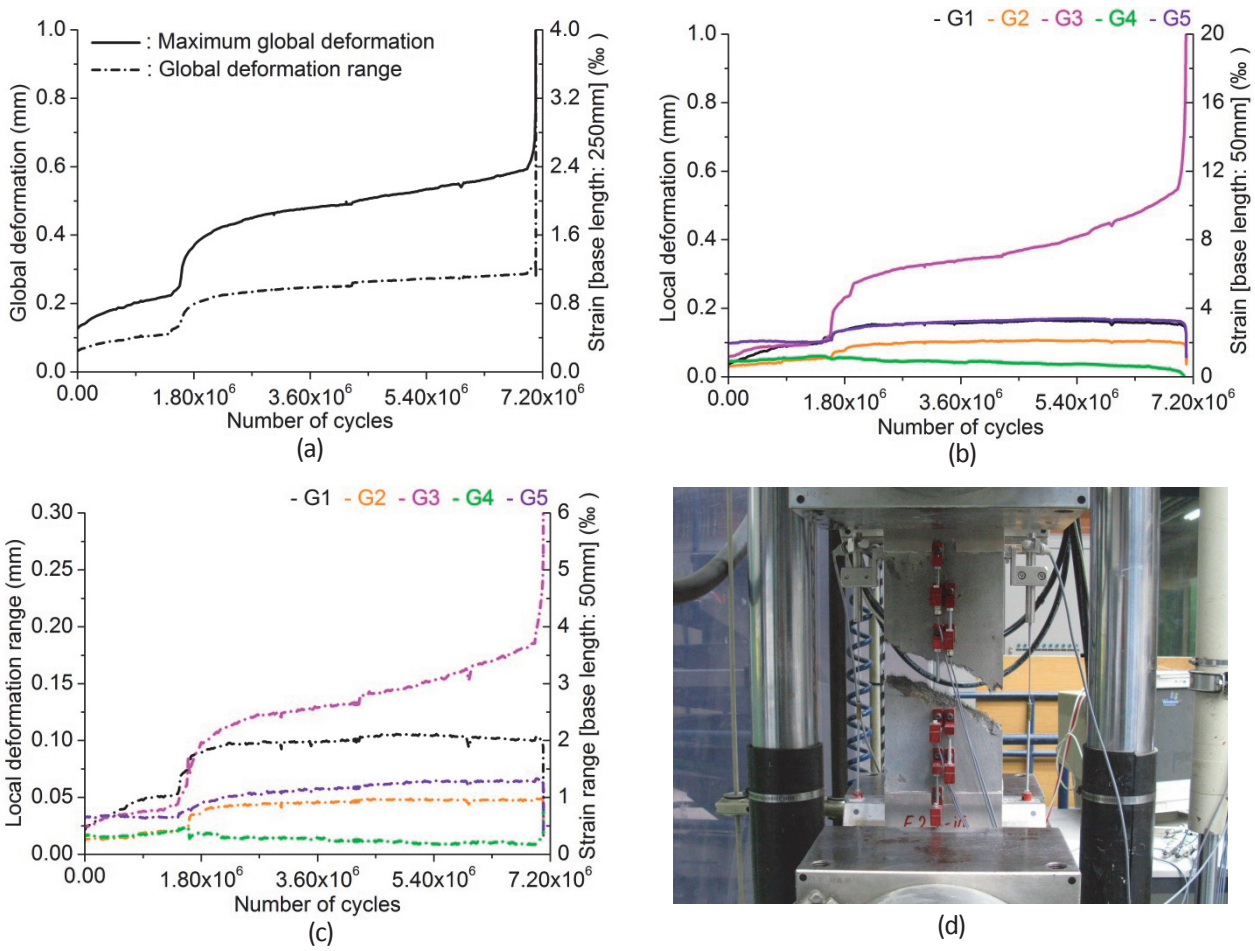


**Figure 71** S3-2_iii test: growth curves of (a) maximum global deformation and global deformation range, (b) maximum local deformation, (c) local deformation range and (d) fractured S3-2 test specimen

***Fatigue fracture surface of S3-2 test specimen:***

Fatigue cracked area is enclosed with a line in Fig. 72, which was identified with rust-coloured powdery products. Smoother part was identified in the fatigue cracked area and fatigue fracture crack was supposed to initiate from the smoother part. Direction of the fatigue fracture crack propagation was extrapolated and indicated with two arrows in Fig. 72.

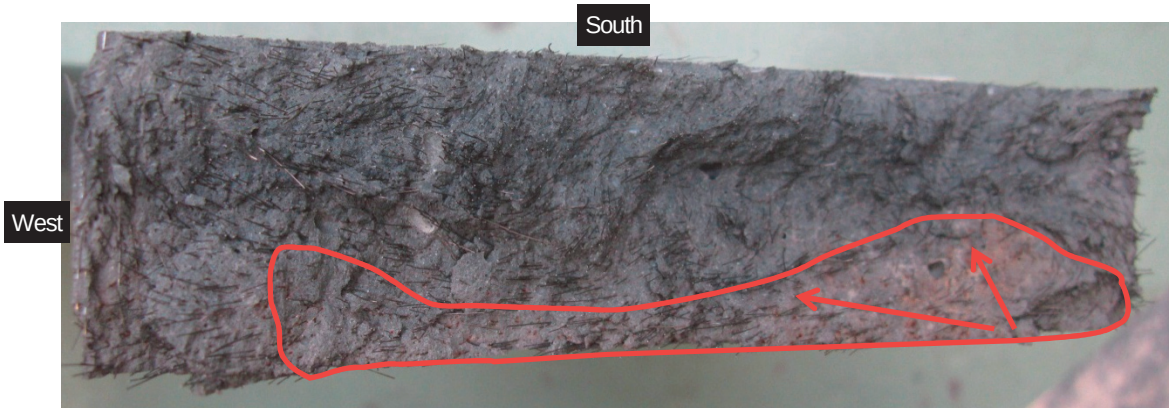


**Figure 72** Fatigue fracture surface of S3-2 test specimen (upper half of the fractured specimen)

### 5.5.3 S3-3 test

***Mechanical properties of the specimen***

| $f_{e,i}$ [MPa] | $\varepsilon_{e,i}$ [‰] | $E$ [GPa] |
|---|---|---|
| 10.5 | 0.28 | 49.8 |

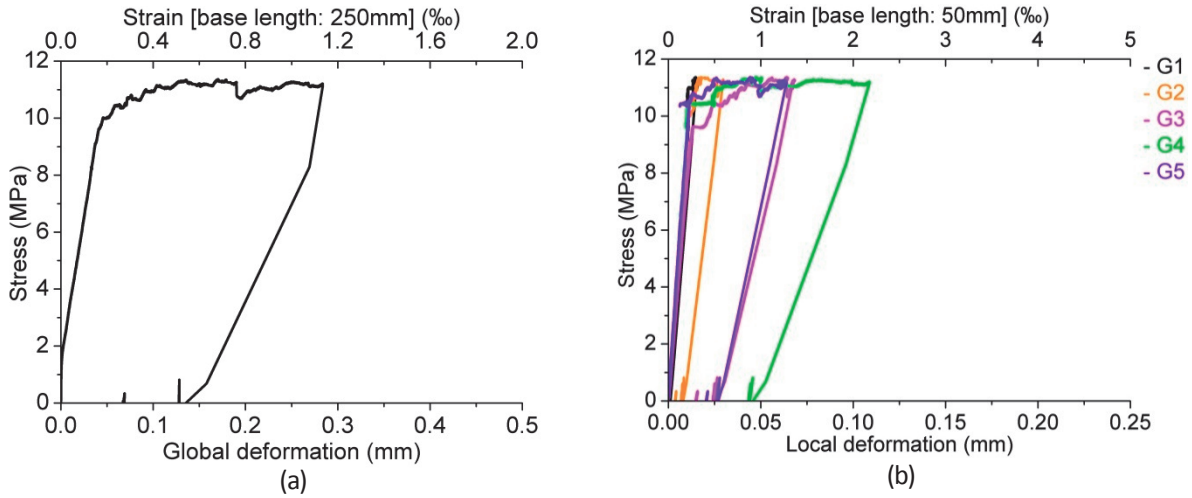


**Figure 73** Stress-deformation curves obtained from quasi-static tensile preloading preceding the S3-3 test (a) global deformation and (b) local deformation

**First fatigue test**

***Test parameters and results***

| $\sigma_{max}$ [MPa] | $\sigma_{min}$ [MPa] | $\varepsilon_{pre}$ [‰] | $\sigma_{max}/f_{e,i}$ | $N$ | Deformation localisation |
|---|---|---|---|---|---|
| 5.9 | 0.59 | 1.13 | 0.56 | 10,000,000 | run-out |

Comment: Stress causing 0.10 ‰ global strain was determined as maximum fatigue stress from the stress-deformation curve obtained from quasi-static tensile preloading.

***Behaviour of S3-3 test specimen during the first fatigue test***

Maximum global deformation, global deformation range, maximum local deformation and local deformation range at all local zones kept approximately constant.

Variations were observed on local deformation range.

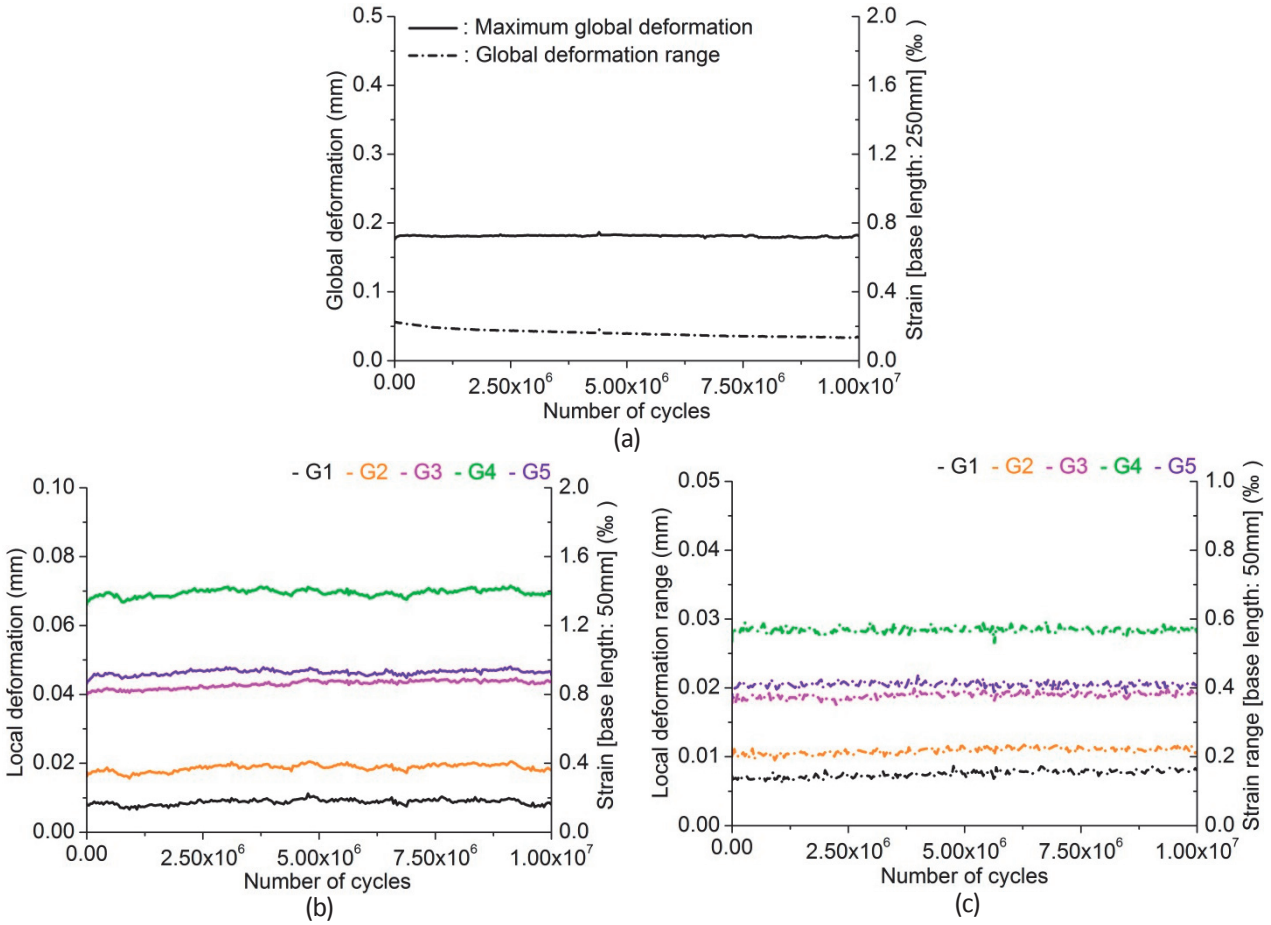


**Figure 74** S3-3_i test: growth curves of (a) maximum global deformation and global deformation range, (b) maximum local deformation and (c) local deformation range

**Second fatigue test**

***Test parameters and results***

| $\sigma_{max}$ [MPa] | $\sigma_{min}$ [MPa] | $\sigma_{max}/f_{e,i}$ | $N$ | Deformation localisation |
|---|---|---|---|---|
| 8.4 MPa | 0.84 MPa | 0.80 | 7,107,413 | G5 zone and outside of G5 zone |

Comment: Stress causing 0.15 ‰ global strain was determined as maximum fatigue stress from the stress-deformation curve obtained from quasi-static tensile preloading.

***Behaviour of S3-3 test specimen during the second fatigue test***

Maximum global deformation increased changing its growth rate until fracture of the specimen. Behaviour of global deformation range was similar to that of maximum global deformation, while its growth rate was more stable than that of maximum global deformation.

Maximum local deformation at G5 zone gradually decreased until just before deformation localised at G5 zone and outside of G5 zone. Maximum local deformation at the other local zones increased with varying growth rate until deformation localisation at G5 zone, at which UHPFRC at these local zones softened. Behaviour of local deformation range was similar to that of maximum local deformation.

Variations remained on local deformation readings.

Fracture crack propagation path was irregular and inclined from horizontal axis with an angle of about 10˚ in general.

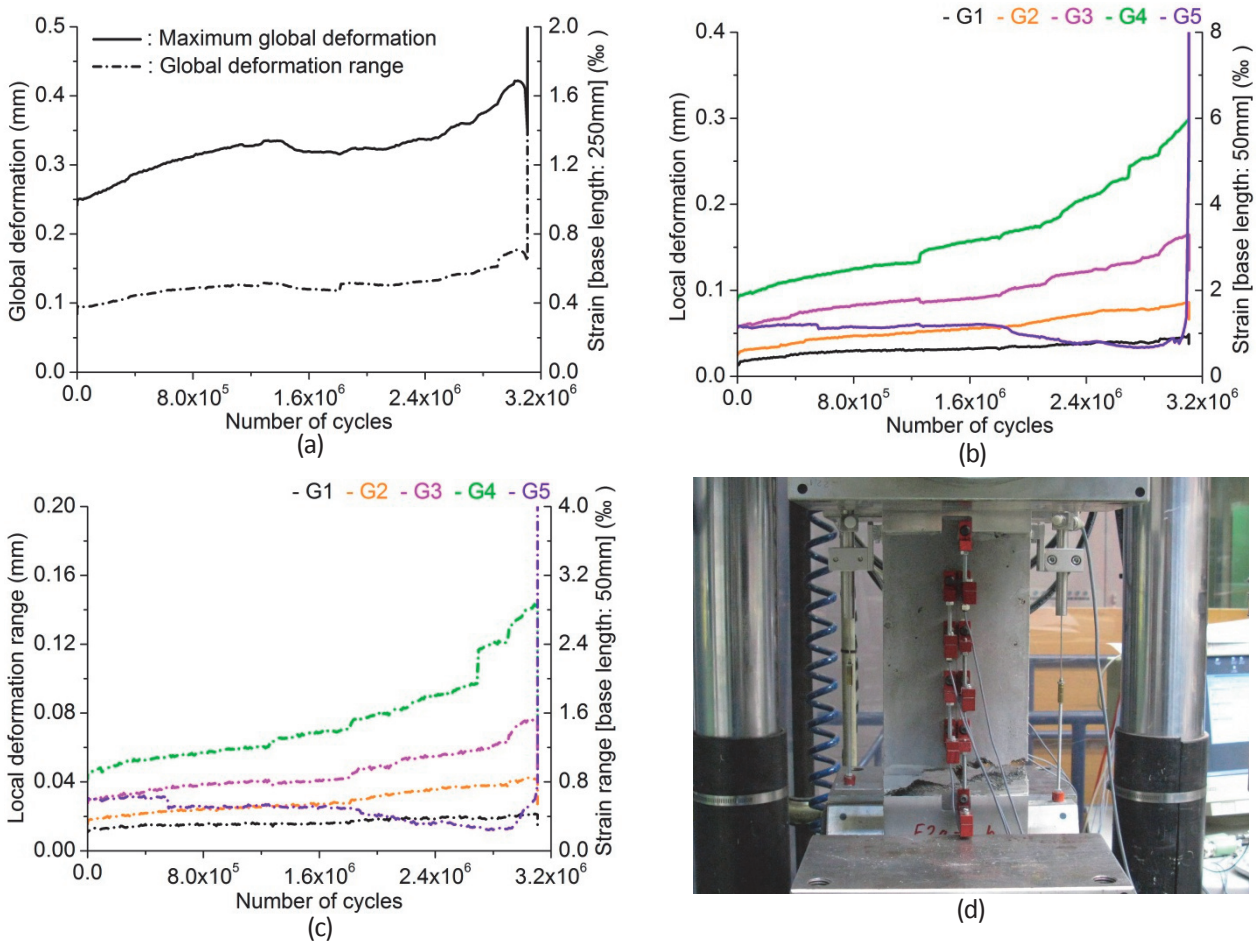


**Figure 75** S3-3_ii test: growth curves of (a) maximum global deformation and global deformation range, (b) maximum local deformation, (c) local deformation range and (d) fractured S3-3 test specimen

***Fatigue fracture surface of S3-3 test specimen:***

Fatigue cracked area was clearly identified with rust-coloured powdery products covering a part of the fracture surface (enclosed with a line in Fig. 76). Its surface was smooth and few fibres were observed on the fatigue cracked area, while the other part of the fracture surface was rough and lots of fibres remained on it. Where fatigue fracture crack initiated was extrapolated from geometry of the fatigue cracked area. Direction of the fatigue fracture crack propagation is indicated with two arrows in Fig. 76.

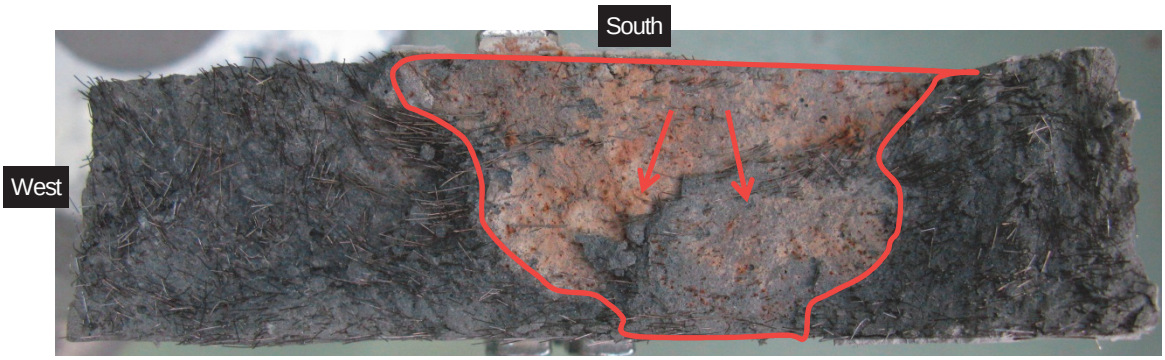


**Figure 76** Fatigue fracture surface of S3-3 test specimen (upper half of the fractured specimen)

### 5.5.4 S3-4 test

***Mechanical properties of the specimen***

| $f_{e,i}$ [MPa] | $\varepsilon_{e,i}$ [‰] | $E$ [GPa] |
|---|---|---|
| 10.7 | 0.25 | 63.8 |

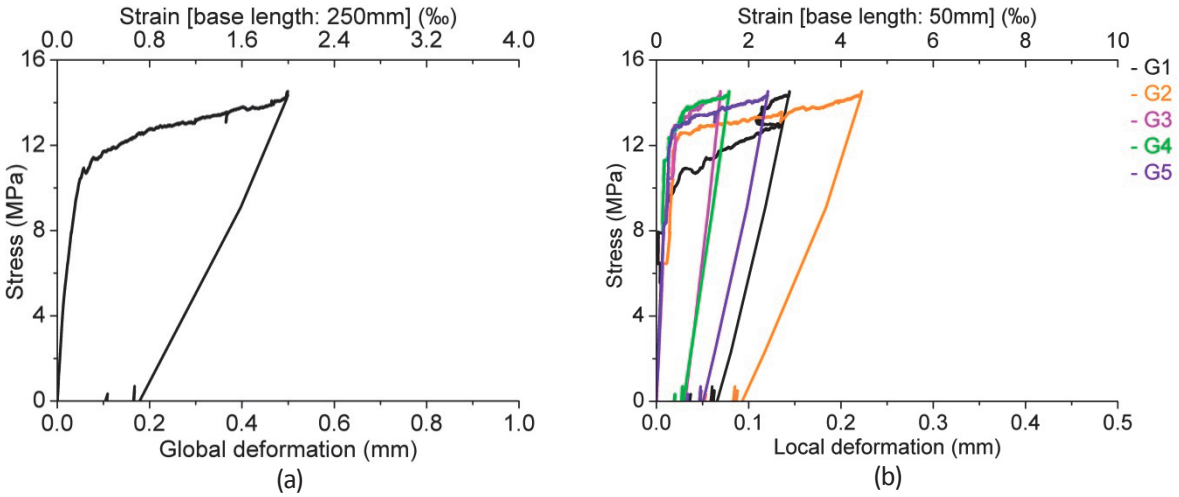


**Figure 77** Stress-deformation curves obtained from quasi-static tensile preloading preceding the S3-4 test (a) global deformation and (b) local deformation

**First fatigue test**

***Test parameters and results***

| $\sigma_{max}$ [MPa] | $\sigma_{min}$ [MPa] | $\varepsilon_{pre}$ [‰] | $\sigma_{max}/f_{e,i}$ | $N$ | Deformation localisation |
|---|---|---|---|---|---|
| 6.9 | 0.69 | 1.99 | 64.5 | 5,002,373 | run-out |

Comment: For the logistics reason, the first fatigue test was stopped at 5 million cycles. Stress causing 0.10 ‰ global strain was determined as maximum fatigue stress from the stress-deformation curve obtained from quasi-static tensile preloading.

***Behaviour of S3-4 test specimen during the first fatigue test***

Maximum global deformation and global deformation range kept approximately constant.

Maximum local deformation and local deformation range at all local zones except G1 zone kept approximately constant. Maximum local deformation at G1 zone kept constant until about 2,182,200 cycles, at which its reading suddenly rose by about 0.15 mm, which was caused by redistribution of localised deformation. Afterwards, it again kept constant. Local deformation range at G1 zone slightly increased until about 2,182,200 cycles and then kept constant.

Variations were observed on local deformation readings.

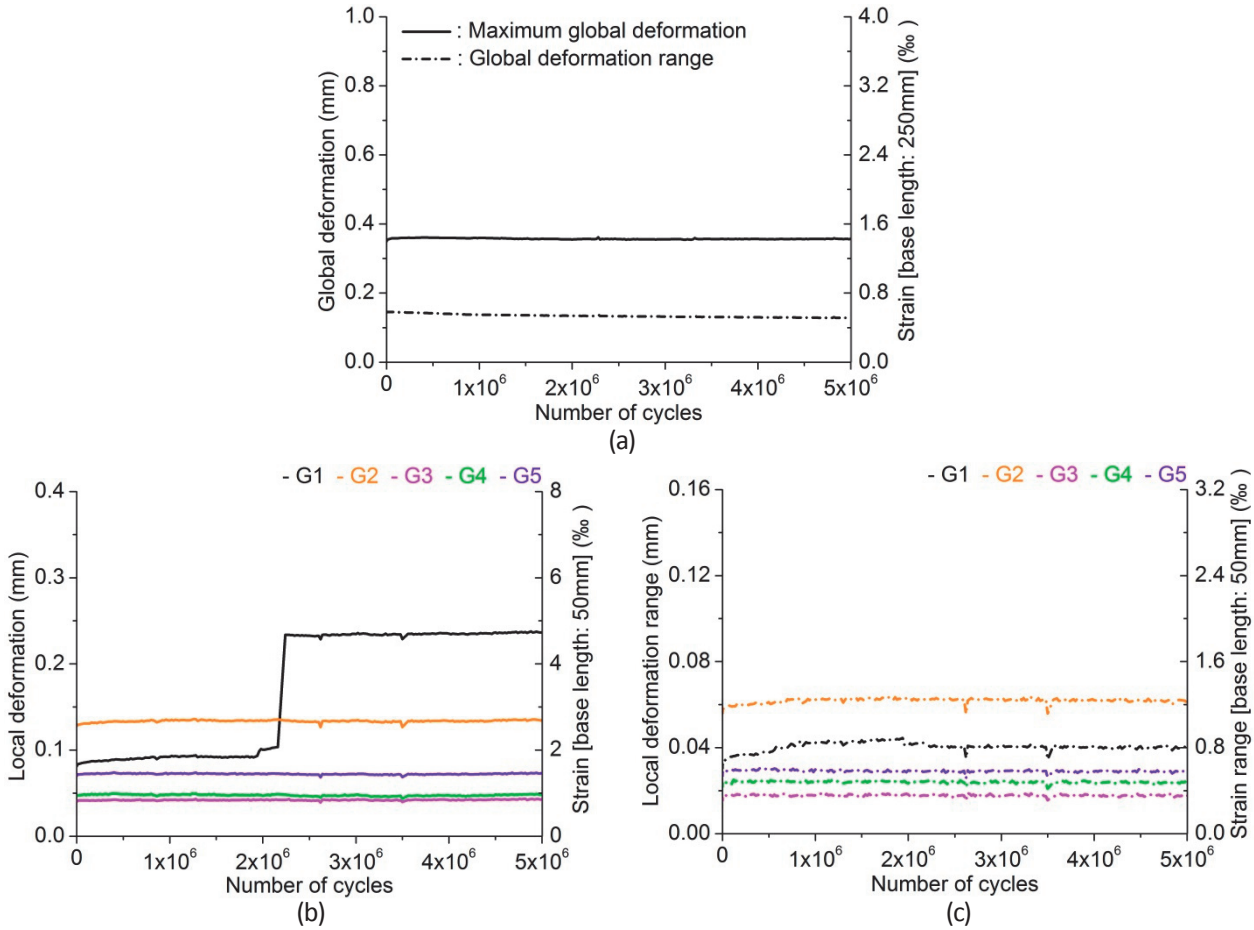


**Figure 78** S3-4_i test: growth curves of (a) maximum global deformation and global deformation range, (b) maximum local deformation and (c) local deformation range

**Second fatigue test**

***Test parameters and results***

| $\sigma_{max}$ [MPa] | $\sigma_{min}$ [MPa] | $\sigma_{max}/f_{e,i}$ | $N$ | Deformation localisation |
|---|---|---|---|---|
| 9.0 MPa | 0.90 MPa | 0.84 | 2,000,072 | run-out |

Comment: For the logistics reason, the second fatigue test was stopped at 2 million cycles. Stress causing 0.15 ‰ global strain was determined as maximum fatigue stress from the stress-deformation curve obtained from quasi-static tensile preloading.

***Behaviour of S3-4 test specimen during the second fatigue test***

Maximum global deformation, global deformation range, maximum local deformation at all local zones except G1 zone and local deformation range at all local zones kept approximately constant.

Maximum local deformation at G1 zone increased quite sharply by about 0.1 mm soon after beginning the test and then kept constant.

Variations were left on local deformation readings.

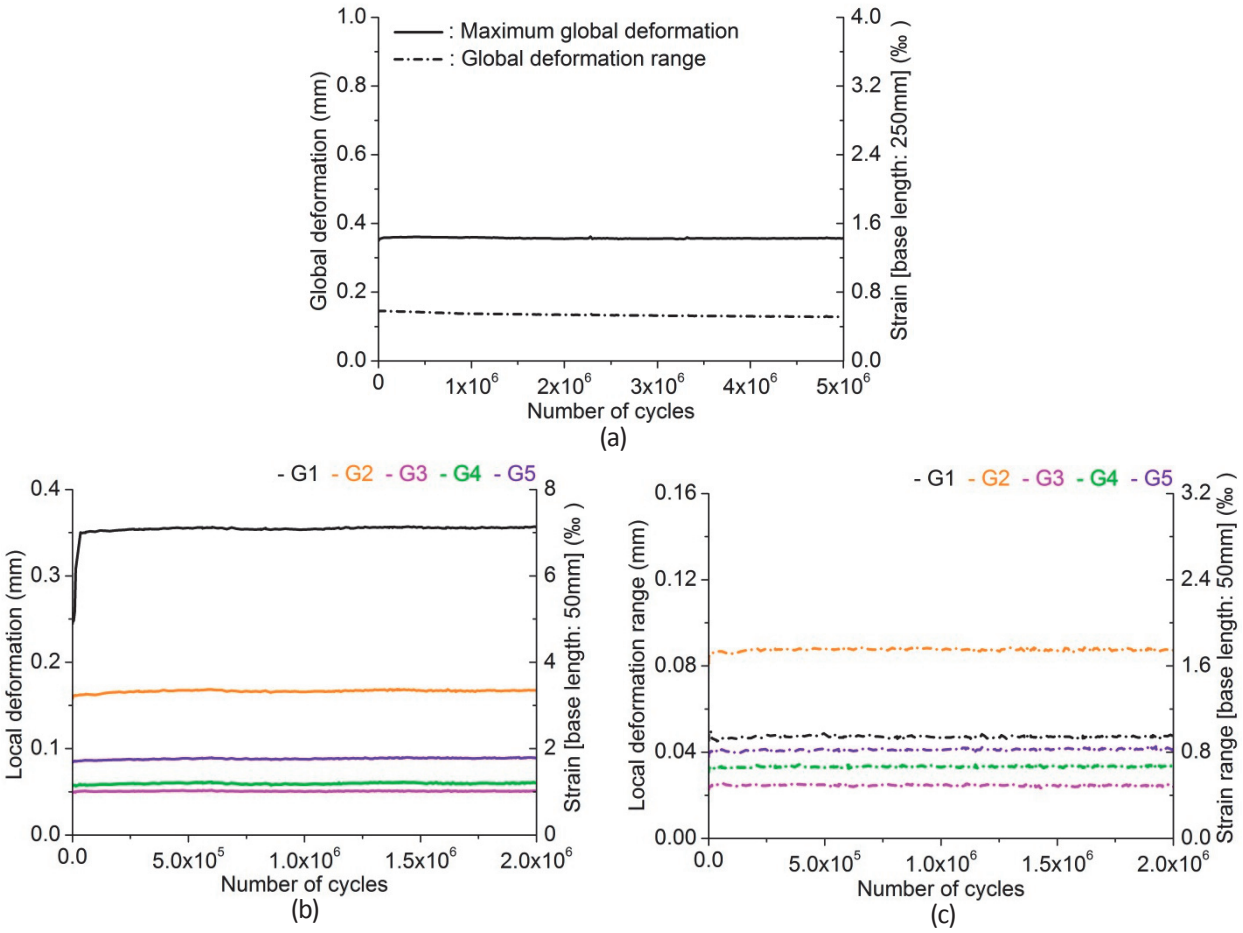


**Figure 79** S3-4_ii test: growth curves of (a) maximum global deformation and global deformation range, (b) maximum local deformation and (c) local deformation range

**Third fatigue test**

***Test parameters and results***

| $\sigma_{max}$ [MPa] | $\sigma_{min}$ [MPa] | $\sigma_{max}/f_{e,i}$ | $N$ | Deformation localisation |
|---|---|---|---|---|
| 10.4 MPa | 1.04 MPa | 0.97 | 64,717 | G1 zone and outside of G1 zone |

Comment: Stress causing 0.20 ‰ global strain was determined as maximum fatigue stress from the stress-deformation curve obtained from quasi-static tensile preloading.

***Behaviour of S3-4 test specimen during the third fatigue test***

Maximum global deformation increased constantly. When maximum global deformation reached about 2.4 ‰ strain, its growth rate started to increase and eventually the specimen fractured. Behaviour of global deformation range was similar to that of maximum global deformation, while its growth rate was smaller than growth rate of maximum global deformation.

Maximum local deformation at all local zones except G1 zone kept approximately constant or increased slightly. Maximum local deformation at G1 zone also kept constant, but at about 30,000 cycles it started to decrease, which might be due to micro- and macrocracking under the base of LVDTs. Eventually deformation localised at G5 zone. Behaviour of local deformation range was similar to that of maximum local deformation at all local zones except G5 zone; local deformation range at G5 zone gradually decreased and its reading wasn't the largest among all local zones like maximum local deformation.

Variations were left on local deformation readings.

Although slightly curved, fracture crack propagation path was almost perpendicular to fatigue force direction.

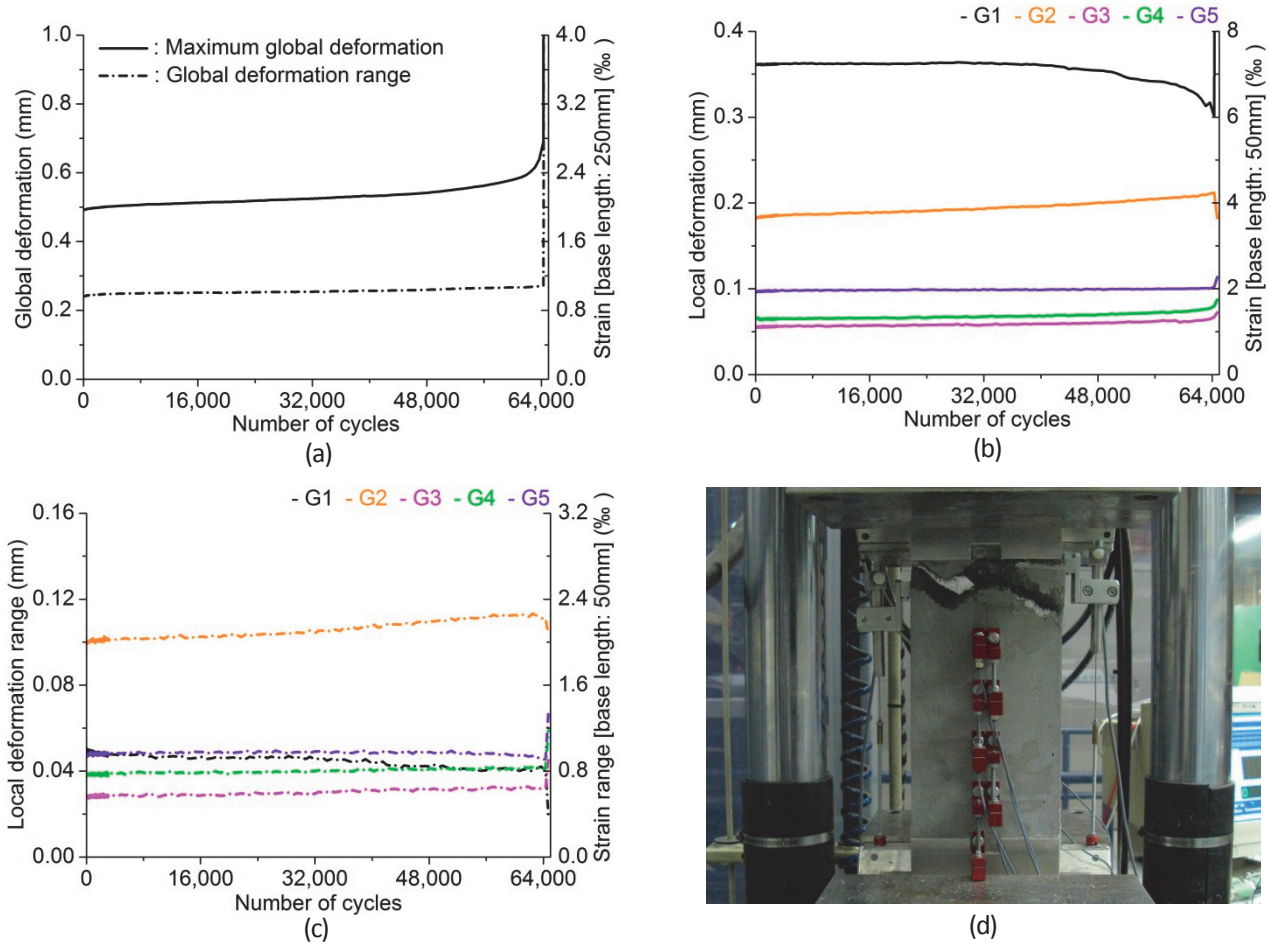


**Figure 80** S3-4_iii test: growth curves of (a) maximum global deformation and global deformation range, (b) maximum local deformation, (c) local deformation range and (d) fractured S3-4 test specimen

***Fatigue fracture surface of S3-4 test specimen:***

Two separated areas with few fibres were observed on the fatigue fracture surface (enclosed with lines in Fig. 81). One of the areas was covered with small amount of rust-coloured powdery products. The other area might have had few fibres initially. Propagation direction of the fatigue fracture crack wasn't understood.

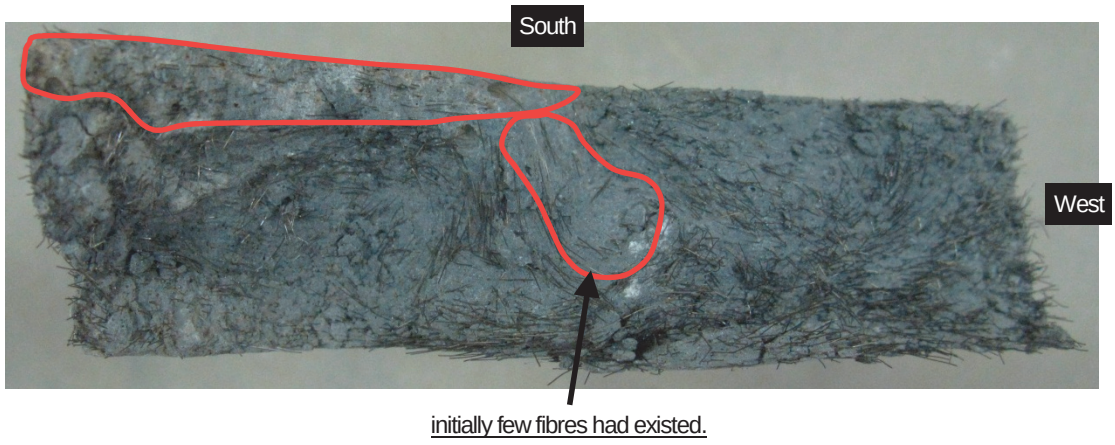


**Figure 81** Fatigue fracture surface of S3-4 test specimen (lower half of the fractured specimen)

### 5.5.5 S3-5 test

***Mechanical properties of the specimen***

| $f_{e,i}$ [MPa] | $\varepsilon_{e,i}$ [‰] | $E$ [GPa] |
|---|---|---|
| 12.5 | 0.24 | 75.8 |

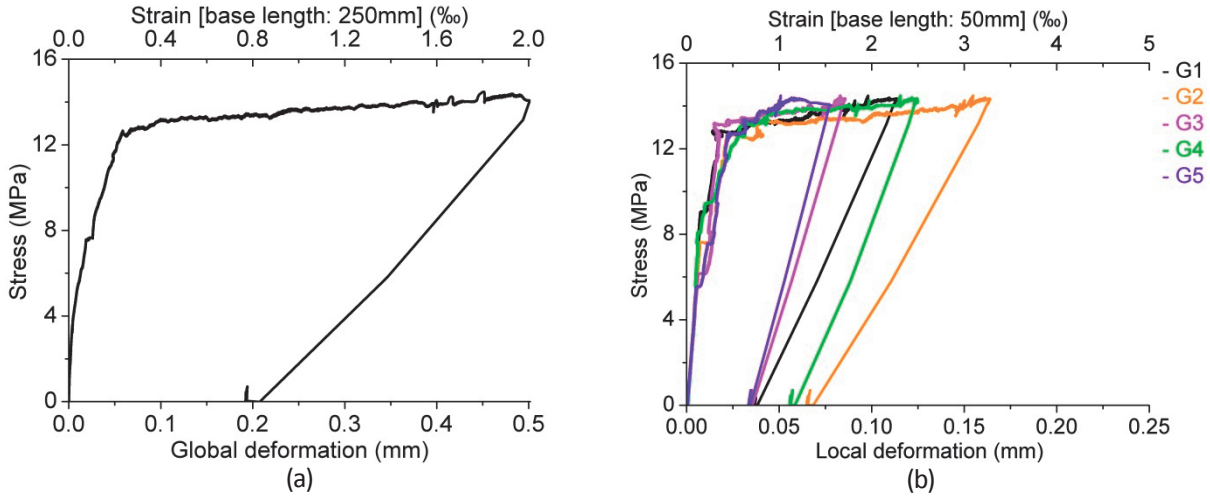


**Figure 82** Stress-deformation curves obtained from quasi-static tensile preloading preceding the S3-5 test (a) global deformation and (b) local deformation

**First fatigue test**

***Test parameters and results***

| $\sigma_{max}$ [MPa] | $\sigma_{min}$ [MPa] | $\varepsilon_{pre}$ [‰] | $\sigma_{max}/f_{e,i}$ | $N$ | Deformation localisation |
|---|---|---|---|---|---|
| 7.6 | 0.76 | 2.01 | 0.61 | 10,000,000 | run-out |

Comment: Stress causing 0.10 ‰ global strain was determined as maximum fatigue stress from the stress-deformation curve obtained from quasi-static tensile preloading.

***Behaviour of S3-5 test specimen during the first fatigue test***

Maximum global deformation and global deformation range kept approximately constant.

Maximum local deformation at G1 and G2 zones decreased until about 6,530,000 cycles and then kept approximately constant. Maximum local deformation at G3 to G5 zones increased until about 4,540,000 cycles and then gradually decreased. Behaviour of local deformation range was relatively similar to that of maximum local deformation at all local zones, while growth and decrease rate of local deformation range was much smaller than those of maximum local deformation.

Variations were observed on local deformation readings.

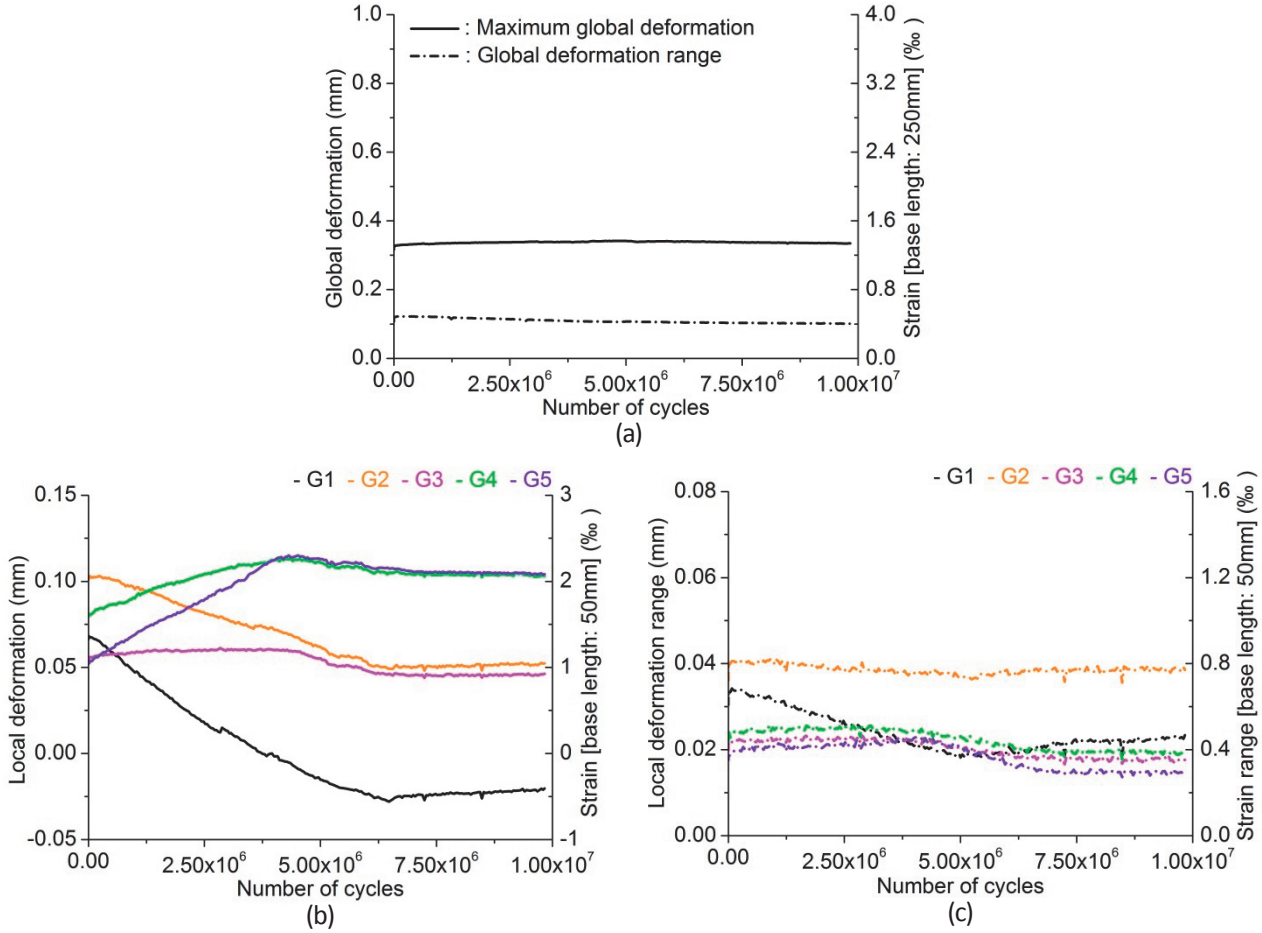


**Figure 83** S3-5_i test: growth curves of (a) maximum global deformation and global deformation range, (b) maximum local deformation and (c) local deformation range

**Second fatigue test**

***Test parameters and results***

| $\sigma_{max}$ [MPa] | $\sigma_{min}$ [MPa] | $\sigma_{max}/f_{e,i}$ | $N$ | Deformation localisation |
|---|---|---|---|---|
| 11.7 MPa | 1.17 MPa | 0.94 | 113,500 | outside of G1 zone |

Comment: Stress causing 0.20 ‰ global strain was determined as maximum fatigue stress from the stress-deformation curve obtained from quasi-static tensile preloading.

***Behaviour of S3-5 test specimen during the second fatigue test***

Since deformation localised outside the measuring devices, deformation growth due to fracture of the specimen wasn't captured.

Maximum global deformation and global deformation range slightly increased.

Maximum local deformation at G1 to G3 zone increased, while maximum local deformation at G4 and G5 zones slightly decreased. Growth rate of maximum local deformation at G1 and G2 zones gradually increased from about 70,000 cycles to the end of the test. All local deformation range gradually decreased.

Variations were left on local deformation readings.

Fracture crack propagation path was perpendicular to fatigue force direction.

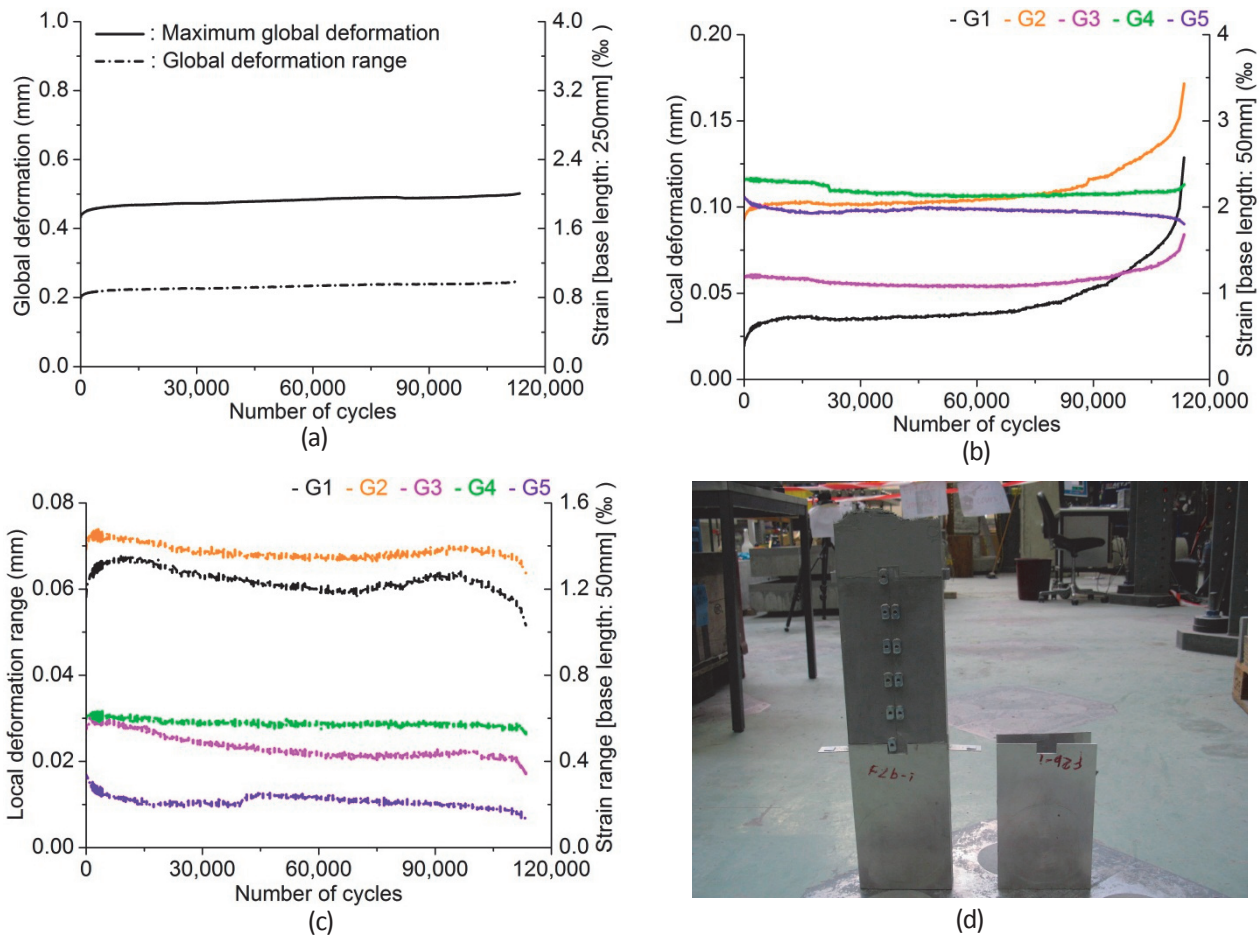


**Figure 84** S3-5_ii test: growth curves of (a) maximum global deformation and global deformation range, (b) maximum local deformation, (c) local deformation range and (d) fractured S3-5 test specimen

***Fatigue fracture surface of S3-5 test specimen:***

Fatigue cracked area wasn't observed on the fatigue fracture surface. The entire fracture surface was rough and uniformly distributed fibres were observed on it. Orientation of fibres in the central part of the fracture surface was roughly perpendicular to fatigue force direction (enclosed with a line in Fig. 85).

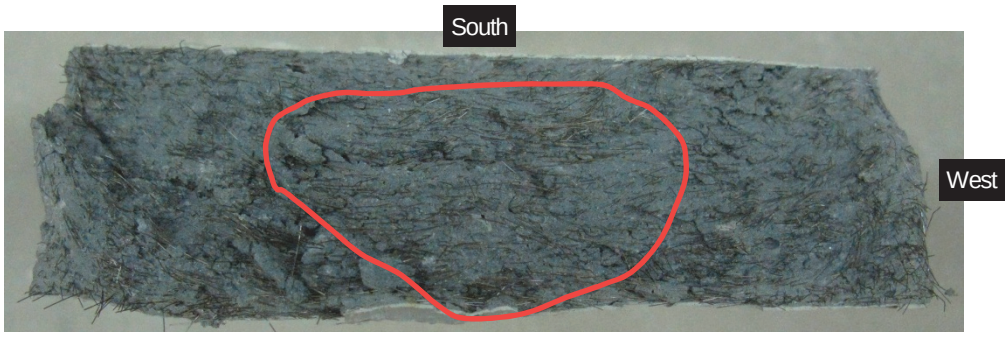


**Figure 85** Fatigue fracture surface of S3-5 test specimen (lower half of the fractured specimen)

### 5.5.6 S3-6 test

***Mechanical properties of the specimen***

| $f_{e,i}$ [MPa] | $\varepsilon_{e,i}$ [‰] | $E$ [GPa] |
|---|---|---|
| 9.0 | 0.31 | 36.8 |

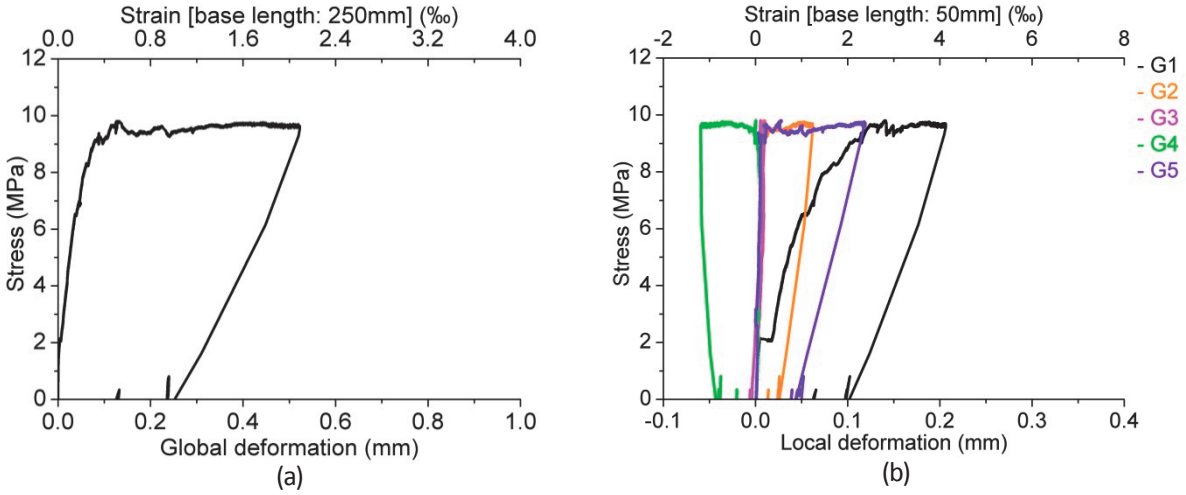


**Figure 86** Stress-deformation curves obtained from quasi-static tensile preloading preceding the S3-6 test (a) global deformation and (b) local deformation

***Test parameters and results***

| $\sigma_{max}$ [MPa] | $\sigma_{min}$ [MPa] | $\varepsilon_{pre}$ [‰] | $\sigma_{max}/f_{e,i}$ | $N$ | Deformation localisation |
|---|---|---|---|---|---|
| 5.2 | 0.52 | 2.09 | 0.58 | 7,869,999 | G4 zone and outside of G5 zone |

Comment: Stress causing 0.15 ‰ global strain was determined as maximum fatigue stress from the stress-deformation curve obtained from quasi-static tensile preloading.

***Behaviour of S3-6 test specimen***

Since deformation localised outside the measuring devices, deformation growth due to fracture of the specimen wasn't captured.

Maximum global deformation gradually increased. At about 6,901,100 cycles, it suddenly rose due to redistribution of localised deformation, after which its growth rate became larger than before. When maximum global deformation reached about 1.7 ‰ strain, its growth rate started to increase and the specimen fractured. Global deformation range kept approximately constant.

Maximum local deformation and local deformation range at all local zones kept approximately constant.

Variations were observed on local deformation readings.

Two fracture cracks appeared due to in-plane bending of the specimen. Propagation path of both fracture cracks was almost perpendicular to fatigue force direction.

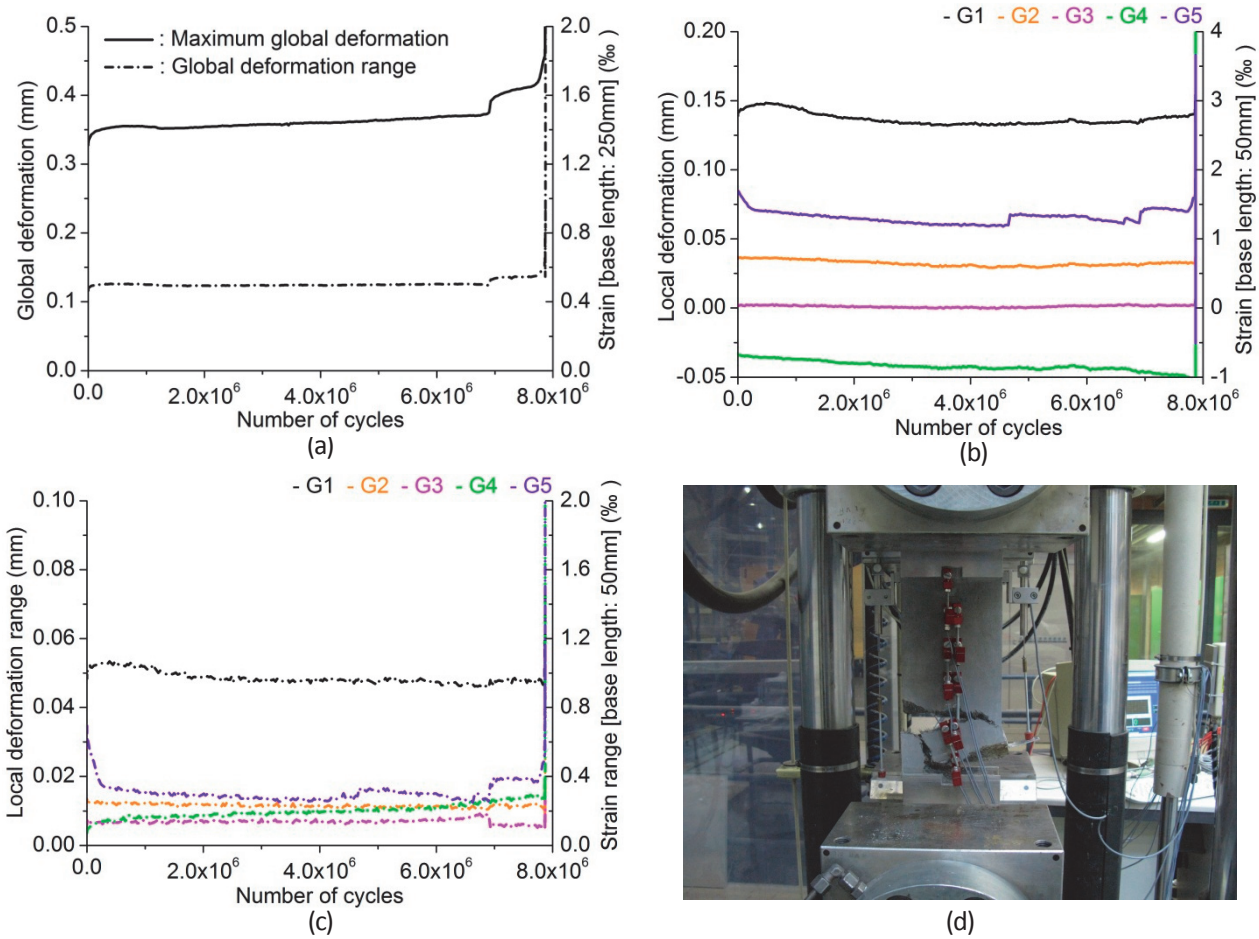


**Figure 87** S3-6 test: growth curves of (a) maximum global deformation and global deformation range, (b) maximum local deformation, (c) local deformation range and (d) fractured specimen

***Fatigue fracture surface of S3-6 test specimen:***

Western area of the fracture surface was covered with rust-coloured powdery products and smoother than the other area (enclosed with a line in Fig. 88). It was understood as fatigue cracked area. Based on the idea that a part of fatigue cracked area covered with deeper rust-coloured products in the fatigue cracked area is where fatigue fracture crack initiated, direction of fatigue fracture crack propagation was extrapolated (indicated with an arrow in Fig. 88).


**Figure 88** Fatigue fracture surface of S3-6 test specimen (lower half of the fractured specimen)

### 5.5.7 S3-7 test

***Mechanical properties of the specimen***

| $f_{e,i}$ [MPa] | $\varepsilon_{e,i}$ [‰] | $E$ [GPa] |
|---|---|---|
| 10.3 | 0.32 | 45.1 |

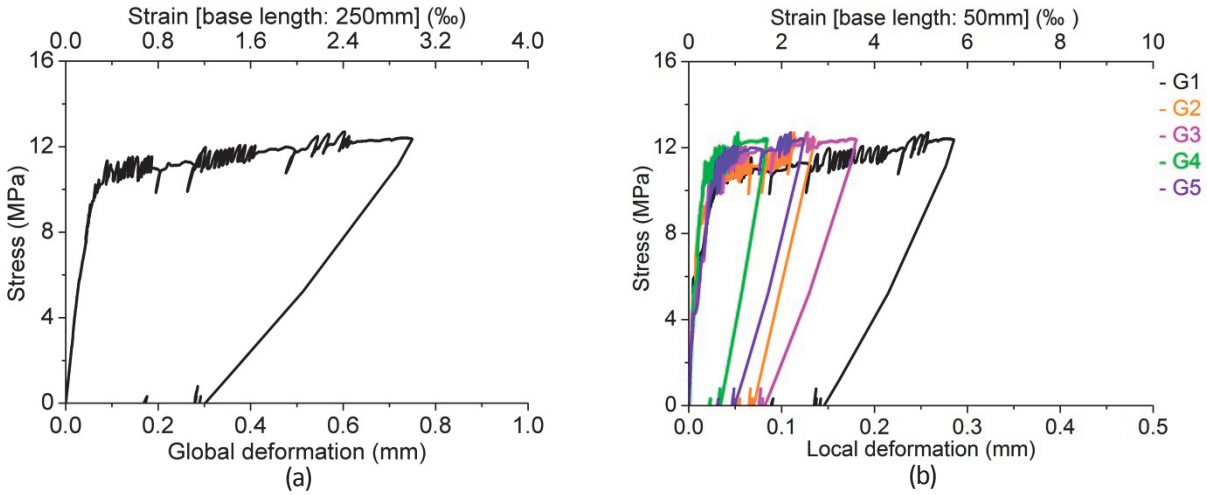


**Figure 89** Stress-deformation curves obtained from quasi-static tensile preloading preceding the S3-7 test (a) global deformation and (b) local deformation

**First fatigue test**

***Test parameters and results***

| $\sigma_{max}$ [MPa] | $\sigma_{min}$ [MPa] | $\varepsilon_{pre}$ [‰] | $\sigma_{max}/f_{e,i}$ | $N$ | Deformation localisation |
|---|---|---|---|---|---|
| 6.7 | 0.67 | 3.00 | 0.65 | 10,082,808 | run-out |

Comment: Stress causing 0.15 ‰ global strain was determined as maximum fatigue stress from the stress-deformation curve obtained from quasi-static tensile preloading.

***Behaviour of S3-7 test specimen during the first fatigue test***

Maximum global deformation, global deformation range, maximum local deformation and local deformation range at all local zones kept almost constant.

Variations were observed on local deformation readings.

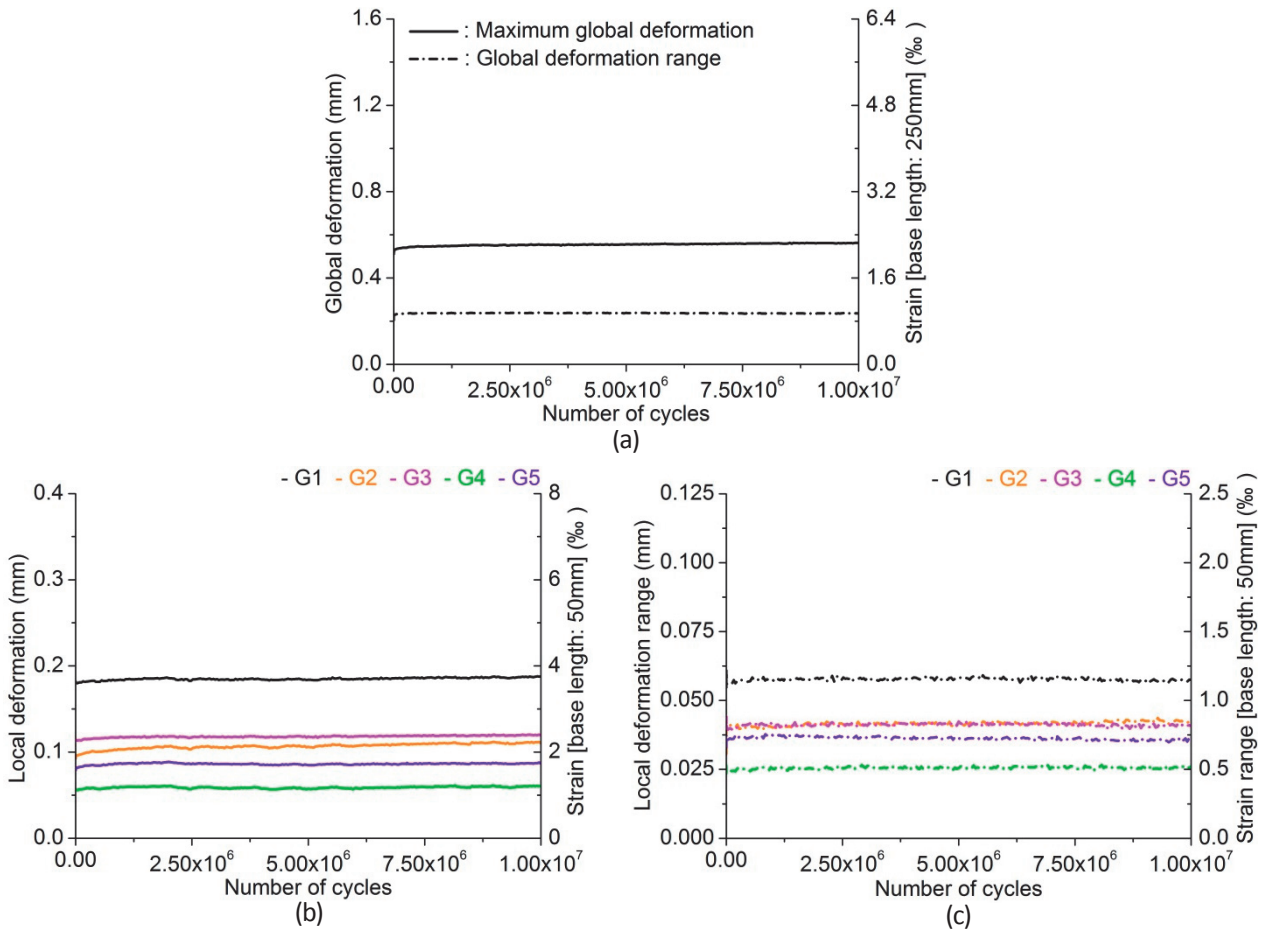


**Figure 90** S3-7_i test: growth curves of (a) maximum global deformation and global deformation range, (b) maximum local deformation and (c) local deformation range

**Second fatigue test**

***Test parameters and results***

| $\sigma_{max}$ [MPa] | $\sigma_{min}$ [MPa] | $\sigma_{max}/f_{e,i}$ | $N$ | Deformation localisation |
|---|---|---|---|---|
| 8.7 MPa | 0.87 MPa | 0.84 | 84,075 | G2 zone |

Comment: Stress causing 0.20 ‰ global strain was determined as maximum fatigue stress from the stress-deformation curve obtained from quasi-static tensile preloading.

***Behaviour of S3-7 test specimen during the second fatigue test***

Maximum global deformation gradually increased. When maximum global deformation reached about 3.7 ‰ strain, its growth rate started to increase and eventually the specimen fractured. Global deformation range also increased, but it didn't grow as significantly as maximum global deformation when the specimen fractured.

Maximum local deformation at G2 zone increased with higher growth rate than the other local zones. At about 20,400 cycles, it suddenly rose due to redistribution of localised deformation, after which its growth rate became lower than before. Its growth rate started to increase at the same time as the beginning of increase of maximum global deformation growth rate. Maximum local deformation at G1 and G3 zones slightly increased, and when growth rate of maximum local deformation at G2 zone started to increase, maximum local deformation at G1 and G3 zones started to decrease. Maximum local deformation at G4 and G5 zones kept approximately constant. When deformation localised at G2 zone, UHPFRC at the other local zones softened. Behaviour of local deformation range at all local zones except G2 zone was similar to that of maximum local deformation. Local deformation range at G2 zone kept approximately constant until deformation localisation. Variations remained on local deformation readings.

Fracture crack propagated in a path almost perpendicular to fatigue force direction.

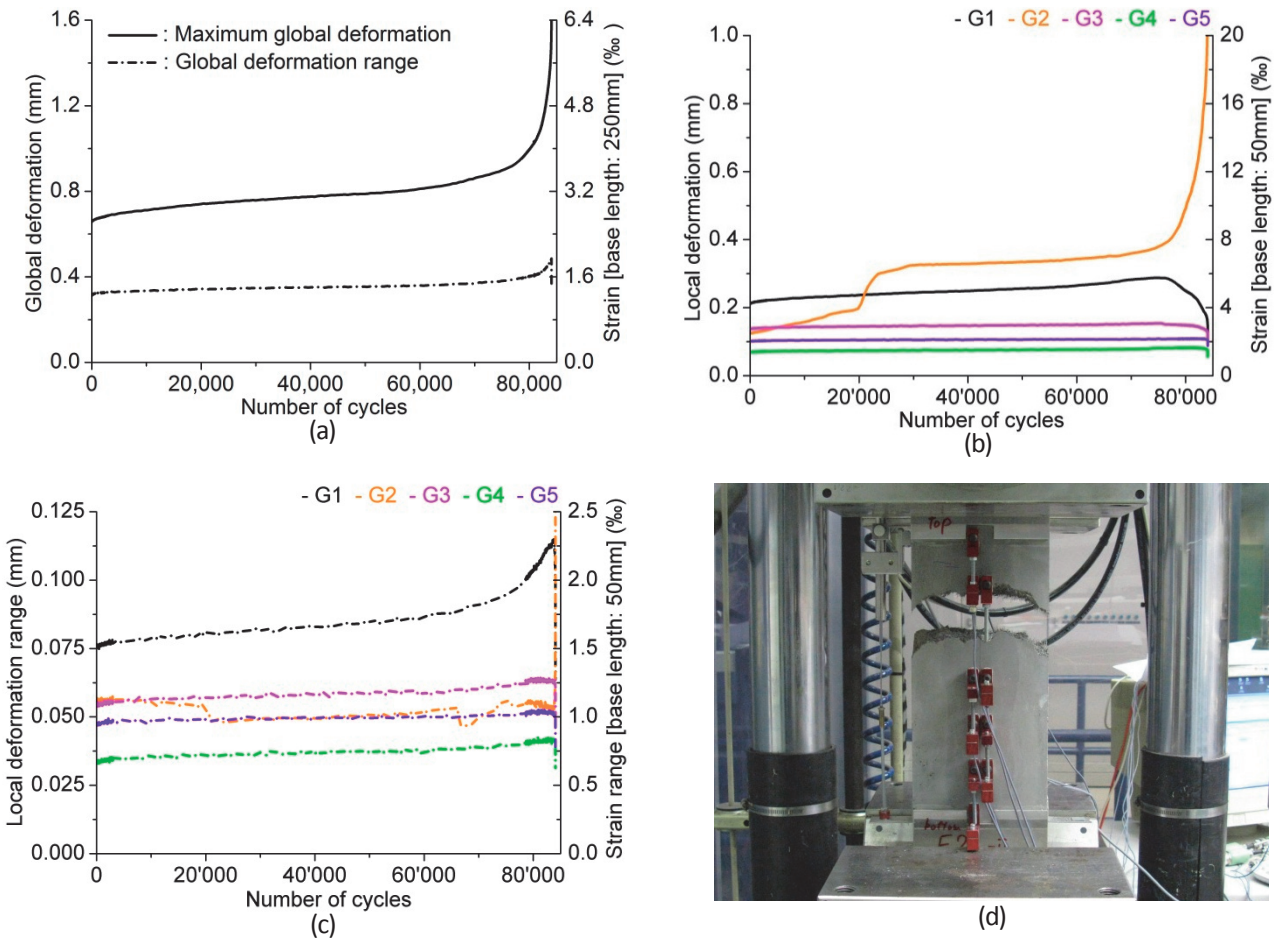


**Figure 91** S3-7_ii test: growth curves of (a) maximum global deformation and global deformation range, (b) maximum local deformation, (c) local deformation range and (d) fractured S3-7 test specimen

***Fatigue fracture surface of S3-7 test specimen:***

South eastern part of the fracture surface was smooth and covered with rust-coloured powdery products, from which it is understood as fatigue cracked area (enclosed with a line in Fig. 92). Fatigue fracture crack was supposed to initiate from the eastern part of the specimen, and its propagation direction was extrapolated from the geometry of smooth surface and indicated with arrows in Fig. 92.

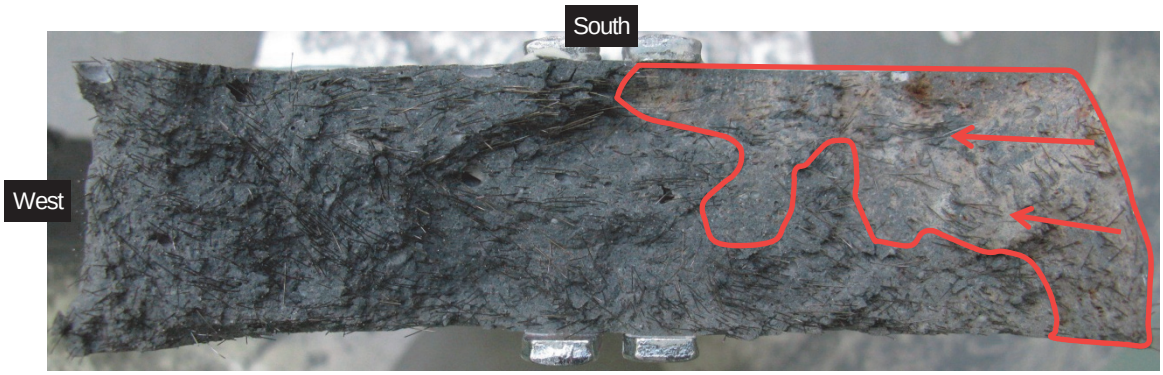


**Figure 92** Fatigue fracture surface of S3-7 test specimen (upper half of the fractured specimen)

### 5.5.8 S3-8 test

***Mechanical properties of the specimen***

| $f_{e,i}$ [MPa] | $\varepsilon_{e,i}$ [‰] | $E$ [GPa] |
|---|---|---|
| 10.3 | 0.28 | 52.0 |

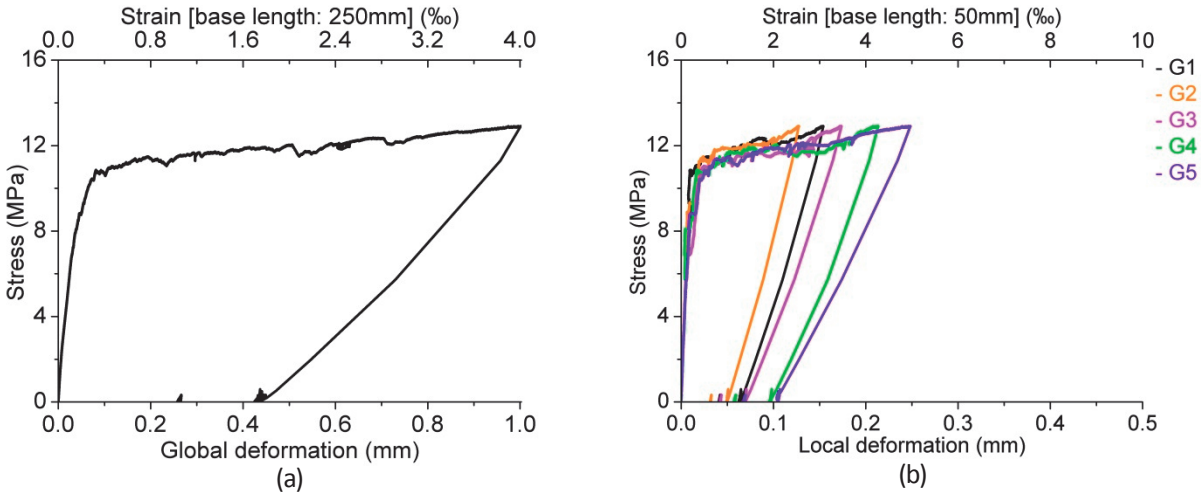


**Figure 93** Stress-deformation curves obtained from quasi-static tensile preloading preceding the S3-8 test (a) global deformation and (b) local deformation

**First fatigue test**

***Test parameters and results***

| $\sigma_{max}$ [MPa] | $\sigma_{min}$ [MPa] | $\varepsilon_{pre}$ [‰] | $\sigma_{max}/f_{e,i}$ | $N$ | Deformation localisation |
|---|---|---|---|---|---|
| 6.0 | 0.60 | 4.00 | 0.58 | 11,363,737 | run-out |

Comment: Stress causing 0.10 ‰ global strain was determined as maximum fatigue stress from the stress-deformation curve obtained from quasi-static tensile preloading.

***Behaviour of S3-8 test specimen during the first fatigue test***

Maximum global deformation, global deformation range, maximum local deformation and local deformation range at all local zones kept almost constant.

Variations were observed on local deformation readings.

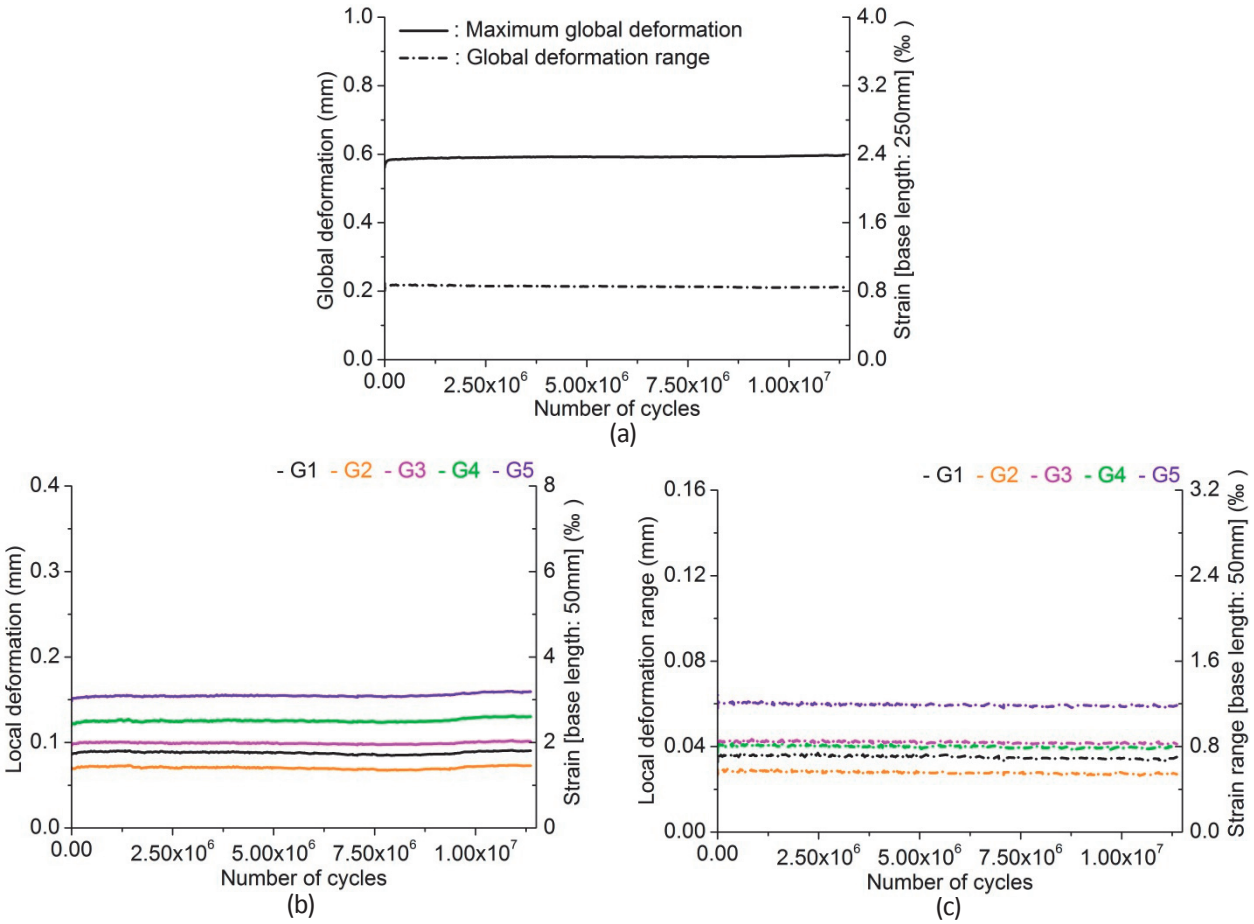


**Figure 94** S3-8_i test: growth curves of (a) maximum global deformation and global deformation range, (b) maximum local deformation and (c) local deformation range

**Second fatigue test**

***Test parameters and results***

| $\sigma_{max}$ [MPa] | $\sigma_{min}$ [MPa] | $\sigma_{max}/f_{e,i}$ | $N$ | Deformation localisation |
|---|---|---|---|---|
| 7.9 | 0.79 | 0.77 | 1,602,088 | G5 zone |

Comment: Stress causing 0.15 ‰ global strain was determined as maximum fatigue stress from the stress-deformation curve obtained from quasi-static tensile preloading.

***Behaviour of S3-8 test specimen during the second fatigue test***

Rapid increase at the beginning and end of the test with long and slow increase at the intermediate stage of the test was identified on the fatigue growth curve of maximum global deformation. When maximum global strain reached about 3.3 ‰, its growth rate began to increase and eventually the specimen fractured. Global deformation range gradually increased, but it didn't rose as significantly as maximum global deformation when the specimen fractured.

Maximum local deformation at all local zones except G5 zone kept approximately constant. Behaviour of maximum local deformation at G5 zone was similar to that of maximum global deformation. Eventually deformation localised at G5 zone. Behaviour of local deformation range at all local zones was quite similar to that of maximum local deformation.

Variations remained on local deformation readings.

Although slightly curved, fracture crack propagated in a path nearly perpendicular to fatigue force direction.

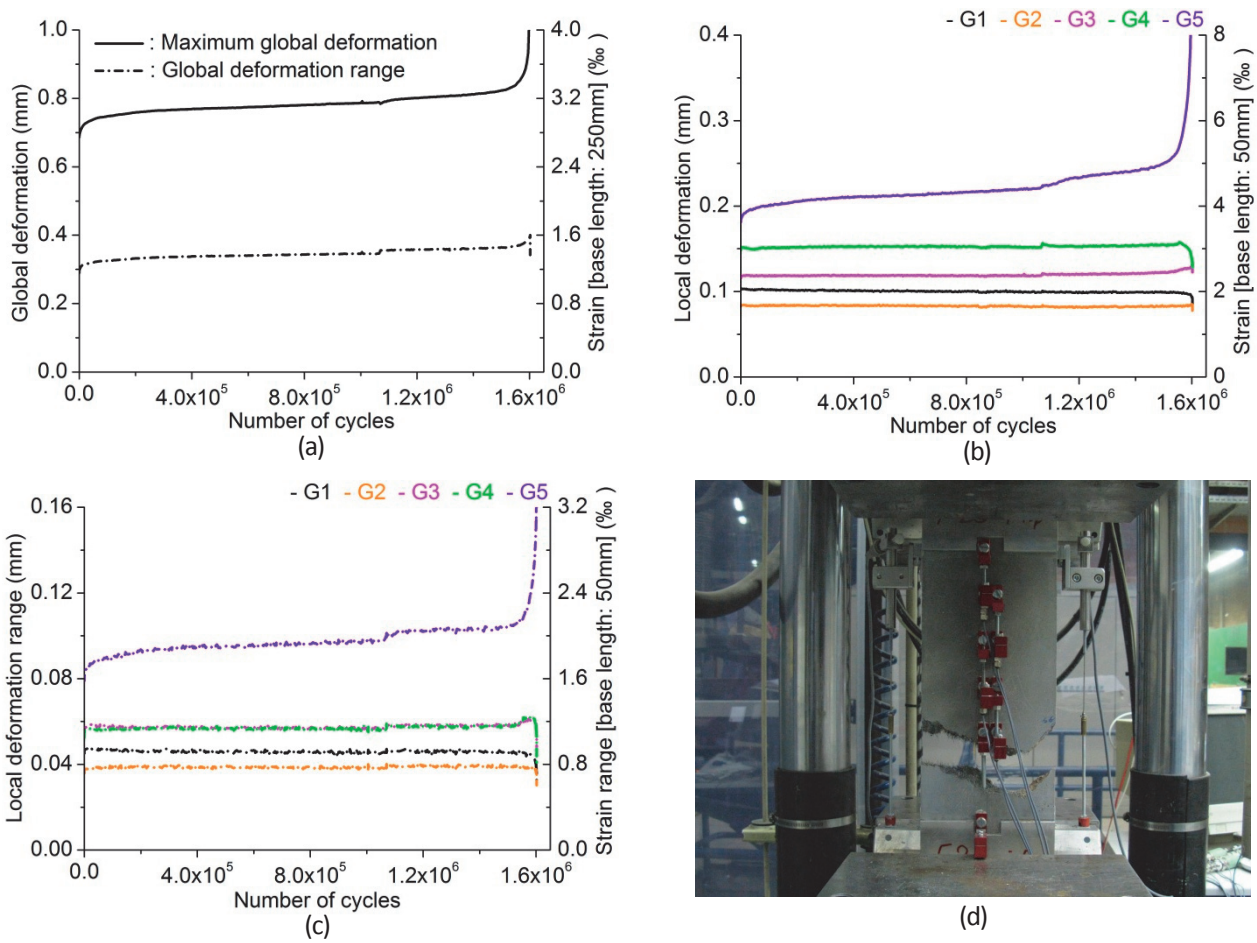


**Figure 95** S3-8_ii test: growth curves of (a) maximum global deformation and global deformation range, (b) maximum local deformation, (c) local deformation range and (d) fractured S3-8 test specimen

***Fatigue fracture surface of S3-8 test specimen:***

Smooth area covered with rust-coloured powdery products was distinguished at the western part of the fracture surface, ranging around 30 % of the total surface area. It was understood as fatigue cracked area (enclosed with a line in Fig. 96. Direction of fatigue fracture crack propagation wasn't understood from examination of fracture surface.

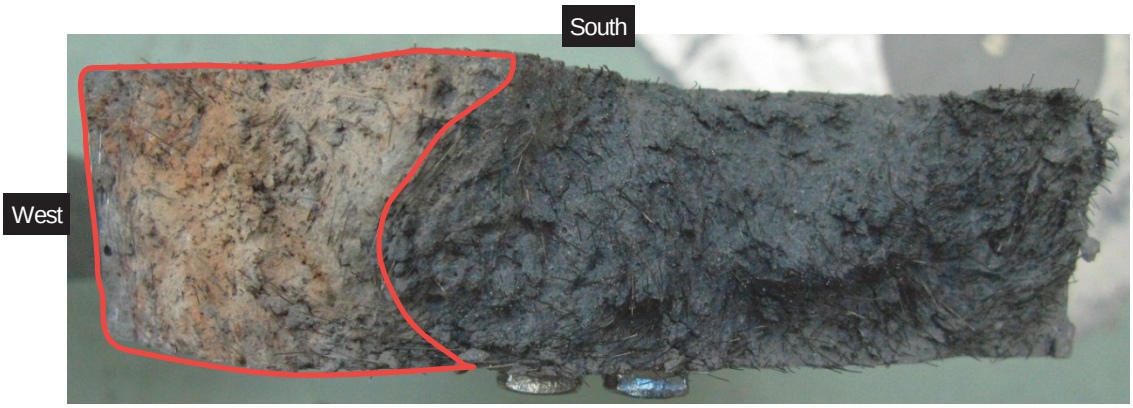


**Figure 96** Fatigue fracture surface of S3-8 test specimen (upper half of the fractured specimen)

### 5.5.9 S3-9 test

***Mechanical properties of the specimen***

| $f_{e,i}$ [MPa] | $\varepsilon_{e,i}$ [‰] | $E$ [GPa] |
|---|---|---|
| 10.0 | 0.31 | 39.0 |

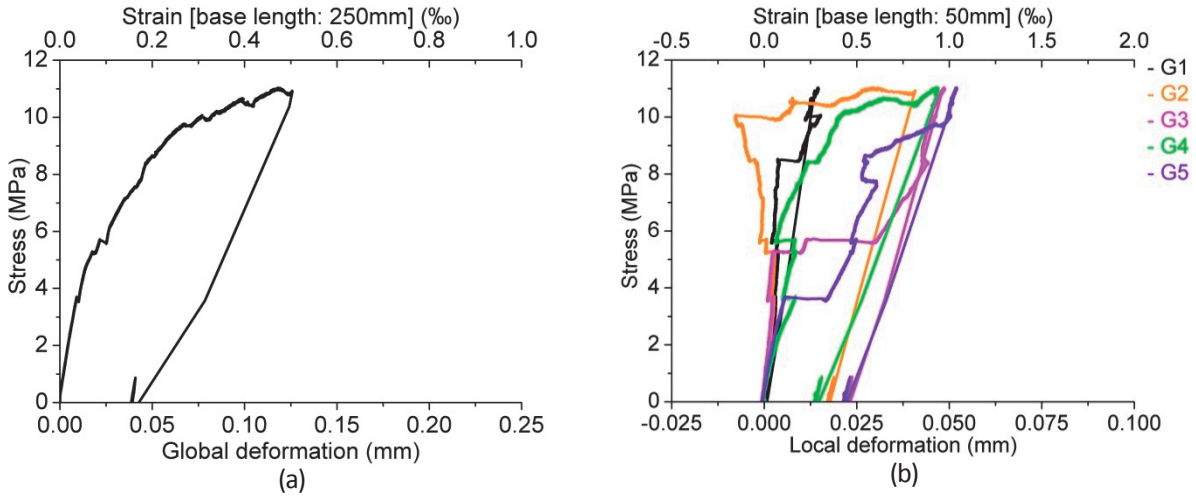


**Figure 97** Stress-deformation curves obtained from quasi-static tensile preloading preceding the S3-9 test (a) global deformation and (b) local deformation

***Test parameters and results***

| $\sigma_{max}$ [MPa] | $\sigma_{min}$ [MPa] | $\varepsilon_{pre}$ [‰] | $\sigma_{max}/f_{e,i}$ | $N$ | Deformation localisation |
|---|---|---|---|---|---|
| 7.2 | 0.72 | 0.50 | 0.72 | 10,000,004 | run-out |

Comment: Stress causing 0.10 ‰ global strain was determined as maximum fatigue stress from the stress-deformation curve obtained from quasi-static tensile preloading.

***Behaviour of S3-9 test specimen***

Maximum global deformation kept unchanged, while global deformation range slightly decreased.

Maximum local deformation at all local zones slightly increased and local deformation range at all local zones kept almost constant.

Variations were observed on local deformation readings.

* Due to operational mistakes of testing machine, S3-9 test specimen was fractured before starting the second fatigue test.

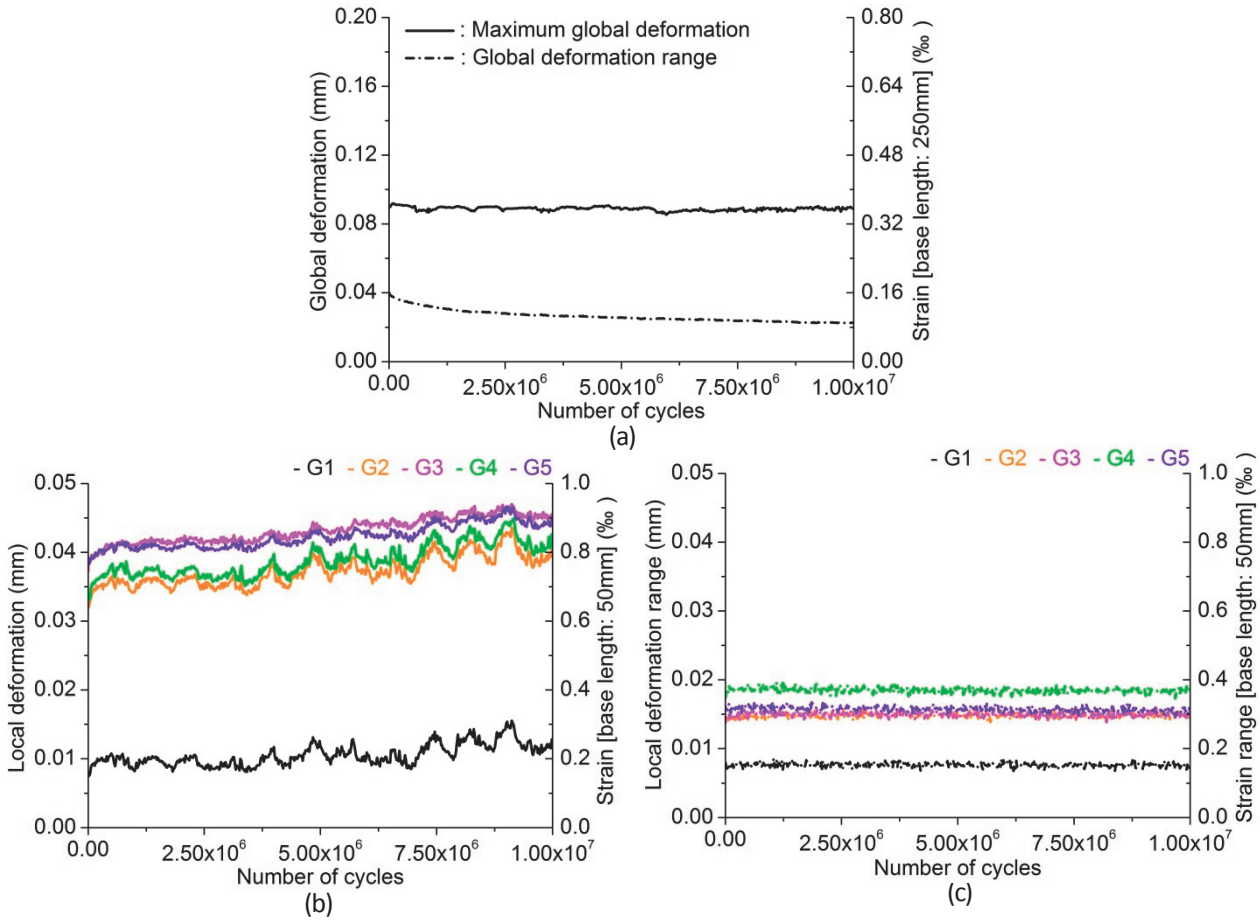


**Figure 98** S3-9 test: growth curves of (a) maximum global deformation and global deformation range, (b) maximum local deformation and (c) local deformation range

### 5.6 Results of S4 series

Table 8 lists the summary of S2.5 series test results.

**Table 10** Results of S4 series tensile fatigue tests of UHPFRC

| Test No. | | $\sigma_{max}$ [MPa] | $\sigma_{min}$ [MPa] | $\varepsilon_{pre}$ [‰] | $\sigma_{max}/f_{e,i}$ | $N$ | Remarks |
|---|---|---|---|---|---|---|---|
| 1 | i | 6.0 | 0.60 | 3.02 | 0.60 | 10,000,000 | run-out |
| | ii | 7.2 | 0.72 | | 0.72 | 10,023,857 | run-out |
| | iii | 8.3 | 0.83 | | 0.83 | 3,005,917 | |
| 2 | | 5.3 | 0.53 | 4.00 | 0.46 | 9,201,019 | |
| 3 | i | 4.9 | 0.49 | 5.01 | 0.46 | 10,000,050 | run-out |
| | ii | 6.7 | 0.67 | | 0.63 | 2,608,168 | |
| 4 | i | 4.5 | 0.45 | 5.03 | 0.54 | 10,000,050 | run-out |
| | ii | 6.6 | 0.66 | | 0.79 | 14,146 | |
| 5 | | 4.4 | 0.44 | 6.11 | 0.50 | 25,228 | |

### 5.6.1 S4-1 test

***Mechanical properties of the specimen***

| $f_{e,i}$ [MPa] | $\varepsilon_{e,i}$ [‰] | $E$ [GPa] | $f_{u,i}$ [MPa] | $\varepsilon_{u,i}$ [‰] |
|---|---|---|---|---|
| 10.0 | 0.31 | 37.4 | 14.3 | 2.45 |

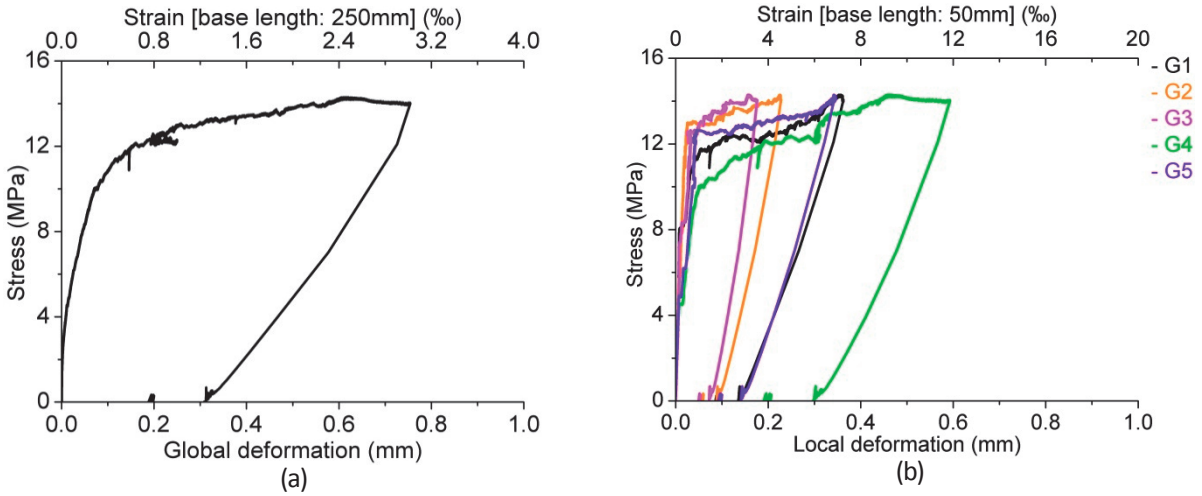


**Figure 99** Stress-deformation curves obtained from quasi-static tensile preloading preceding the S4-1 test (a) global deformation and (b) local deformation

**First fatigue test**

***Test parameters and results***

| $\sigma_{max}$ [MPa] | $\sigma_{min}$ [MPa] | $\varepsilon_{pre}$ [‰] | $\sigma_{max}/f_{e,i}$ | $N$ | Deformation localisation |
|---|---|---|---|---|---|
| 6.0 | 0.60 | 3.02 | 0.60 | 10,000,000 | run-out |

Comment: Stress causing 0.10 ‰ global strain was determined as maximum fatigue stress from the stress-deformation curve obtained from quasi-static tensile preloading.

***Behaviour of S4-1 test specimen during the first fatigue test***

Maximum global deformation, global deformation range, maximum local deformation and local deformation range at all local zones kept almost constant.

Variations were observed on local deformation readings.

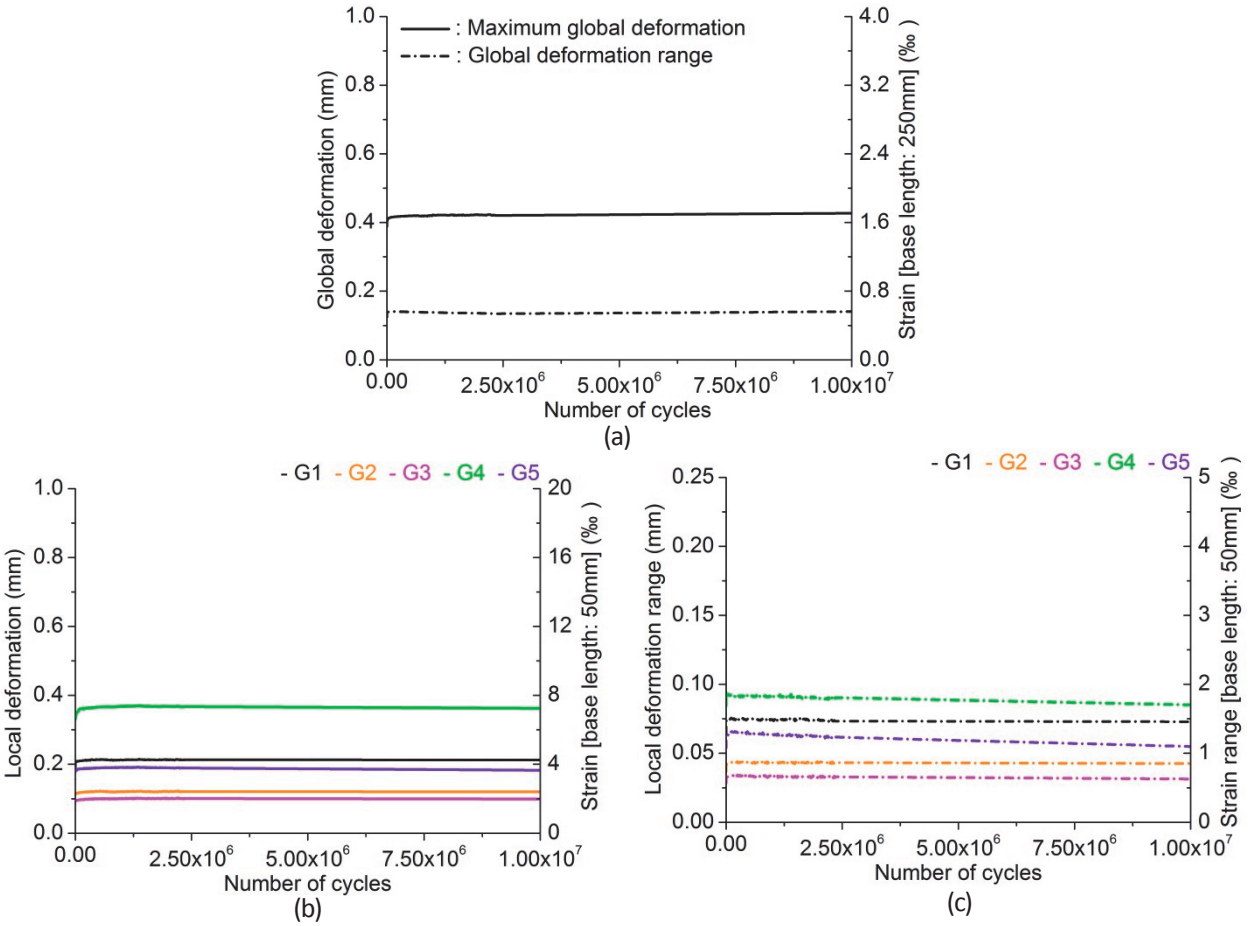


**Figure 100** S4-1_i test: growth curves of (a) maximum global deformation and global deformation range, (b) maximum local deformation and (c) local deformation range

**Second fatigue test**

***Test parameters and results***

| $\sigma_{max}$ [MPa] | $\sigma_{min}$ [MPa] | $\sigma_{max}/f_{e,i}$ | $N$ | Deformation localisation |
|---|---|---|---|---|
| 7.2 | 0.29 | 0.72 | 10,023,857 | run-out |

Comment: Stress causing 0.15 ‰ global strain was determined as maximum fatigue stress from the stress-deformation curve obtained from quasi-static tensile preloading.

***Behaviour of S4-1 test specimen during the second fatigue test***

Maximum global deformation, global deformation range, maximum local deformation at all local zones except G4 zone and local deformation range at all local zones kept almost constant.

Maximum local deformation at G4 zone kept constant until about 1,889,100 cycles at which its reading suddenly rose. After that, maximum local deformation at G4 zone kept again constant.

Variation remained on local deformation readings.

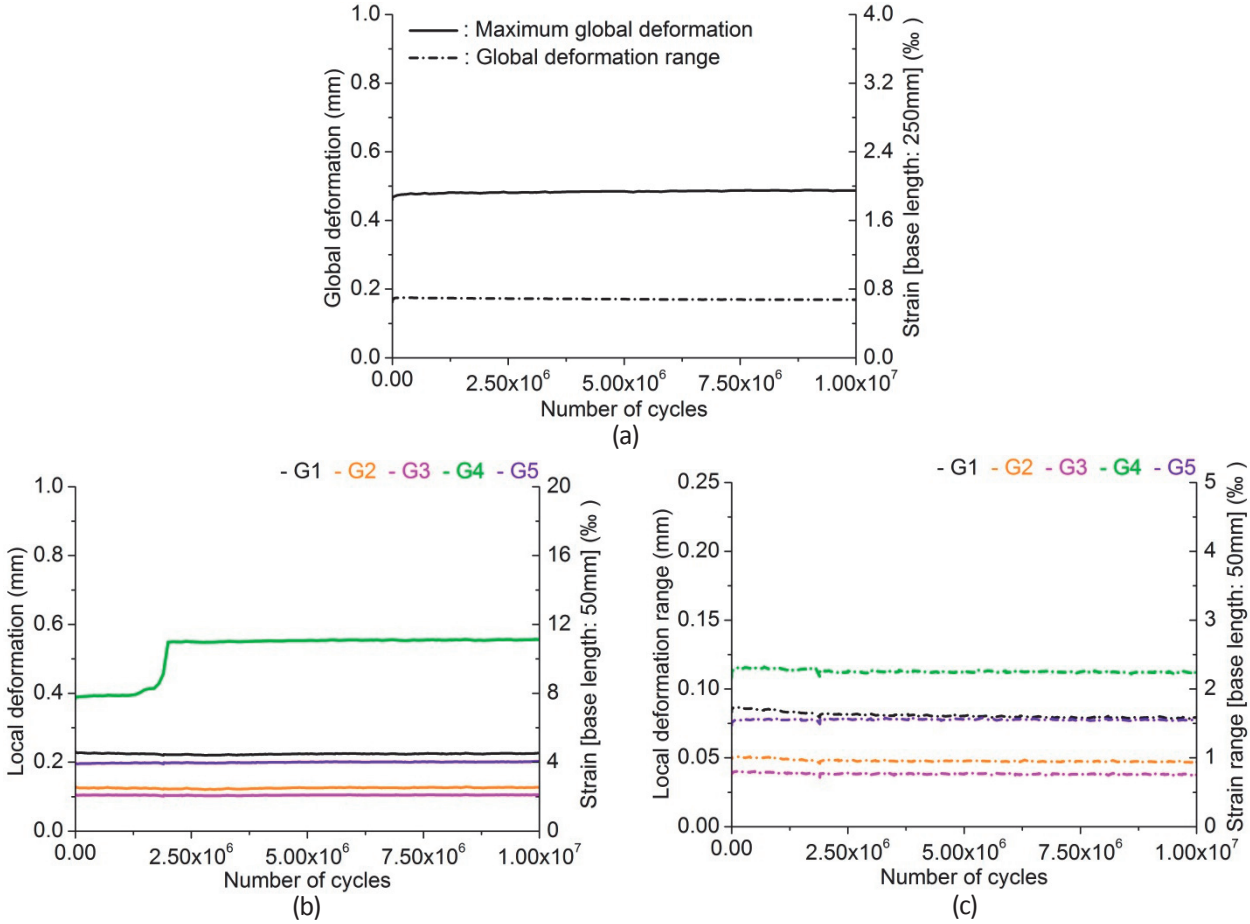


**Figure 101** S4-1_ii test: growth curves of (a) maximum global deformation and global deformation range, (b) maximum local deformation and (c) local deformation range

**Third fatigue test**

***Test parameters and results***

| $\sigma_{max}$ [MPa] | $\sigma_{min}$ [MPa] | $\sigma_{max}/f_{e,i}$ | $N$ | Deformation localisation |
|---|---|---|---|---|
| 8.3 | 0.83 | 0.83 | 3,005,917 | G4 zone |

Comment: Stress causing 0.20 ‰ global strain was determined as maximum fatigue stress from the stress-deformation curve obtained from quasi-static tensile preloading.

***Behaviour of S4-1 test specimen during the third fatigue test***

Maximum global deformation and global deformation range kept almost constant until deformation localised at G4 zone.

Behaviour of maximum local deformation and local deformation range at G4 zone was similar to that of maximum global deformation. Maximum local deformation and local deformation range at the other local zones kept approximately constant.

When deformation localised at G4 zone, UHPFRC at the other local zones softened.

Variation remained on local deformation readings.

Fracture crack propagated diagonally with an angle of about 35˚ from horizontal axis.

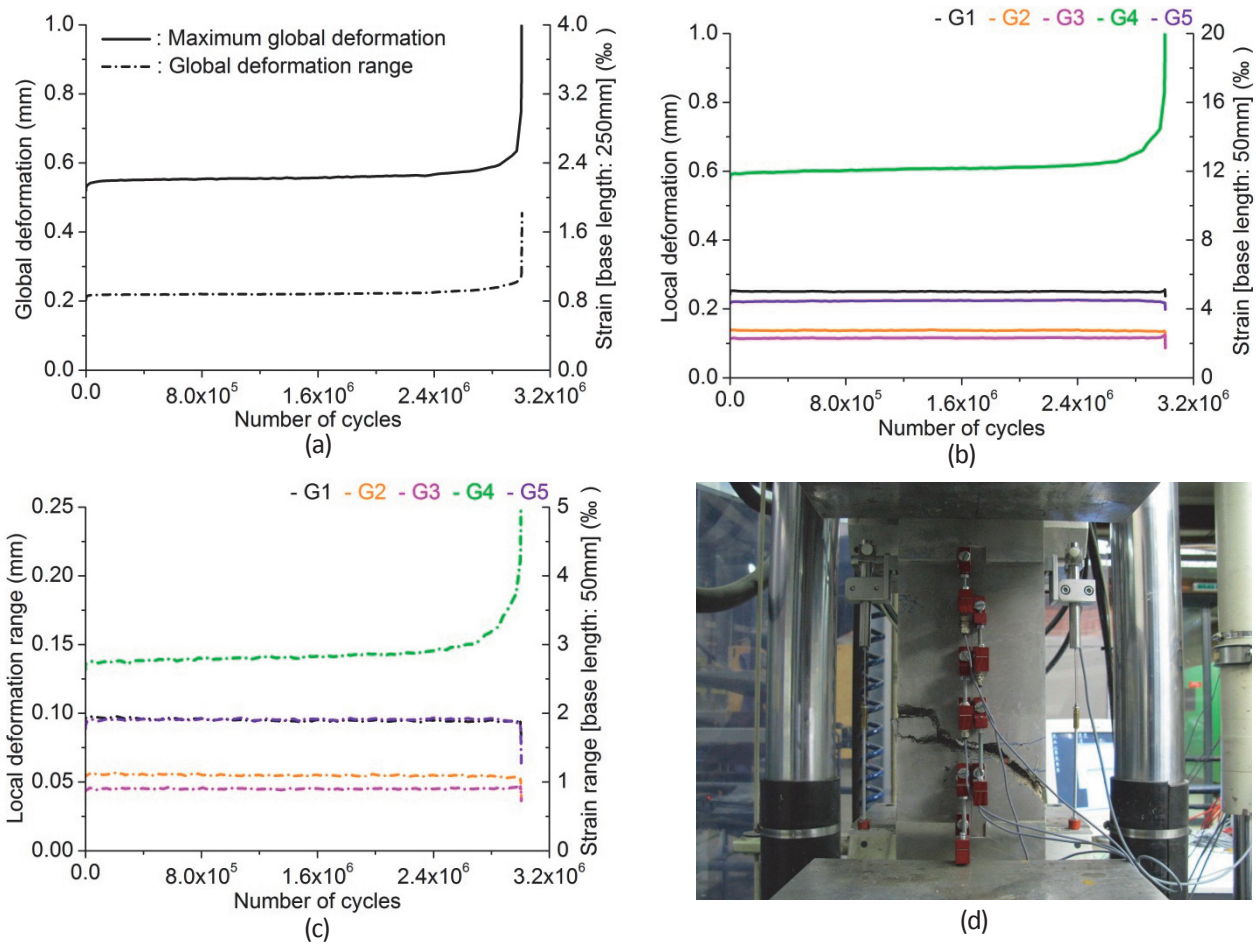


**Figure 102** S4-1_iii test: growth curves of (a) maximum global deformation and global deformation range, (b) maximum local deformation, (c) local deformation range and (d) fractured S4-1 test specimen

***Fatigue fracture surface of S4-1 test specimen:***

A part of the fracture surface was smooth and covered with rust-coloured powdery products. That was understood to be fatigue cracked area (enclosed with a line in Fig. 103). Direction of fatigue fracture crack propagation wasn't understood from examination of the fracture surface.

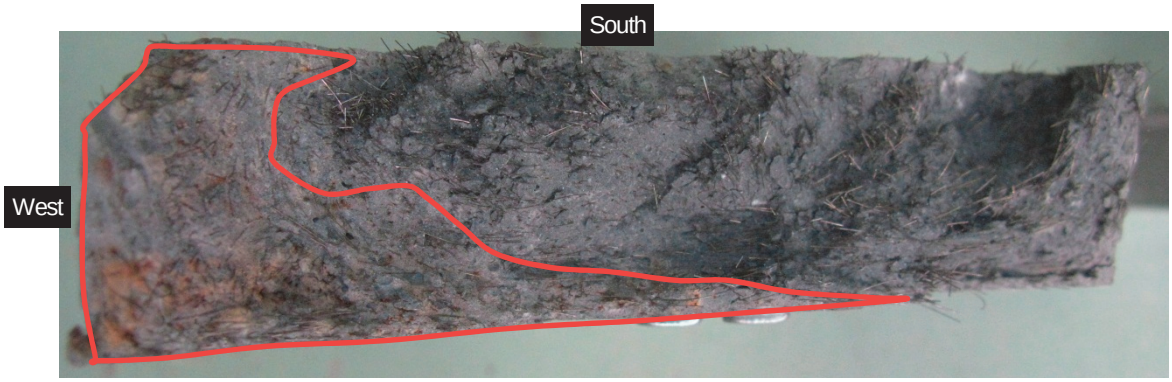


**Figure 103** Fatigue fracture surface of S4-1 test specimen (upper half of the fractured specimen)

### 5.6.2 S4-2 test

***Mechanical properties of the specimen***

| $f_{e,i}$ [MPa] | $\varepsilon_{e,i}$ [‰] | $E$ [GPa] | $f_{u,i}$ [MPa] | $\varepsilon_{u,i}$ [‰] |
|---|---|---|---|---|
| 11.5 | 0.32 | 51.2 | 13.0 | 2.12 |

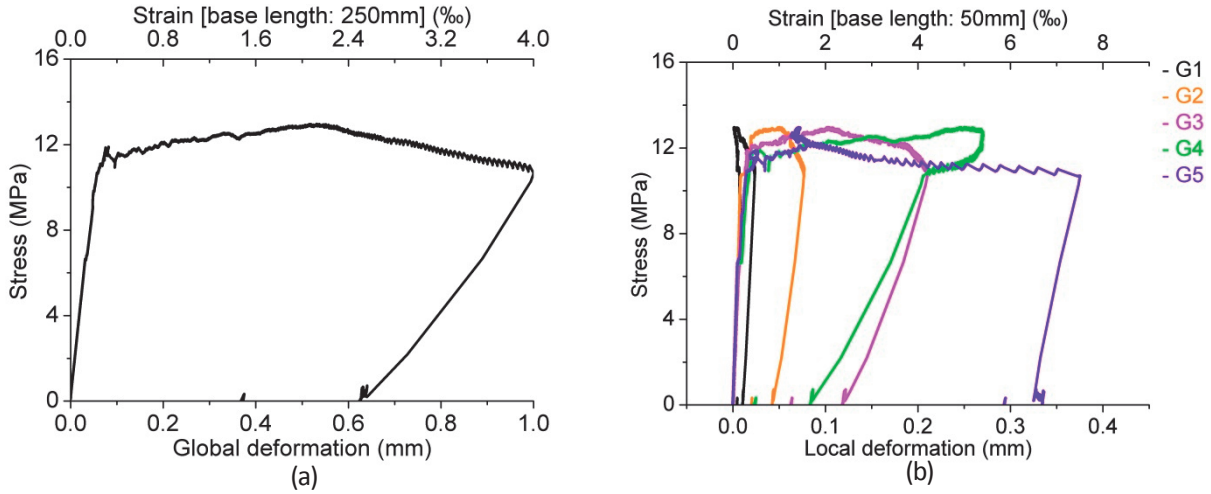


**Figure 104** Stress-deformation curves obtained from quasi-static tensile preloading preceding the S4-2 test (a) global deformation and (b) local deformation

***Test parameters and results***

| $\sigma_{max}$ [MPa] | $\sigma_{min}$ [MPa] | $\varepsilon_{pre}$ [‰] | $\sigma_{max}/f_{e,i}$ | $N$ | Deformation localisation |
|---|---|---|---|---|---|
| 5.3 | 0.53 | 4.00 | 0.46 | 9,201,019 | G5 zone and outside of G5 zone |

Comment: Stress causing 0.10 ‰ global strain was determined as maximum fatigue stress from the stress-deformation curve obtained from quasi-static tensile preloading.

***Behaviour of S4-2 test specimen***

Maximum global deformation gradually increased until deformation localised at G5 zone. Behaviour of global deformation range was similar to that of maximum global deformation, while growth rate of global deformation range was smaller than that of maximum global deformation.

Behaviour of maximum local deformation at G5 zone was similar to that of maximum global deformation. Local deformation range at G5 zone slightly decreased in the early stage of the test, and then gradually increased until deformation localisation occurred. Maximum local deformation and local deformation range at the other local zones kept approximately constant.

Variations were observed on local deformation readings.

Fracture crack propagated in a path with an angle of about 30˚ from horizontal axis.

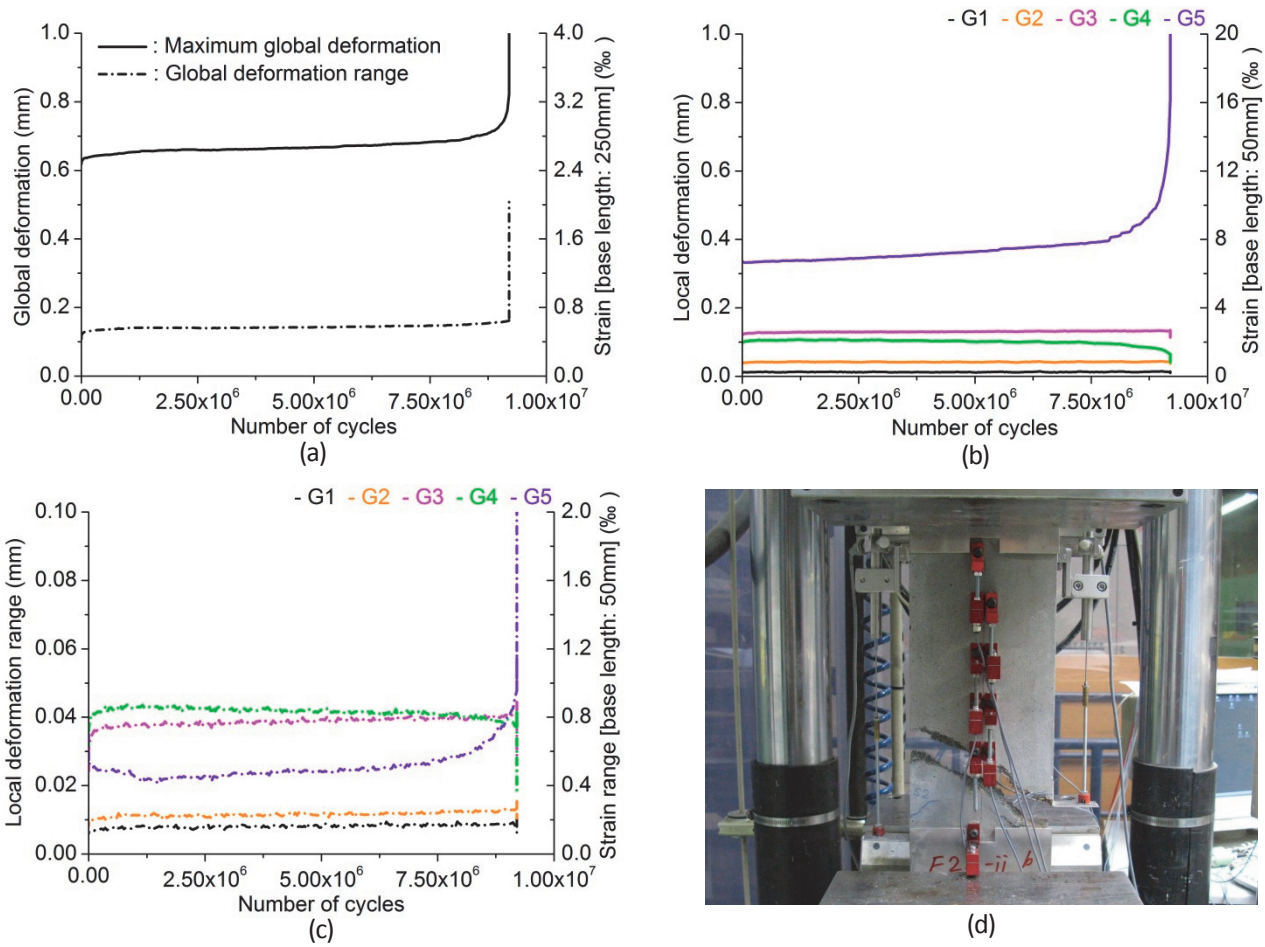


**Figure 105** S4-2 test: growth curves of (a) maximum global deformation and global deformation range, (b) maximum local deformation, (c) local deformation range and (d) fractured specimen

***Fatigue fracture surface of S4-2 test specimen:***

A part of the fracture surface was covered with rust-coloured powdery products and smooth with few fibres, which was understood as fatigue cracked area (enclosed with a line in Fig. 106). Direction of fatigue fracture crack propagation was extrapolated from the depth of rust-coloured powdery products, which are indicated with arrows in Fig. 106.


**Figure 106** Fatigue fracture surface of S4-2 test specimen (lower half of the fractured specimen)

### 5.6.3 S4-3 test

***Mechanical properties of the specimen***

| $f_{e,i}$ [MPa] | $\varepsilon_{e,i}$ [‰] | $E$ [GPa] | $f_{u,i}$ [MPa] | $\varepsilon_{u,i}$ [‰] |
|---|---|---|---|---|
| 10.7 | 0.35 | 40.6 | 15.6 | 3.50 |

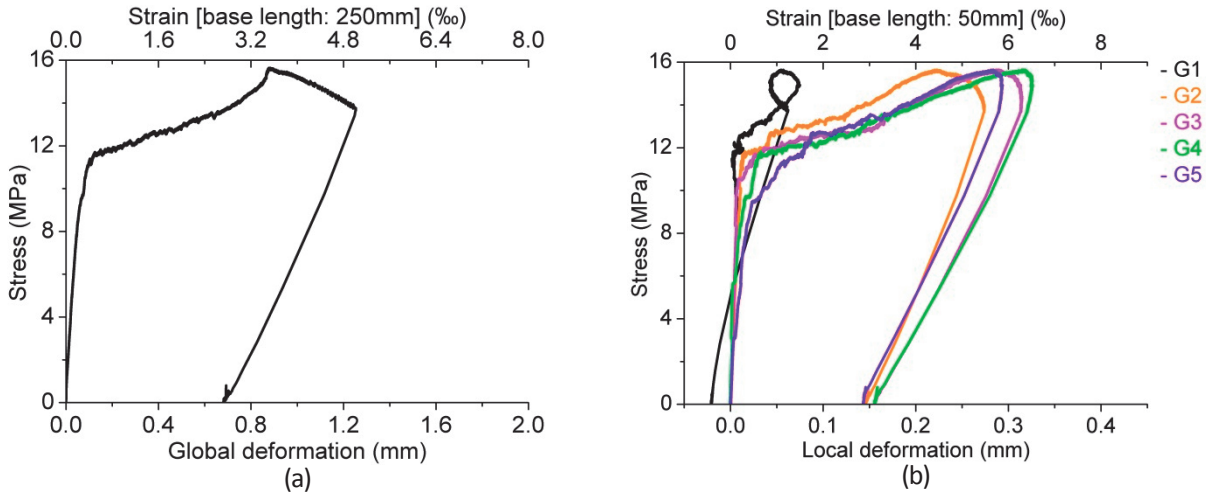


**Figure 107** Stress-deformation curves obtained from quasi-static tensile preloading preceding the S4-3 test (a) global deformation and (b) local deformation

**First fatigue test**

***Test parameters and results***

| $\sigma_{max}$ [MPa] | $\sigma_{min}$ [MPa] | $\varepsilon_{pre}$ [‰] | $\sigma_{max}/f_{e,i}$ | $N$ | Deformation localisation |
|---|---|---|---|---|---|
| 4.9 | 0.49 | 5.01 | 0.46 | 10,000,005 | run-out |

Comment: Stress causing 0.10 ‰ global strain was determined as maximum fatigue stress from the stress-deformation curve obtained from quasi-static tensile preloading.

***Behaviour of S4-3 test specimen during the first fatigue test***

Maximum global deformation, global deformation range, maximum local deformation at all local zones except G1 zone and local deformation range at all local zones kept approximately constant.

Maximum local deformation at G1 zone gradually increased until about 2,754,400 cycles at which its reading suddenly rose. After that, it kept approximately constant.

Variations were observed on local deformation readings.

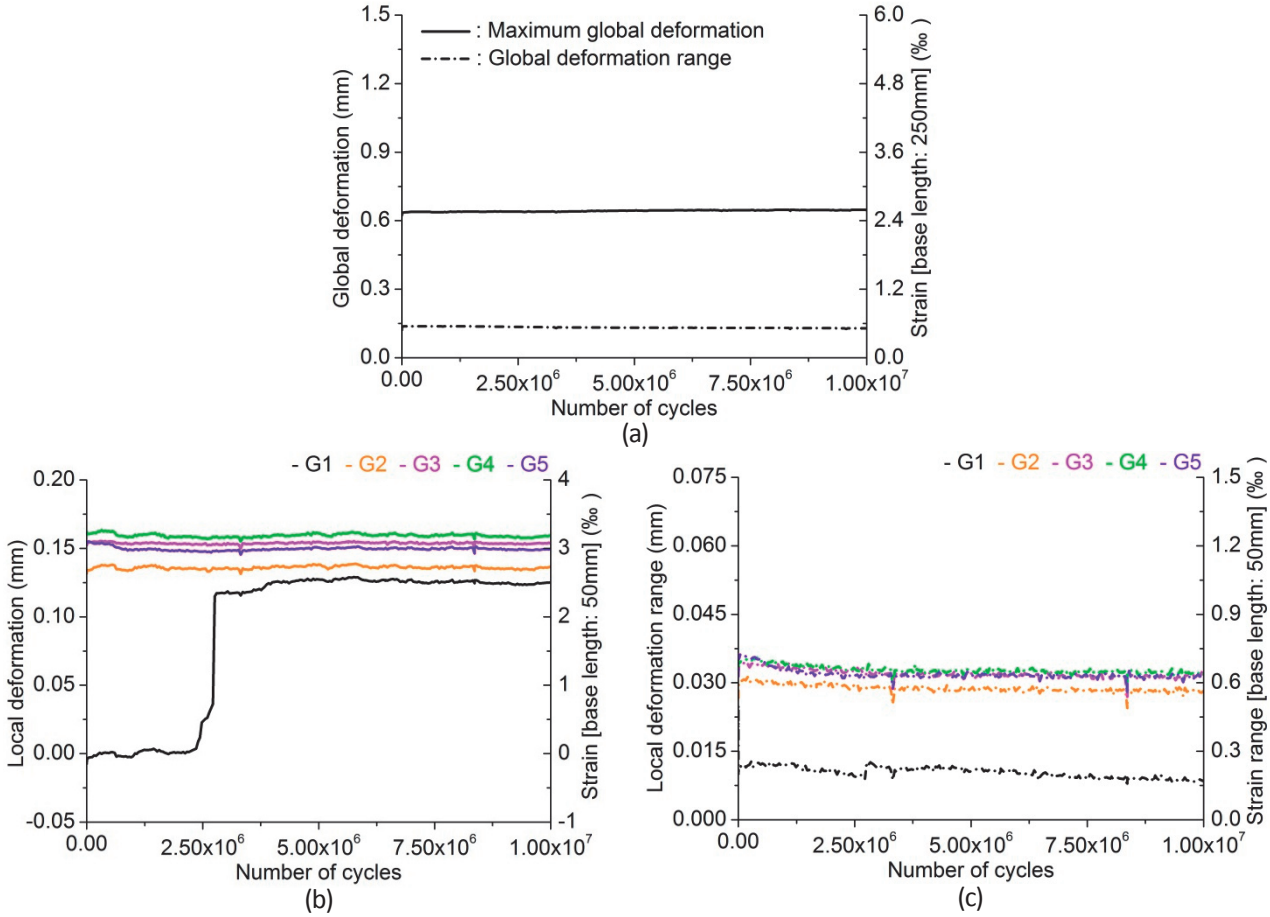


**Figure 108** S4-3_i test: growth curves of (a) maximum global deformation and global deformation range, (b) maximum local deformation and (c) local deformation range

**Second fatigue test**

***Test parameters and results***

| $\sigma_{max}$ [MPa] | $\sigma_{min}$ [MPa] | $\sigma_{max}/f_{e,i}$ | $N$ | Deformation localisation |
|---|---|---|---|---|
| 6.7 | 0.67 | 0.63 | 2,608,168 | G1 zone |

Comment: Stress causing 0.15 ‰ global strain was determined as maximum fatigue stress from the stress-deformation curve obtained from quasi-static tensile preloading.

***Behaviour of S4-3 test specimen during the second fatigue test***

Maximum global deformation and global deformation range gradually increased until the specimen fractured.

Behaviour of maximum local deformation at G1 zone was irregular. Maximum local deformation at G1 zone gradually decreased until about 420,300 cycles at which its reading suddenly decreased, and then fluctuated. At about 651,300 cycles, its reading suddenly decreased again and then kept approximately constant until the specimen fractured. Maximum local deformation at G2 and G3 zones increased, while maximum local deformation at G4 and G5 zones kept approximately constant. Local deformation range at G1 zone repeated increasing and decreasing until fracture of the specimen. Local deformation range at the other zones had similar behaviour to maximum local deformation.

Variations remained on local deformation readings.

Although curved, fracture crack propagation path was roughly perpendicular to fatigue force direction.

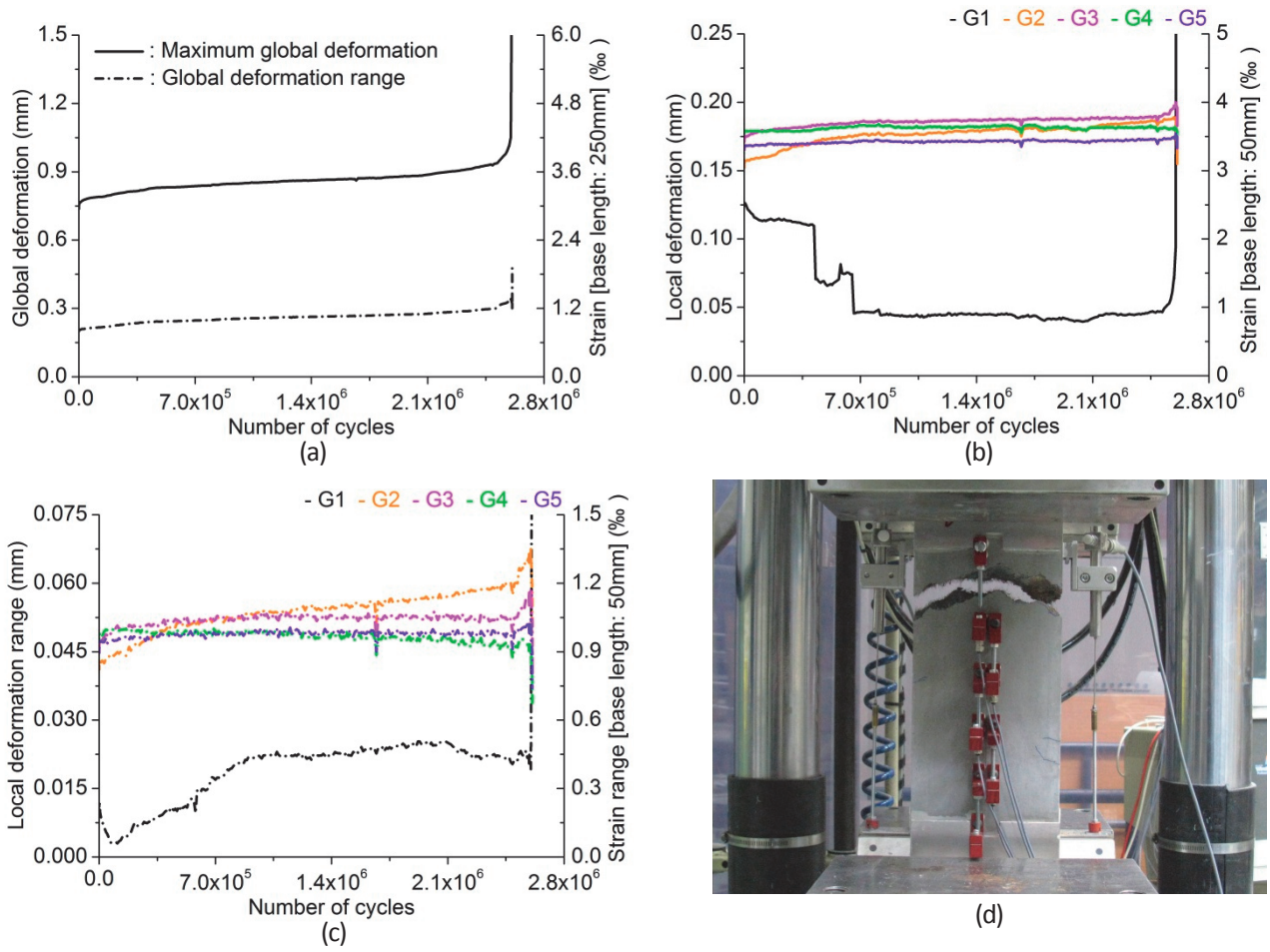


**Figure 109** S4-3_ii test: growth curves of (a) maximum global deformation and global deformation range, (b) maximum local deformation, (c) local deformation range and (d) fractured S4-3 test specimen

***Fatigue fracture surface of S4-3 test specimen:***

Western part of the fracture surface was covered with rust-coloured powdery product, which was identified as fatigue cracked area (enclosed with a line in Fig. 110). Direction of fatigue fracture crack propagation wasn't understood.

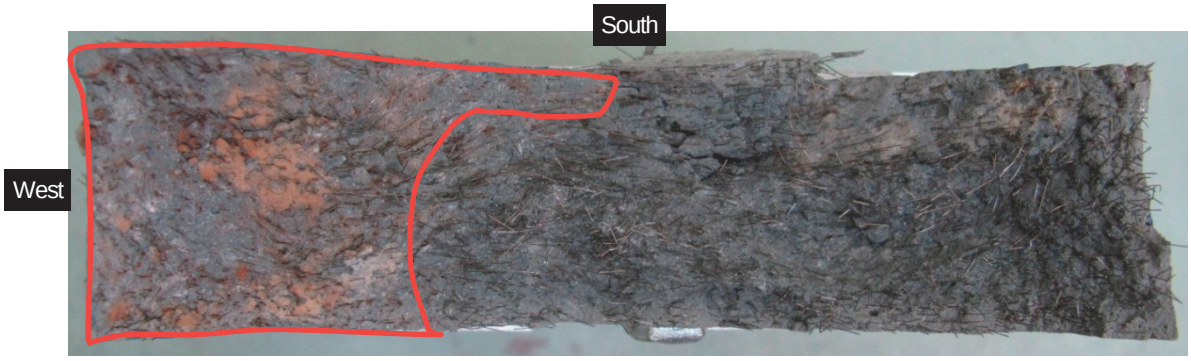


**Figure 110** Fatigue fracture surface of S4-3 test specimen (upper half of the fractured specimen)

### 5.6.4 S4-4 test

***Mechanical properties of the specimen***

| $f_{e,i}$ [MPa] | $\varepsilon_{e,i}$ [‰] | $E$ [GPa] | $f_{u,i}$ [MPa] | $\varepsilon_{u,i}$ [‰] |
|---|---|---|---|---|
| 8.4 | 0.29 | 43.8 | 10.5 | 2.73 |

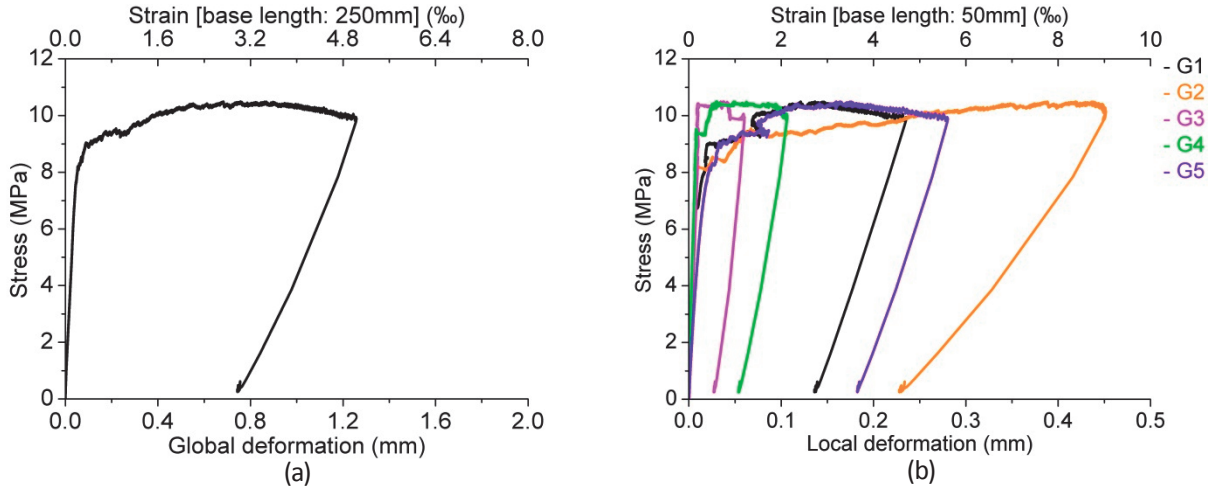


**Figure 111** Stress-deformation curves obtained from quasi-static tensile preloading preceding the S4-4 test (a) global deformation and (b) local deformation

**First fatigue test**

***Test parameters and results***

| $\sigma_{max}$ [MPa] | $\sigma_{min}$ [MPa] | $\varepsilon_{pre}$ [‰] | $\sigma_{max}/f_{e,i}$ | $N$ | Deformation localisation |
|---|---|---|---|---|---|
| 4.5 | 0.45 | 5.03 | 0.54 | 10,000,005 | run-out |

Comment: Stress causing 0.10 ‰ global strain was determined as maximum fatigue stress from the stress-deformation curve obtained from quasi-static tensile preloading.

***Behaviour of S4-4 test specimen during the first fatigue test***

Maximum global deformation, global deformation range, maximum local deformation and local deformation range at all local zones kept almost constant.

Variations were observed on local deformation readings.

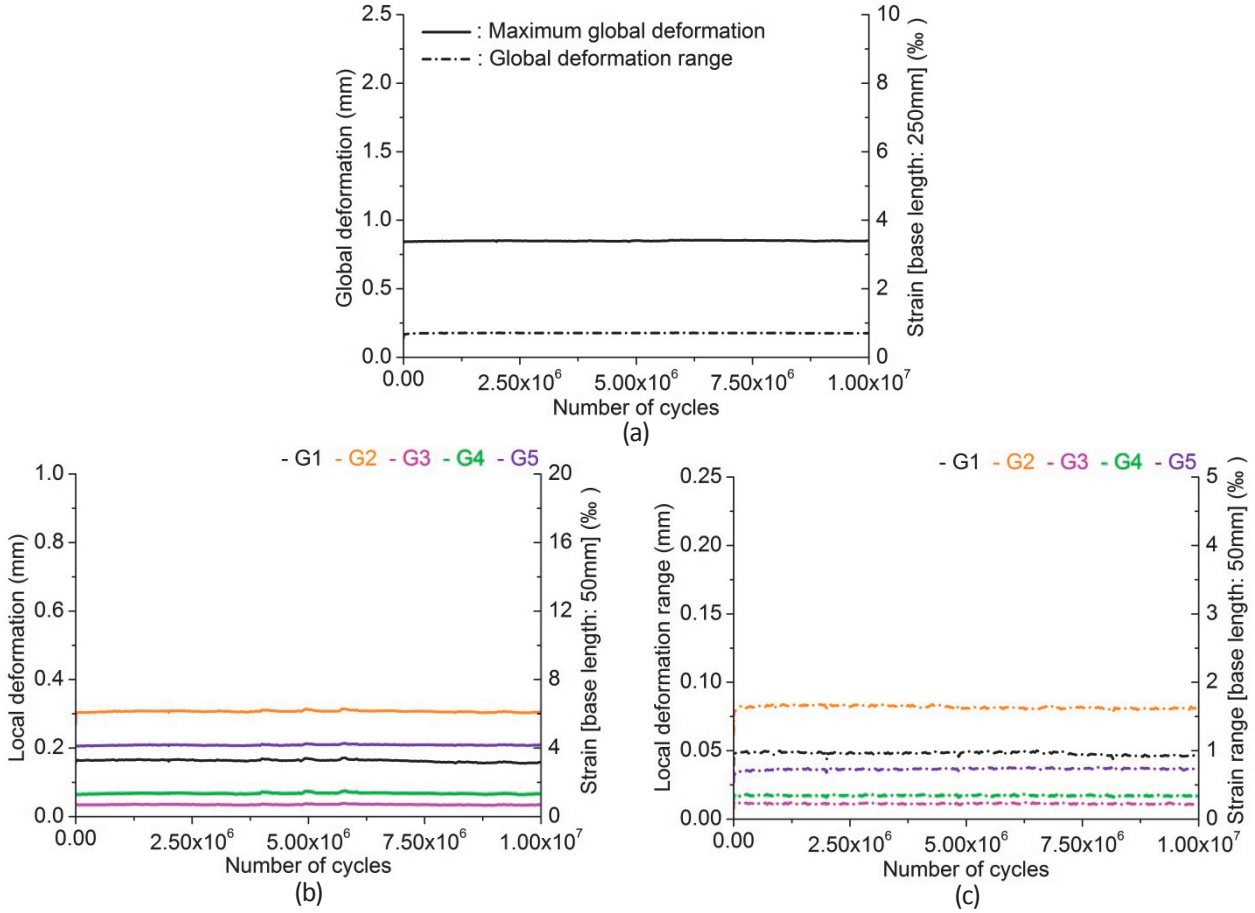


**Figure 112** S4-4_i test: growth curves of (a) maximum global deformation and global deformation range, (b) maximum local deformation and (c) local deformation range

**Second fatigue test**

***Test parameters and results***

| $\sigma_{max}$ [MPa] | $\sigma_{min}$ [MPa] | $\sigma_{max}/f_{e,i}$ | $N$ | Deformation localisation |
|---|---|---|---|---|
| 6.6 | 0.66 | 0.79 | 14,146 | G1 and G5 zones |

Comment: Stress causing 0.15 ‰ global strain was determined as maximum fatigue stress from the stress-deformation curve obtained from quasi-static tensile preloading.

***Behaviour of S4-4 test specimen during the second fatigue test***

Maximum global deformation gradually increased until about 10,000 cycles at which its growth rate started to increase, and eventually the specimen fractured. Global deformation range constantly increased with lower growth rate than maximum global deformation until fracture of the specimen.

Maximum local deformation at G1 and G5 zones had similar behaviour to maximum global deformation, while maximum deformation reading of G5 zone was larger than that of G1 zone. Maximum local deformation at the other local zones kept approximately constant, and when deformation localised at G1 and G5 zones, UHPFRC at the other local zones softened. Local deformation range at G5 zone gradually increased, while local deformation range at the other local zones kept approximately constant.

Variations remained on local deformation readings, being the same degree as the first fatigue test.

Two fracture cracks appeared and both propagated in paths with an angle of about 20˚ from horizontal axis.

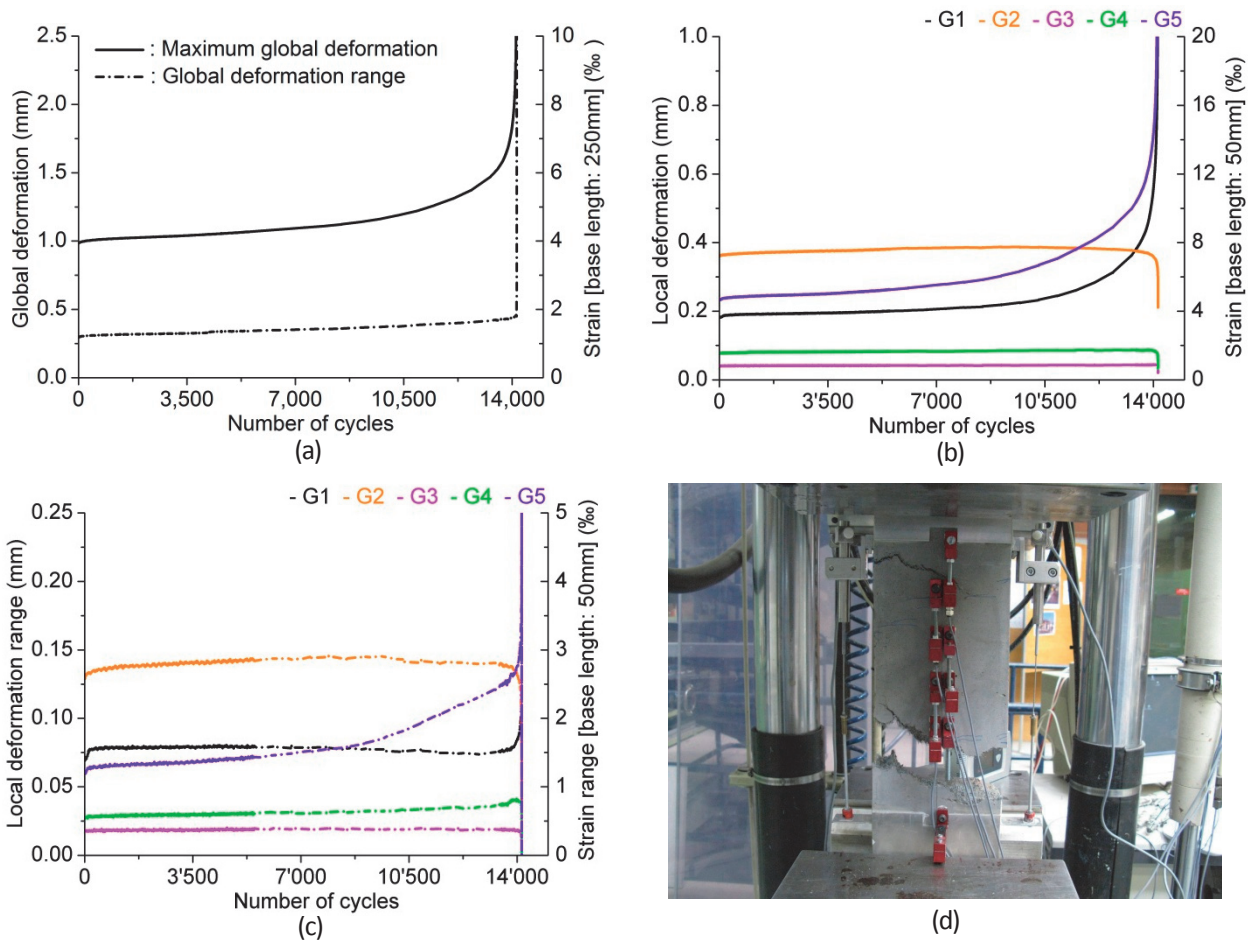


**Figure 113** S4-4_ii test: growth curves of (a) maximum global deformation and global deformation range, (b) maximum local deformation, (c) local deformation range and (d) fractured S4-4 test specimen

***Fatigue fracture surface of S4-4 test specimen:***

The area with few fibres is indicated with an enclosing line in Fig. 114. Since holes caused by fibre pull-out were not observed in the area devoid of fibres, few fibres were supposed to exist initially in that area due to the UHPFRC fabrication process.


**Figure 114** Fatigue fracture surface of S4-4 test specimen (lower half of the fractured specimen)

### 5.6.5 S4-5 test

***Mechanical properties of the specimen***

| $f_{e,i}$ [MPa] | $\varepsilon_{e,i}$ [‰] | $E$ [GPa] | $f_{u,i}$ [MPa] | $\varepsilon_{u,i}$ [‰] |
|---|---|---|---|---|
| 8.8 | 0.35 | 29.8 | 9.3 | 2.47 |

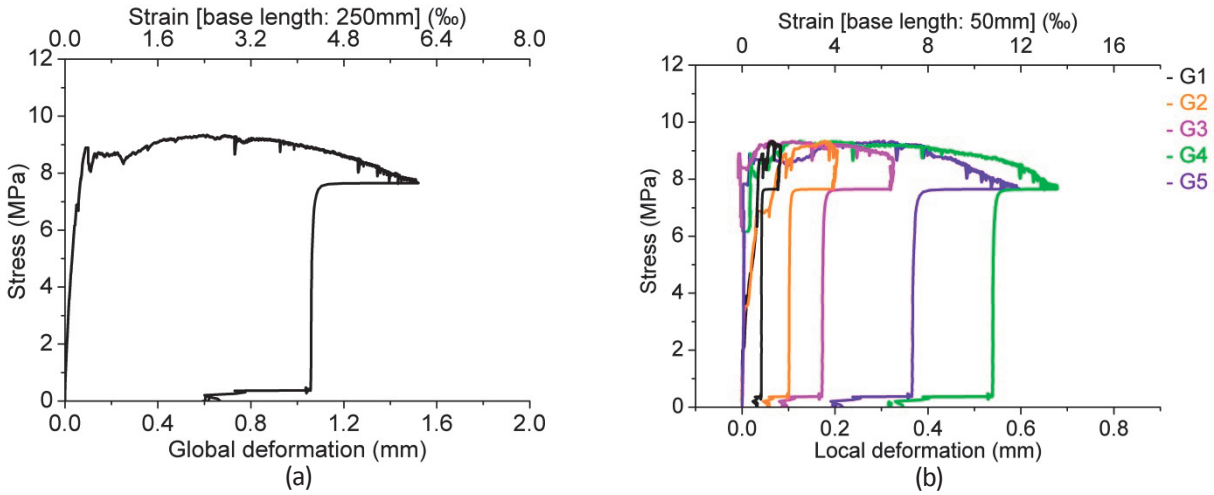


**Figure 115** Stress-deformation curves obtained from quasi-static tensile preloading preceding the S4-4 test (a) global deformation and (b) local deformation

***Test parameters and results***

| $\sigma_{max}$ [MPa] | $\sigma_{min}$ [MPa] | $\varepsilon_{pre}$ [‰] | $\sigma_{max}/f_{e,i}$ | $N$ | Deformation localisation |
|---|---|---|---|---|---|
| 4.4 | 0.44 | 6.11 | 0.50 | 25,228 | G4 and G5 zones |

Comment: Stress causing 0.10 ‰ global strain was determined as maximum fatigue stress from the stress-deformation curve obtained from quasi-static tensile preloading.

***Behaviour of S4-5 test specimen***

Maximum global deformation gradually increased. At about 21,000 cycles, its growth rate started to increase and eventually the specimen fractured. Global deformation range kept approximately constant.

Behaviour of maximum local deformation at G4 zone where deformation localised was quite similar to that of maximum global deformation. Maximum local deformation at G5 zone gradually increased. At about 23,000 cycles, its growth rate started to increase and deformation also localised at G5 zone. Maximum local deformation at G1 to G3 zone kept constant. Local deformation range at G4 zone gradually increased and when deformation localised, it suddenly rose. Local deformation range at G5 zone gradually increased and when deformation localised, it suddenly dropped. Local deformation range at G1 to G3 zone kept approximately constant and when deformation localised, it suddenly dropped.

Variations were observed on local deformation readings.

Two fracture cracks appeared. One of them propagated through all width of the specimen at G4 zone and another propagated only in the western half of the specimen. Both were almost perpendicular to fatigue force direction.

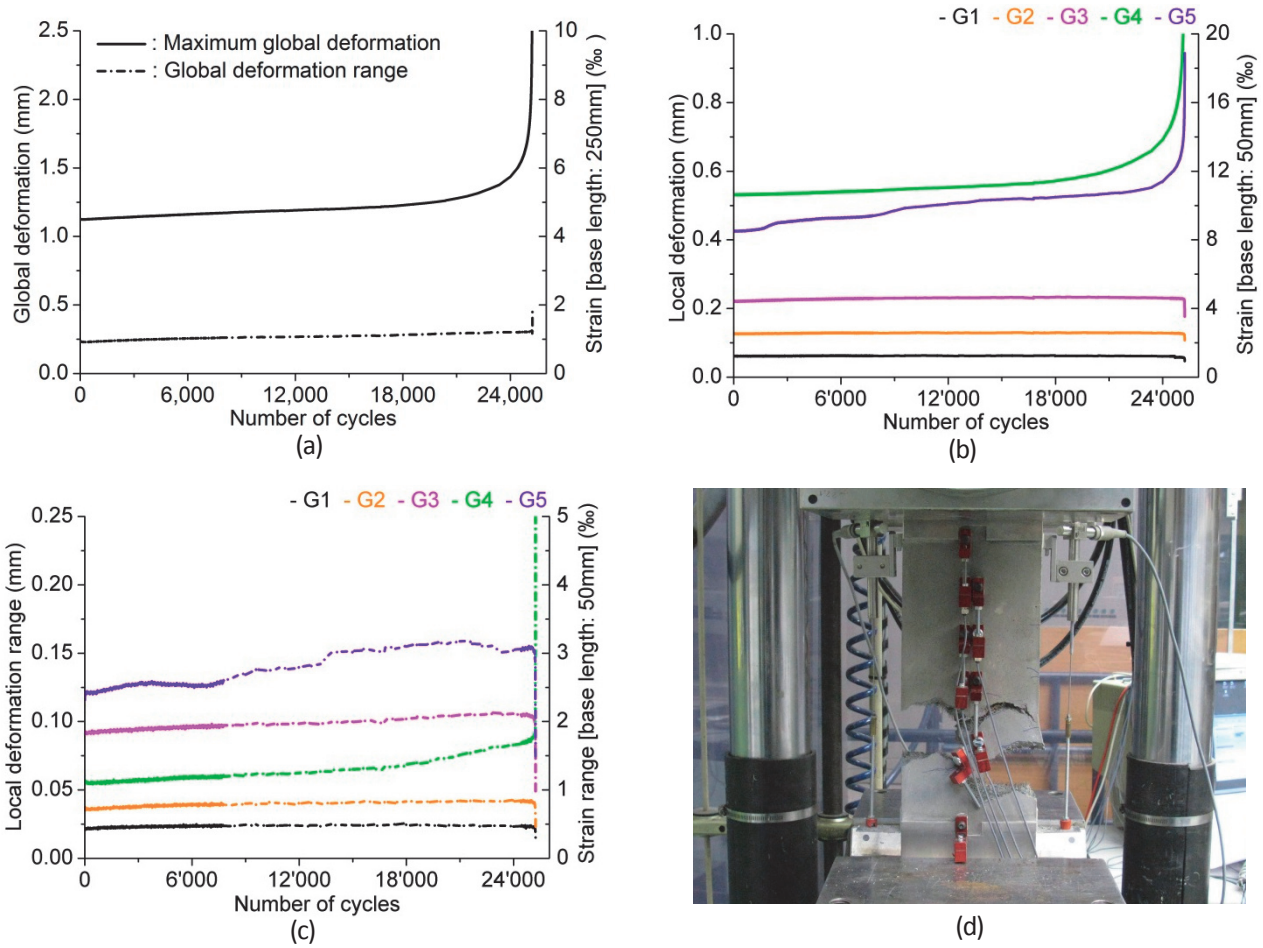


**Figure 116** S4-5 test: growth curves of (a) maximum global deformation and global deformation range, (b) maximum local deformation, (c) local deformation range, (d) fractured specimen

***Fatigue fracture surface of S4-5 test specimen:***

Fatigue cracked area wasn't identified. The area void of fibres was observed on south part of the fracture surface and it was supposed to have few fibres initially (enclosed with a line in Fig. 117).


**Figure 117** Fatigue fracture surface of S4-5 test specimen (lower half of the fractured specimen)

## 6 Conclusion

This report presents the tests results of an experimental campaign carried out by the author to investigate the tensile fatigue behaviour of UHPFRC. The results were used to draw *S-N* diagrams to determine the fatigue endurance limit and deduce empirical laws concerning fatigue damage of UHPFRC. For discussion and analysis of the results, refer to the papers or the thesis of the author.

The following conclusions were drawn:

1) Behaviour of global deformation range was similar to that of maximum global deformation. Minimum global deformation kept more or less constant and thus minimum fatigue stress didn't cause significant damage on UHPFRC.

2) Variations were observed on local deformation despite the fact that tensile fatigue stress was uniform in UHPFRC specimen. This might be due to local variations of material properties of UHPFRC.

3) In most specimens, fatigue fracture crack propagated in a path approximately perpendicular to fatigue force direction.

4) Regardless of macrocracking during the fatigue tests, UHPFRC kept to carry fatigue stress by redistributing localised deformation.

5) On the fatigue fracture surface, a smooth surface area was observed. It was often covered by rust-coloured powdery products.

6) In some specimens, behaviour of maximum local deformation at a specific zone was approximately the same as that of maximum global deformation.

7) In the S3 and S4 series, specimens didn't show significant deformation growth. This is due to initial deformation caused by the preloading prior to the fatigue test.

8) UHPFRC has sufficient fatigue stress resistance even after preloading beyond the elastic limit strength.

**7 Reference**

[1] Makita T., Brühwiler E., (2013) "Tensile fatigue behaviour of ultra-high performance fibre reinforced concrete (UHPFRC)", Materials and Structures, Published online: 23 April, 2013